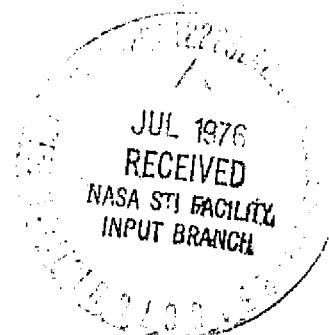# NASA TECHNICAL MEMORANDUM

NASA TM X- 73,139

WIND TUNNEL INVESTIGATION OF A LARGE-SCALE

MODEL OF A LIFT/CRUISE FAN V/STOL AIRCRAFT

Bruno J. Gambucci, Kiyoshi Aoyagi, and L. Stewart Rolls

Ames Research Center
Moffett Field, Calif. 94035

May 1976

1. Report No. NASA TM X-73,139	2. Government Accession No.	3. Recipient's Catalog No.
4. Title and Subtitle WIND TUNNEL INVESTIGATION OF A LARGE-SCALE MODEL OF A LIFT/CRUISE FAN V/STOL AIRCRAFT		5. Report Date
		6. Performing Organization Code
7. Author(s) Bruno J. Gambucci, Kiyoshi Aoyagi, and L. Stewart Rolls		8. Performing Organization Report No. A-6619
		10. Work Unit No. 505-10-35
9. Performing Organization Name and Address Ames Research Center Moffett Field, Calif. 94035		11. Contract or Grant No.
		13. Type of Report and Period Covered Technical Memorandum
12. Sponsoring Agency Name and Address National Aeronautics and Space Administration Washington, D. C. 20546		14. Sponsoring Agency Code
15. Supplementary Notes		

16. Abstract

An investigation was conducted in the Ames 40- by 80-Foot Wind Tunnel to determine the aerodynamic characteristics of a large-scale model of a lift/cruise fan V/STOL aircraft. The model was equipped with three fans, one mounted in the forward section of the fuselage in a lift mode, and two mounted on top of the wing adjacent to the fuse ge in a lift/cruise mode.

The data that were obtained include longitudinal and lateral-directional characteristics of the model, with the horizontal tail on and off, for both the powered-lift and cruise configurations. Powered-lift data were obtained at several wind tunnel velocities and at several lift/cruise fan thrust vector angles by varying the position of the hooded deflectors from 0° (the cruise condition) to 90°.

17. Key Words (Suggested by Author(s)) Lift cruise fan V/STOL Powered lift	18. Distribution Statement Unlimited STAR Category - 02		
19. Security Classif. (of this report) Unclassified	20. Security Classif. (of this page) Unclassified	21. No. of Pages 108	22. Price* $5.25

WIND TUNNEL INVESTIGATION OF A LARGE-SCALE MODEL OF A LIFT/CRUISE

FAN V/STOL AIRCRAFT

Bruno J. Gambucci, Kiyoshi Aoyagi, and L. Stewart Rolls

Ames Research Center, NASA
Moffett Field, Calif. 94035

SUMMARY

An investigation was conducted in the Ames 40- by 80-Foot Wind Tunnel to
determine the aerodynamic characteristics of a large-scale model of a lift/
cruise fan V/STOL aircraft. The model was equipped with three fans, one
mounted in the forward section of the fuselage in a lift mode, and two mounted
on top of the wing adjacent to the fuselage in a lift/cruise mode.

The data that were obtained include longidudinal and lateral-directional
characteristics of the model, with the horizontal tail on and off, for both
the powered-lift and cruise configurations. Powered-lift data were obtained
at several wind tunnel velocities and at several lift/cruise fan thrust vector
angles by varying the position of the hooded deflectors from 0° (the cruise
condition) to 90°.

INTRODUCTION

The NASA/Navy Lift/Cruise Fan Technology Aircraft Program is a cooperative
effort between NASA and the Navy; its purpose is to establish a firm technology
base for the design of lift/cruise fan V/STOL multimission aircraft for both
military and civilian applications. The program's ultimate objective is the
design, fabrication, and flight test of an aircraft that uses a lift/cruise
fan propulsion system. The operational suitability of the aircraft in multi-
mission V/STOL roles will then be investigated. This objective will be pre-
ceded by design studies (refs. 1 and 2), wind tunnel tests of small- and
large-scale models, and systems evaluation tests and simulation to develop
the base for the Technology Aircraft design. This report contains the results
of a large-scale wind tunnel test of a lift/cruise fan model typical of a con-
figuration being investigated for the Technology Aircraft. The tests were
conducted in the Ames Research Center 40- by 80-Foot Wind Tunnel.

The large-scale lift-cruise fan V/STOL model used in this test was pow-
ered by three lift fans each of which was driven by a gas generator. Data
were obtained for two modes of operation, powered lift and cruise. For the
cruise-mode operation, only the two generators over the wing-mounted lift/
cruise fans were powered; the forward fan was covered. Static tests planned
for the hover mode will be the subject of a separate report.

The longitudinal force and moment characteristics of the model, as well as its lateral-directional characteristics, are presented for both modes of operation. Results for powered lift were obtained at a constant fan speed over a range of wind tunnel velocities; the cruise configuration was run at three lift/cruise fan exit velocities and at constant wind tunnel speed.

The test data are not analyzed here; their analyses will be the subject of future reports.

NOTATION

b	wing span, m (ft)
C_D	drag coefficient about the wind axis, $\dfrac{D}{qS}$
$C_{D_{ram}}$	ram drag coefficient about the body axis, $\dfrac{Wv}{gqS}$
C_ℓ	rolling moment coefficient about the stability axis, $\dfrac{\ell}{qSb}$
C_L	lift coefficient about the wind axis, $\dfrac{L}{qS}$
C_m	pitching moment coefficient about the stability axis at $0.25\bar{c}$, $\dfrac{m}{qS\bar{c}}$
C_n	yawing moment coefficient about the stability axis, $\dfrac{n}{qSb}$
C_y	side force coefficient about the stability axis, $\dfrac{y}{qS}$
c	wing chord parallel to the plane of symmetry, m (ft)
$\bar{c}$	mean aerodynamic chord, $\dfrac{2}{S}\displaystyle\int_0^{b/2} c^2 dy$, m (ft)
D	drag, N (lb)
F_A	static axial force, N (lb)
F_g	gross thrust with $\delta_{cn} = 0°$, N (lb)
F_N	static normal force, N (lb)
g	acceleration of gravity, 9.81 m/sec^2 (32.2 ft/sec^2)
i_t	horizontal tail incidence angle, deg
L	total lift on the model, N (lb)
ℓ	rolling moment, N-m (ft-lb)
m	pitching moment, N-m (ft-lb)
n	yawing moment, N-m (ft-lb)

2

P_O standard absolute pressure, 101352.9 (14.7 psi) N/m^2

P_s freestream static pressure, N/m^2 (lb/ft^2)

q freestream dynamic pressure, N/m^2 (lb/ft^2)

$RPM/\sqrt{\theta}$ corrected fan rotational speed

S wing area, m^2 (ft^2)

V_O freestream velocity, m/sec (ft/sec)

V_j fan exit velocity, m/sec (ft/sec)

y side force, N (lb)

α angle of attack, deg

β angle of sideslip, deg

β_v lift fan exit louver deflection angle, deg

δ relative static pressure, $\dfrac{P_s}{P_O}$

δ_{ail} aileron deflection, deg

δ_{cn} lift/cruise fan exhaust duct angle, deg

δ_f trailing-edge flap deflection, deg

δ_j front fan exhaust static turning angle, $\tan^{-1} \dfrac{F_N}{F_A}$, deg

δ_R rudder deflection, deg

η percent of wing semispan or static turning efficiency, $\dfrac{\sqrt{F_N^2 + F_A^2}}{F_g}$

θ ratio of ambient temperature to standard temperature (519° Rankine)

θ_j lift/cruise fan exhaust static turning angle, deg

Subscripts

ail   aileron

J   fan exit

R   rudder

S   static conditions

u   uncorrected data

MODEL DESCRIPTION

Photographs of the model mounted in the Ames 40- by 80-Foot Wind Tunnel are shown in figure 1. Model geometric details and pertinent dimensions are presented in figure 2. The model was equipped with adjustable flaps, ailerons, horizontal stabilizer, and rudder. The horizontal tail is removable. The ailerons and horizontal tail were remotely controlled.

Wing

The wing aspect ratio was 4.5, taper ratio 0.30, and sweep along the quarter chord line 25°. An NACA 4416 airfoil section was the basic wing section at the exposed root. This became a modified supercritical airfoil with wing station (0.442 η) and tip having a thickness-to-chord ratio of 0.14 and 0.08, respectively. The wing incidence was 3.23° at the exposed root and -2.77° at the theoretical tip; this resulted in a wing twist of 6°. Wing airfoil ordinates are presented in table 1.

Empennage

The horizontal tail was an NACA 64A0 series airfoil section with a thickness-to-chord ratio at the root of 0.10 and of 0.08 at the tip. The all-movable horizontal tail could be remotely actuated and had an incidence range of ±20°.

The vertical tail had an NACA 65A010 airfoil section and was equipped with a movable rudder. For the tail-off tests, only the horizontal tail was removed.

Propulsion System

The model was equipped with three 36-in. diameter General Electric X-376 turbo-tip fans with a design pressure ratio of 1.1. As shown in figure 2(a), one lift fan was mounted in the forward fuselage section with the thrust axis tilted 15° forward with respect to the horizontal plane. Two lift/cruise fans were mounted in nacelles on the upper surface of the wing adjacent to the fuselage. Each of these fans was powered by a modified T58-δB gas generator. The relationship between the fans and gas generators is shown by the schematic in figure 3.

Thrust vectoring of the forward fan was obtained by a cascade of fourteen 0.102-m (0.333 ft) chord plain louvers that were mounted at the duct exit as shown in figure 2(b). These louvers were remotely operated and varied from 103° to complete closure (0°). Two yaw vectoring vanes were located below the louvers and 0.235 m (0.771 ft) symmetrically off the model centerline. The vanes had a chord of 0.298 m (0.978 ft) and could be deflected ±20°. For the cruise configuration ($\delta cn = 0°$), the inlet and the exit of the forward lift fan were covered for most cases with the exit louvers and yaw vanes removed.

4

Thrust vectoring of the lift/cruise fans was obtained by using the same hooded deflectors and cruise nozzle (0°) of reference 3. Geometric angles of 90°, 71°, 56°, 38°, and 23° were obtained by removing or adding circular sections as shown in figure 2(c). Two yaw vectoring vanes were located at the hooded deflector exit and could be deflected ±20° as shown in the figure 2(b). The nozzle geometric area of the hooded deflector was 0.7678 m^2 (1190 in^2). When the cruise nozzle was used, the nozzle geometric area was 0.6937 m^2 (1075 in^2).

For the cruise configuration the nozzle with the 0° geometric angle was used. This nozzle configuration was used without the yaw vanes.

TESTS AND PROCEDURE

Longitudinal force and moment data were obtained at discrete lift/cruise fan exit nozzle deflections for model angle of attack and wind tunnel speed ranges with the horizontal tail on and off. Lateral-directional data were obtained for a range of sideslip angles at model angles of attack of 0°, 8°, and 16°. A summary of the principal test variables for the powered-lift configuration is presented in the following table:

q, N/m^2 (psf)	67.032 to 952.817 N/m^2 (1.4 to 19.9 psf)
δ_{cn}	90° to 23°
α_u	-4° to 32°
β	-12° to 4°
i_t	-20° to 20°
fan RPM/$\sqrt{\theta}$	3600 (nominal)

Similar data were obtained for the cruise configuration. A summary of the variables for this mode of operation is presented below:

q, N/m^2 (psf)	1699.749 N/m^2 (35.5 psf)
δ_{cn}	0°
α_u	-4° to 32°
β	-12° to 4°
i_t	-20° to 20°
fan RPM/$\sqrt{\theta}$	2700 to 1600 (nominal)

When either the angle of attack or angle of sideslip was varied in the data acquisition process, the fan RPM, wind tunnel dynamic pressure, flap deflection, and fan exit nozzle deflection were held constant. In the cruise configuration, data were obtained with the forward fan covered.

CORRECTIONS

Force and moment data with the lift fans windmilling (power off) were corrected for wind tunnel wall constraints in the following manner:

$$\alpha = \alpha_u + 0.410 \ C_{L_u}$$

$$C_D = C_{D_u} + 0.0071 \ (C_{L_u})^2$$

$$C_m = C_{m_u} + 0.0112 \ C_{L_u} \quad \text{(only with the horizontal tail on)}$$

None of the power-on data (i.e., lift fans driven by the gas generators) was corrected for wind tunnel wall constraints. Corrections have not been applied for the effects of the exposed tips on the model support struts, or for ram drag.

PRESENTATION OF DATA

Static fan performance (i.e., at wind tunnel free stream dynamic pressure of zero q = 0 psf) for the lift/cruise and forward fans is presented in figures 4 through 6. Lift/cruise fan deflector static turning and turning efficiency is presented in figure 7. In figure 8, the variation of jet velocity ratio with wind tunnel velocity is presented for the three fans. The variation of jet velocity ratio with the angle of attack and fan RPM for the cruise configuration is presented in figure 9. Wind-milling characteristics of the lift/cruise fans at various thrust vector angles and for the forward lift fan are presented in figure 10. Variation of ram drag coefficient with angle of attack at several jet velocity ratios for each fan (three fans) is presented in figure 11. The variation of fan thrust with angle of attack at several jet velocity ratios is presented in figure 12.

An index to all the figures presenting the basic aerodynamic data is given in table 2. For ease of presentation, the aerodynamic data have been divided into two parts: namely, powered lift and cruise. The longitudinal aerodynamic characteristics of the model in the powered-lift mode, with the horizontal tail on and off the model, are presented in figures 13 and 14. The effects of rudder deflection on the model longitudinal and lateral characteristics are presented in figure 15. The lateral-directional character-istics of the model are presented in figure 16 and horizontal tail sweeps in figures 17 to 21. The effect of forward fan louver sweeps is presented in figures 22 to 24. Other data such as the effect of forward fan RPM, sideslip angle, and aileron effectiveness, are presented in figures 25, 26, and 27 respectively.

The effects of tail incidence on the cruise mode longitudinal charac-teristics are presented in figure 28. Longitudinal characteristics for the

cruise mode with the horizontal tail on and with the tail off, are presented in figures 29 to 33. The data presented also include the effect of lift/cruise fan speed, differential aileron, and horizontal tail incidence (figures 34-37).

REFERENCES

1. Design Definition Study of a Lift/Cruise Fan Technology V/STOL Aircraft -
   Vol. I. V/STOL Aircraft Advanced Engineering, McDonnell Aircraft Co.,
   June 1975, NASA CR-137678.

2. Zabinsky, J. M.; and Higgins, H.C.: Design Definition Study of a Lift/
   Cruise Fan Technology V/STOL Airplane - Summary. Boeing Commercial
   Airplane Company, August 15, 1975, NASA CR-137749.

3. Atencio, Adolph, Jr., Hall, Leo P.; and Kirk, Jerry V.: Low Speed Wind
   Tunnel Investigation of a Large-Scale Lift Fan STOL Transport Model.
   NASA TM X-62,231, 1973.

TABLE I

LARGE SCALE LIFT/CRUISE FAN AIRCRAFT MODEL

AIRFOIL ORDINATES

STATION	EXPOSED ROOT (0.221η) NACA 4416		WING STATION (0.442η) MODIFIED, SUPERCRITICAL, t = 14%c		THEORETICAL TIP (0.941η) MODIFIED, SUPERCRITICAL, t = 8%c	
X, % CHORD	Y_U, %c	Y_L, %c	Y_U, %c	Y_L, %c	Y_U, %c	Y_L, %c
0	0.	0.	0.	0.	0.	0.
1.25	3.275	-1.909	2.471	-2.467	1.422	-1.435
2.5	4.448	-2.645	3.233	-3.218	1.836	-1.840
5.0	6.123	-3.486	4.126	-4.069	2.307	-2.334
7.5	7.371	-3.957	4.729	-4.653	2.641	-2.678
10.0	8.363	-4.245	5.208	-5.099	2.902	-2.944
15.0	9.888	-4.459	5.945	-5.756	3.293	-3.335
20.0	10.933	-4.427	6.481	-6.177	3.569	-3.598
25.0	11.648	-4.245	6.878	-6.433	3.768	-3.766
30.0	12.000	-4.000	7.165	-6.560	3.904	-3.682
40.0	12.000	-3.467	7.478	-6.435	4.029	-3.837
50.0	11.232	-2.901	7.494	-5.753	3.988	-3.531
60.0	9.920	-2.283	7.229	-4.503	3.788	-2.766
70.0	8.139	-1.653	6.662	-2.786	3.420	-1.465
80.0	5.920	-1.099	5.685	-1.091	2.829	-0.084
90.0	3.285	-0.608	3.980	-0.194	1.843	+0.496
95.0	1.781	-0.384	2.616	-0.210	1.090	+0.342
100.0	0.171	-0.171	0.496	-0.447	0.108	-0.214
L.E. RADIUS, % c	2.822		3.041		1.154	
CHORD LENGTH, $\frac{m}{(F_t)}$	2.409 (8.231)		2.049 (6.723)		0.891 (2.922)	
INCIDENCE, DEG.	3.23		2.49		-2.77	

8

TABLE 2 – LIST OF BASIC DATA FIGURES

Run No.	Figure	q (psf)	q (N/m²)	α_u, deg.	δ_f, deg.	δ_{ail}, deg.	δ_{cn}, deg.	i_t, deg.	β_v, deg.	β, deg.	Fan RPM/$\sqrt{\theta}$ Fwd. Fan	Fan RPM/$\sqrt{\theta}$ Wing Fans	δ_R, deg.	Remarks
46	13(a)	3.34	159.9	−4 to 20	15	10	90	OFF	90	0	3609	3609	0	Longitudinal Data
48		7.15	342.3								3578	3578		
49		7.17	343.3								Wind Mill	Wind Mill		
45	13(b)	1.33	63.7	−4 to 32							3607	3607		
51	13(c)	3.29	157.5	−4 to 20			56		43		3633	3633		
53		7.20	344.7								3629	3629		
54		12.34	590.8								3623	3623		
56		19.24	921.2								Wind Mill	Wind Mill		
60	13(d)	7.11	340.4				23				3612	3612		
61		12.30	588.9								3625	3625		
62		19.26	922.2								3617	3617		
63		19.23	920.7								Wind Mill	Wind Mill		
34	14(a)	3.27	156.6				90	0	90		3606	3606		
36		7.13	341.4								3631	3631		
32		7.17	343.3								Wind Mill	Wind Mill		
31	14(b)	1.33	63.7								3597	3597		
115	14(c)	3.33	159.4				71		55		3630	3630		
		7.71	346.2								3612	3612		
114	14(d)	1.4.	67.5	0,8,16							3624	3624		
98	14(e)	3.31	158.5	−4			56		43		3623	3623		
82				0										
90				8										
99				12										
94				16										
98		7.10	339.9	−4							3626	3626		
83				0										
91				8										
99				12										
95				16										

TABLE 2 - LIST OF BASIC DATA FIGURES - CONTINUED

Run No.	Figure	q		α_u deg.	δ_f, deg.	δ_{ail}, deg.	δ_{cn}, deg.	i_t, deg.	β_v, deg.	β, deg.	Fan RPM/$\sqrt{\theta}$		δ_R, deg.	Remarks
		psf	N/m^2								Pod. Fan	Wing Fans		
98	14(e)	12.34	590.8	-4	15	10	56	0	43	0	3627	3627	0	Longitudinal Data
88				0										
92				8										
99				12										
96				16										
100		12.35	591.3	12							Wind Mill	Wind Mill		
97				16										
107	14(f)	7.13	341.4	-4 to 20			38				3627	3627		
103		12.34	590.8								3628	3628		
105		19.23	920.7								3626	3626		
109		19.26	922.2								Wind Mill	Wind Mill		
65	14(g)	7.18	343.8				23				3615	3615		
66		12.31	589.4								3624	3624		
68		19.18	918.3								3617	3617		
67		19.24	921.2								Wind Mill	Wind Mill		
111	15(a)	7.11	340.4				38				3626	3626	23	
111		12.32	589.9								3640	3640		
111	15(b)	7.11	340.4								3626	626		Lateral Data
111		12.32	589.9								3640	3640		
38	16(a)	1.37	65.6	0			90		90	4 to -12	3603	3603	0	Lateral-directional Data
41		3.31	158.5								3622	3622		
42		7.16	342.8								3636	3636		
44		6.97	333.7								Wind Mill	Wind Mill		
76	16(b)	3.32	159.0				56		43	4 to -20	3619	3619		
77		7.02	336.1								3627	3627		
78		12.26	587.0								3619	3619		
79		12.35	591.3								Wind Mill	Wind Mill		

TABLE 2 – LIST OF BASIC DATA FIGURES – CONTINUED

Run No.	Figure	q		α_u, deg.	δ_f, deg.	δ_{ail}, deg.	δ_{cn}, deg.	i_t, deg.	β_v, deg.	β, deg.	Fan RPM/$\sqrt{\theta}$		δ_R, deg.	Remarks
		psf	N/m²								Fwd. Fan	Wing Fans		
80	16(c)	3.19	152.7	8	15	10	56	0	43	4 to -17	3626	3626	0	Lateral-directional
		7.05	337.6								3629	3629		Data
		12.29	588.4								3626	3626		
81		12.33	590.4								Wind Mill	Wind Mill		
72	16(d)	12.36	591.8	0				23			3620	3620		
70		19.34	926.0								3615	3615		
75		19.25	921.7								Wind Mill	Wind Mill		
34	17(a)	3.26	156.1				90	0	90	0	3611	3611		Tail Sweeps
43		3.26	156.1					-10,10,20			3611	3611		
39		7.16	342.8					-20 to 20			3628	3628		
44		6.98	334.2					-20,-10, 10,20			Wind Mill	Wind Mill		
40	17(b)	1.39	66.6					-20 to 20			3612	3612		
34	17(c)	3.19	152.7	8				0			3612	3612		
43		3.19	152.7					-10,10,20			3612	3612		
36		6.96	333.2					0			3633	3633		
43		6.96	333.2					-10,10,20			3633	3633		
31	17(d)	1.15	55.1					0			3607	3607		
40								-20						
43								10,20						
34	17(e)	3.21	153.7	16							3612	3612		
43								-10,10,20						
36		6.94	332.3					0			3631	3631		
43								-20,-10, 10,20						
31	17(f)	1.20	57.5					0			3610	3610		
43								10,20						

11

TABLE 2 - LIST OF BASIC DATA FIGURES - CONTINUED

Run No.	Figure	q psf	q N/m²	α_u, deg.	δ_f, deg.	δ_{ail}, deg.	δ_{cn}, deg.	i_t, deg.	β_v, deg.	β, deg.	Fan RPM/√θ Fwd. Fan	Fan RPM/√θ Wing Fans	δ_R, deg.	Remarks
114	18	3.34	159.9	0	15	10	71	-10,10,20	55	0	3631	3631	0	Tail Sweeps
115		↓	↓		↓	↓	↓	0	↓		↓	↓		
82	19(a)	3.31	158.5				56	-10 to 20	43		3618	3618		
83		7.16	342.8					↓			3644	3644		
88		12.43	595.2					-20 to 20			3626	3626		
87		12.36	591.8	↓			↓	-10 to 20			Wind Mill	Wind Mill		
90	19(b)	3.38	161.8	8							3617	3617		
91		7.12	340.9								3610	3610		
92		12.31	389.4								3618	3618		
93		12.34	590.8								Wind Mill	Wind Mill		
		19.10	'4.5	↓										
94	19(c)	3.29	157.5	16							3618	3618		
95		7.12	340.9								3629	3629		
96		12.28	588.0								3632	3632		
97		12.28	588.0	↓			↓	↓			Wind Mill	Wind Mill		
108	20	7.20	344.7	0			38	-10 to 20			3627	3627		
104		12.37	592.3				↓	↓			3613	3613		
106		19.30	924.1								3626	3626		
64	21(a)	3.21	153.7				23	0,10			3629	3629		
73		7.05	337.6					-20 to 20			3610	3610		
71		12.28	588.0					↓			3619	3619		
69		19.27	922.7								3629	3629		
74		19.23	920.7	↓				↓			Wind Mill	Wind Mill		
73	21(b)	7.03	336.6	8				-10 to 20			3613	3613		
71		12.24	586.1					↓			3616	3616		
69		19.22	920.3					-10 to 10			3627	3627		
67		19.18	918.3	↓				0			Wind Mill	Wind Mill		
74					↓	↓	↓	-10,10	↓	↓			↓	

TABLE 2 - LIST OF BASIC DATA FIGURES - CONTINUED

Run No.	Figure	q psf	q N/m²	α_u, deg.	δ_f, deg.	δ_{ail}, deg.	δ_{cn}, deg.	i_t, deg.	β_v, deg.	β, deg.	Fan RPM/√θ Fwd. Fan	Fan RPM/√θ Wing Fans	δ_R, deg.	Remarks
65	21(c)	6.98	334.2	16	15	10	23	0	43	0	3617	3617	0	Tail Sweeps
73								-10,10						
66		12.16	582.2					0			3622	3622		
71								-10,10						
68		19.14	916.4					0			3616	3616		
69								-10,10						
67		19.23	920.7					0			Wind Mill	Wind Mill		
74								-10,10						
45	22(a)	1.35	64.6	0			90	OFF	70,80,100		3611	3611		Forward Fan Louver Sweeps
47		3.35	160.4								3594	3594		
46									90					
47		7.16	342.8						70,80,100		3586	3586		
48									90					
33	22(b)	1.35	64.6					0	70,80,100		3600	3600		
31									90					
35		3.30	158.0						70,80,100		3604	3604		
34									90					
37		7.14	341.9						70,80,100		3624	3624		
36									90					
19	23(a)	1.39	66.6				0	OFF	50,70,90		3608	3608		
19		5.53	264.8						35 to 90		3616	3616		
19		10.77	515.7						50 to 90		3622	3622		
20		21.92	1049.5								3640	3640		
20		34.25	1639.9								3630	3630		
21	23(b)	1.38	66.1	8							3617	3617		
21		12.28	588.0								3614	3614		
22	24	1.39	66.6	0							3606	Wind Mill		
22		5.54	265.3								3633			
22		12.22	585.1								3607			

13

TABLE 2 - LIST OF BASIC DATA FIGURES - CONTINUED

14

Run No.	Figure	q		α_u, deg.	δ_f, deg.	δ_{ail}, deg.	δ_{cn}, deg.	i_t, deg.	β_v, deg.	β, deg.	Fan RPM/$\sqrt{\theta}$		δ_R, deg.	Remarks
		psf	N/m²								Fwd. Fan	Wing Fans		
89	25	19.28	923.1	0	15	10	56	0	43	0	2000 to 3600	3633	0	Forward Fan RPM Sweep
77	26	7.02	336.1							4 to −20	3626	3626		Sideslip
85		7.19	344.3			25/−25				0 to −12	3619	3619		
84	27(a)	7.10	339.9			25/10 to −25/25				0	3619	3619		Aileron Effectiveness
86		12.37	592.3								3636	3636		
84	27(b)	7.10	339.9								3619	3619		
86		12.37	592.3								3636	3636		
119	28(a)	34.19	1637.0	0 to 32	0	0	0	−20	REMOVED	0	COVERED	2727		Cruise Mode Longitudinal Data
121								−10						
116				−4 to 32				0						Forward Fan Inlet and Exit Covered
124				0 to 32				10						
127								20						
120	28(b)							−20				2170		
123								−10						
117				−4 to 32				0						
126				0 to 32				10						
128								20						
118	28(c)			−4 to 32				0				1614		
140	29	34.24	1639.4					OFF				2726		
141				−4 to 20								1615		
134	30(a)			0 to 32				0				2728	23	
135				0 to 16								1617		
135				16 to 32								2182		
134	30(b)			0 to 32								2728		
135				0 to 16								1617		
135				16 to 32								2182		

TABLE 2 - LIST OF BASIC DATA FIGURES - CONTINUED

Run No.	Figure	q (psf)	q (N/m²)	α_u, deg.	δ_f, deg.	δ_{ail}, deg.	δ_{cn}, deg.	i_t, deg.	β_v, deg.	β, deg.	Fan RPM/$\sqrt{\theta}$ Fwd. Fan	Wing Fans	δ_R, deg.	Remarks
133	31(a)	34.24	1639.4	4 to 32	0	0	0	0	REMOVED	8	COVERED	2730	23	Cruise Mode Longitudinal Data
133	31(b)	▽	↓					↓	↓	↓		2730		
27	32	34.19	1637.0	-4 to 32				OFF	0	0		2723	0	
27				-4 to 20								2166		
28												1629		
28		↓	↓	↓								Wind Mill		
27	33	34.16	1635.6	-4 to 32	↓	↓						2723		
26		↓			15	10						2716		
26				0 to 18	↓	↓		↓	↓	↓		Wind Mill		
129	34(a)			0	0	0		0	REMOVED	4 to -12		2723		Sideslip
130				8								↓		Forward Fan Inlet
131				16										and Exit Covered
129	34(b)			0								1614		
130				8								↓		
131		↓	↓	16		↓				↓		↓		
138	35(a)	34.22	1638.4	8 to 32		25/25				0		2721		Forward Fan Inlet
139				16 to 32								2184		and Exit Covered
139				8 to 16								1621		
138	35(b)			8 to 32								2721		
139				16 to 32								2184		
139		↓	↓	8 to 16		↓						1621		
137	3f(a)	34.2	1638.0	0		25/-25 to -25/25						1610		Differential Aileron Forward Fan Inlet and Exit Covered
136												2709		
137	36(b)	↓	↓	↓	↓	↓	↓	↓	↓	↓	↓	1610	↓	
136												2709		

15

TABLE 2 - LIST OF BASIC DATA FIGURES - CONCLUDED

Run No.	Figure	q		α_u, deg.	δ_f, deg.	δ_{ail}, deg.	δ_{cn}, deg.	i_t, deg.	β_v, deg.	β, deg.	Fan RPM/$\sqrt{\theta}$		δ_R, deg.	Remarks
		psf	N/m^2								Fwd. Fan	Wing Fans		
119	37(a)	34.17	1636.1	0	0	C	0	-20	REMOVED	0	COVERED	2722	0	Tailsweeps
121								-10						Forward Fan Inlet
116								0						and Exit Covered
124								10						
127								20						
120		34.21	1638.0					-20				2164		
123								-10						
117								0						
126								10						
128								20						
118		34.23	1638.9					0				1592		
135	37(b)	34.22	1638.5					-10 to 10				1615	23	
134		34.25	1639.9									2721		
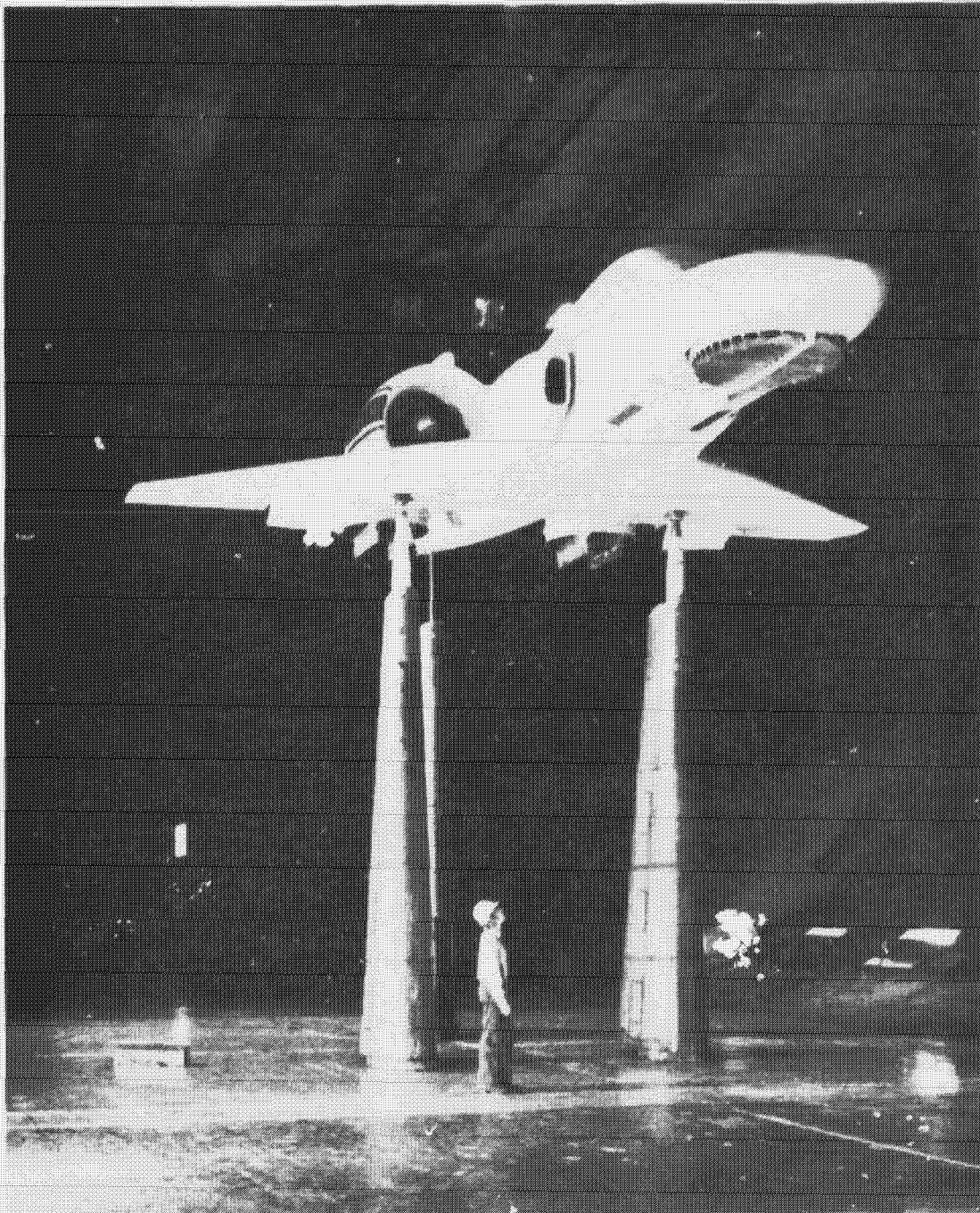
(a) 3/4 front view.

Figure 1.- Photograph of the model mounted in the Ames 40- by 80-foot wind tunnel.

17
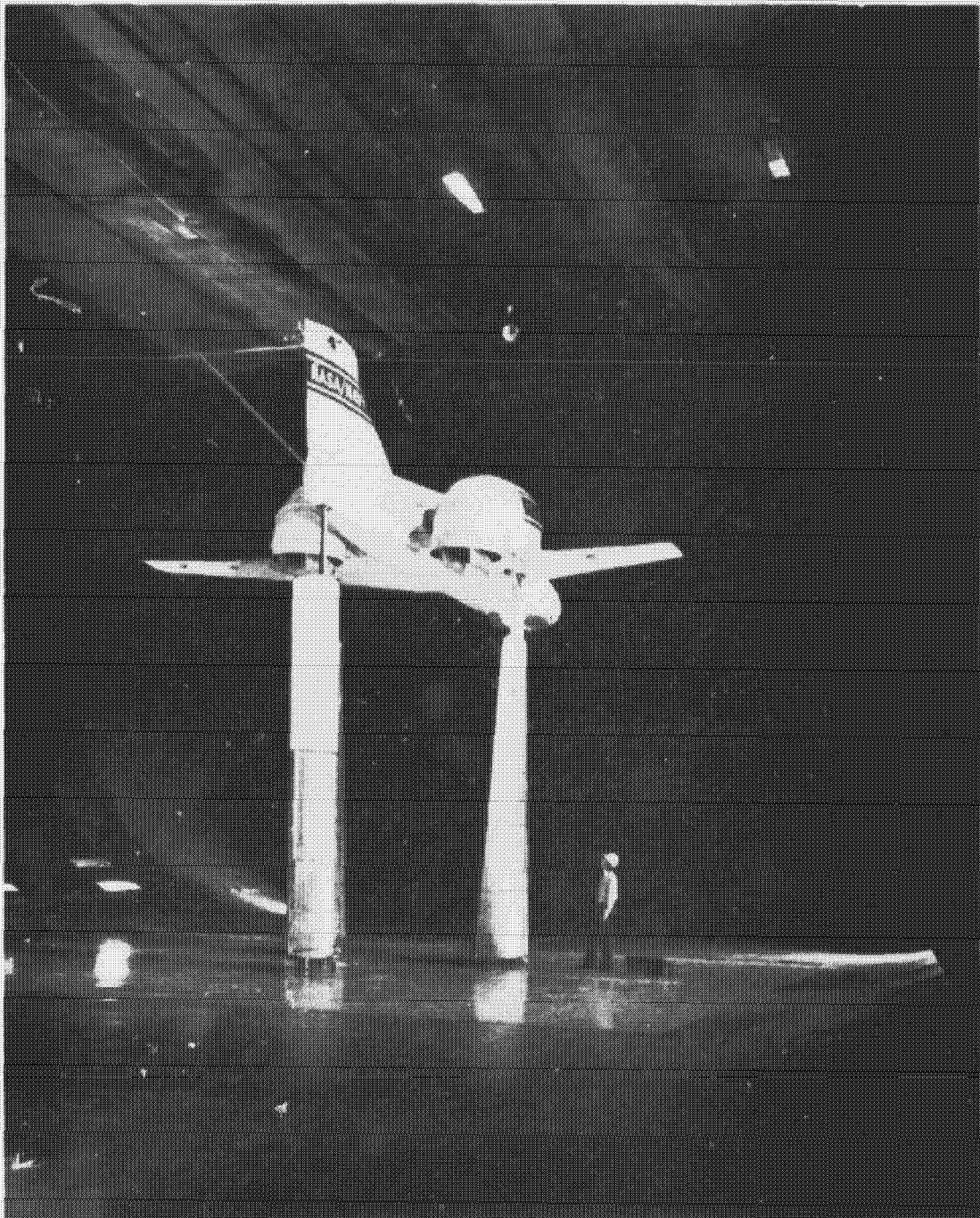
(b) 3/4 rear view.

Figure 1.- Concluded.

19

	WING	HORIZONTAL TAIL	VERTICAL TAIL
AREA, m^2 (FT²)	16.572 (180.32)	4.006 (43.12)	3.096 (33.32)
ASPECT RATIO	4.600	3.665	0.688
TAPER RATIO	0.300	0.405	0.433
b, m (FT.)	8.682 (28.49)	3.832 (12.57)	1.459 (4.787)
C_{ROOT}, m (FT.)	2.968 (9.738)	1.488 (4.882)	2.960 (9.711)
C_{TIP}, m (FT.)	0.890 (2.920)	0.603 (1.978)	1.282 (4.206)
$\bar{c}$, m (FT.)	2.116 (6.942)	1.108 (3.635)	2.232 (7.323)
Λ c/4	25.00°	26.02°	45.50°
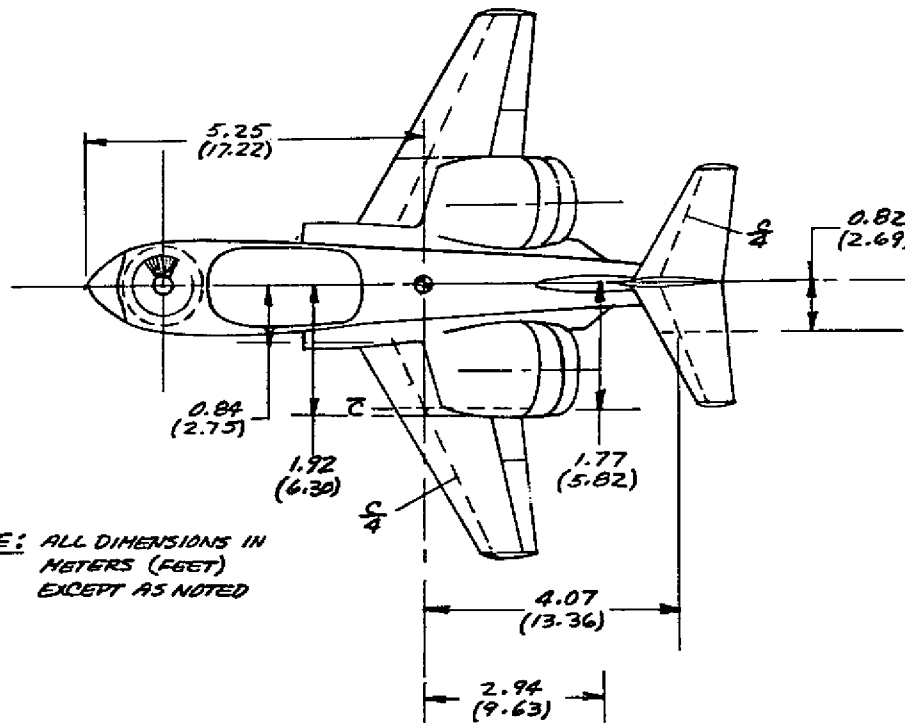
NOTE: ALL DIMENSIONS IN
METERS (FEET)
EXCEPT AS NOTED

5.25 (17.22)
0.82 (2.69)
0.84 (2.75)
1.92 (6.30)
1.77 (5.82)
4.07 (13.36)
2.94 (9.63)

1.30 (4.27)

0.26 (0.84)
0.13 (0.44)
2.28 (7.49)
0.50 (1.64)
9.76 (32.03)
15°
7°
FUSELAGE STATION 0 (0)
1.25 (4.10)
3.41 (11.20)
5.42 (17.78)
10.31 (33.83)
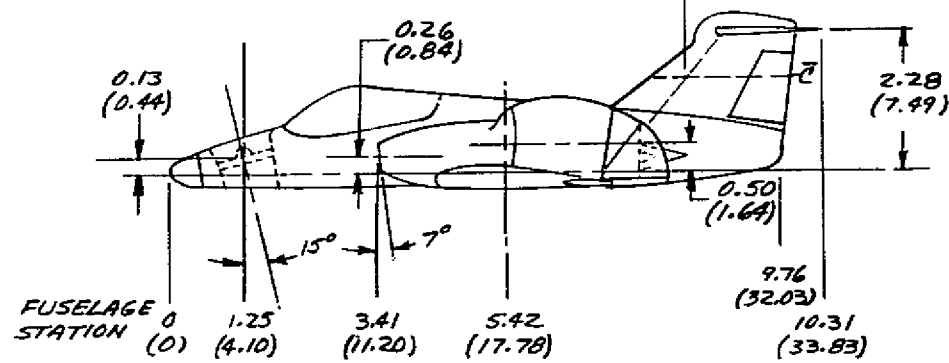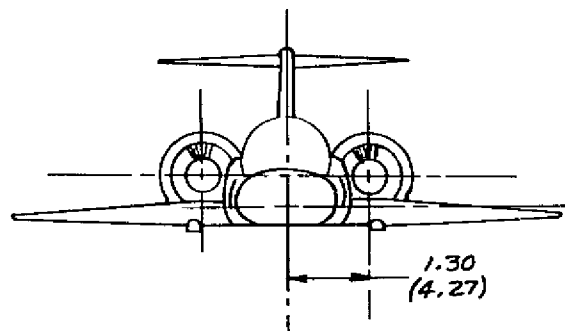
(a) Overall dimensions and geometry.

Figure 2.- Geometric details of the model.

0.5715
(1.875)R

0.656 R
(2.15)

15°

X 376
FAN

LOUVERS

YAW VANES
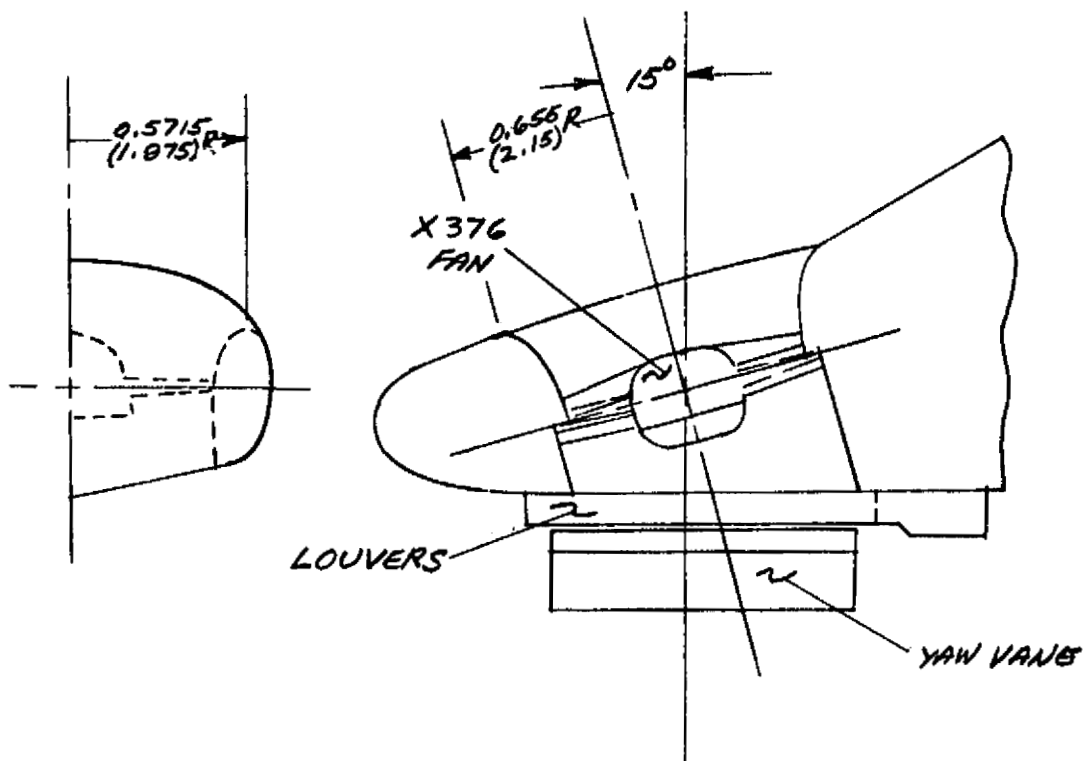
DIMENSIONS IN METERS (FEET)
EXCEPT AS NOTED

(b) Forward fan details.

Figure 2.- Concluded

20

0°

0° 23°

0° 38°

0°

0.0762
(0.25)

56°

0.2286
(0.75)

0.18
(0.58)

0.894
(2.93)

0°

71°

EXIT
NOZZLE

YAW VANE

0°

X376
FAN
DIA.
0.91
(3.00)

DIMENSIONS IN METERS
(FEET)
EXCEPT AS NOTED

90°
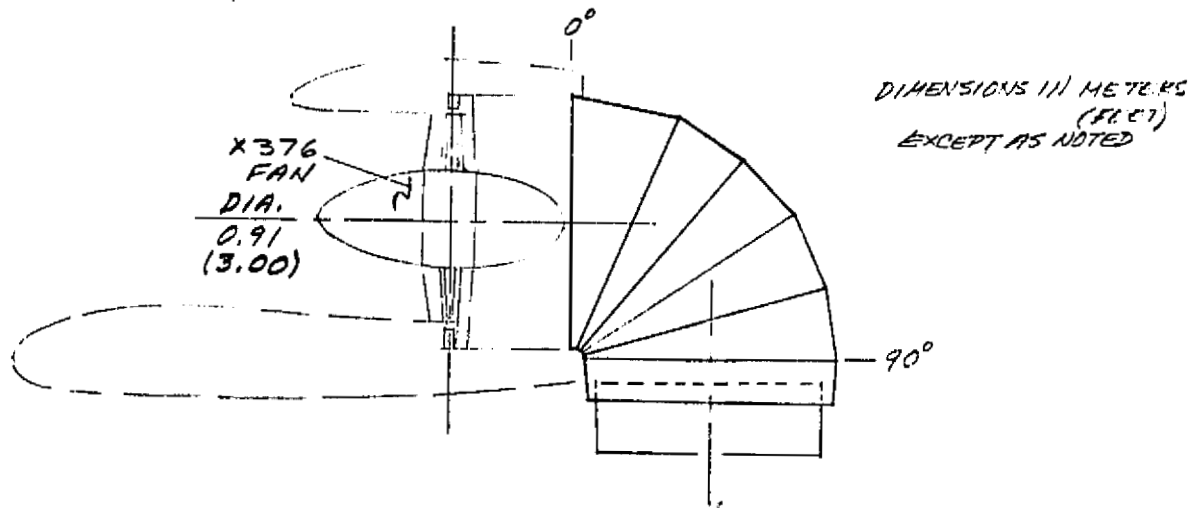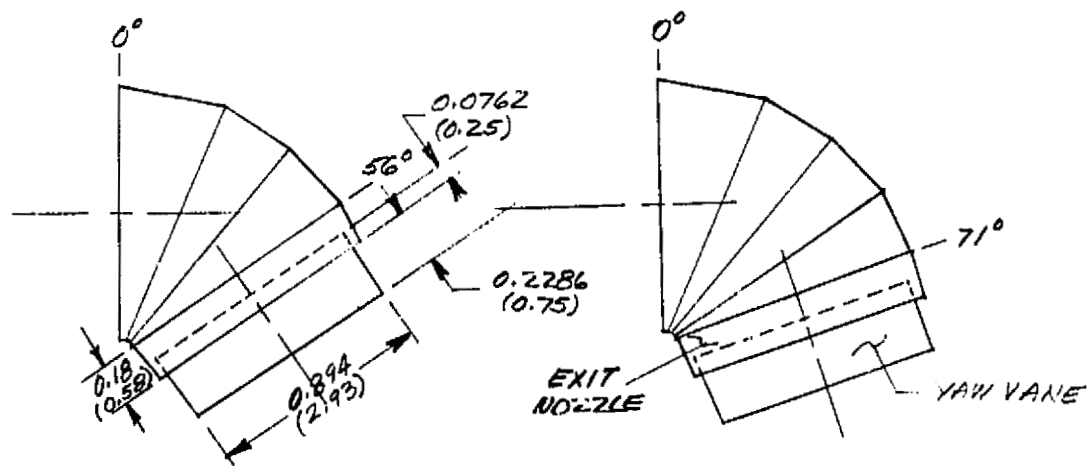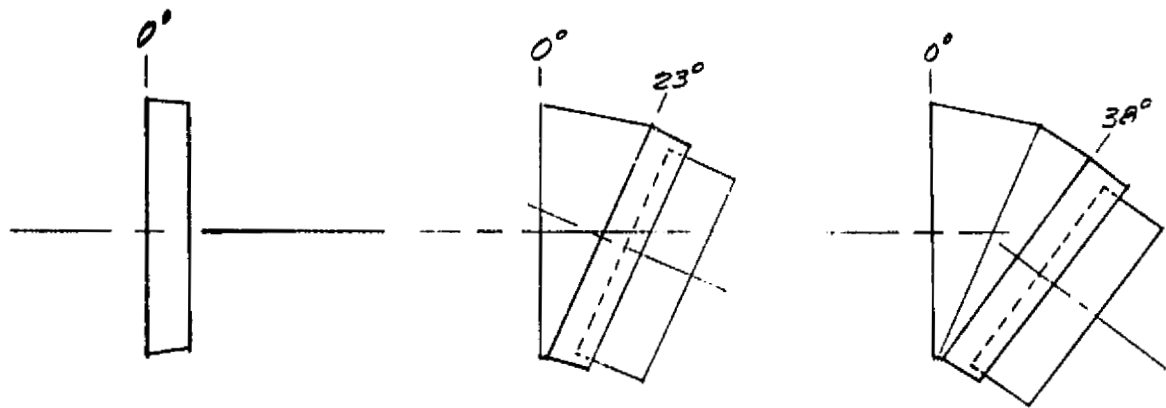
(c) Lift/cruise fan details.

Figure 2.- Continued.

21

L/C FAN
INLET

T58 GAS
GENERATOR

LIFT FAN
INLET

LIFT FAN
VECTORING
LOUVERS

AUXILIARY INLET
FOR THIRD ENGINE

L/C VECTORING
NOZZLE

X376
TURBO-TIP FAN
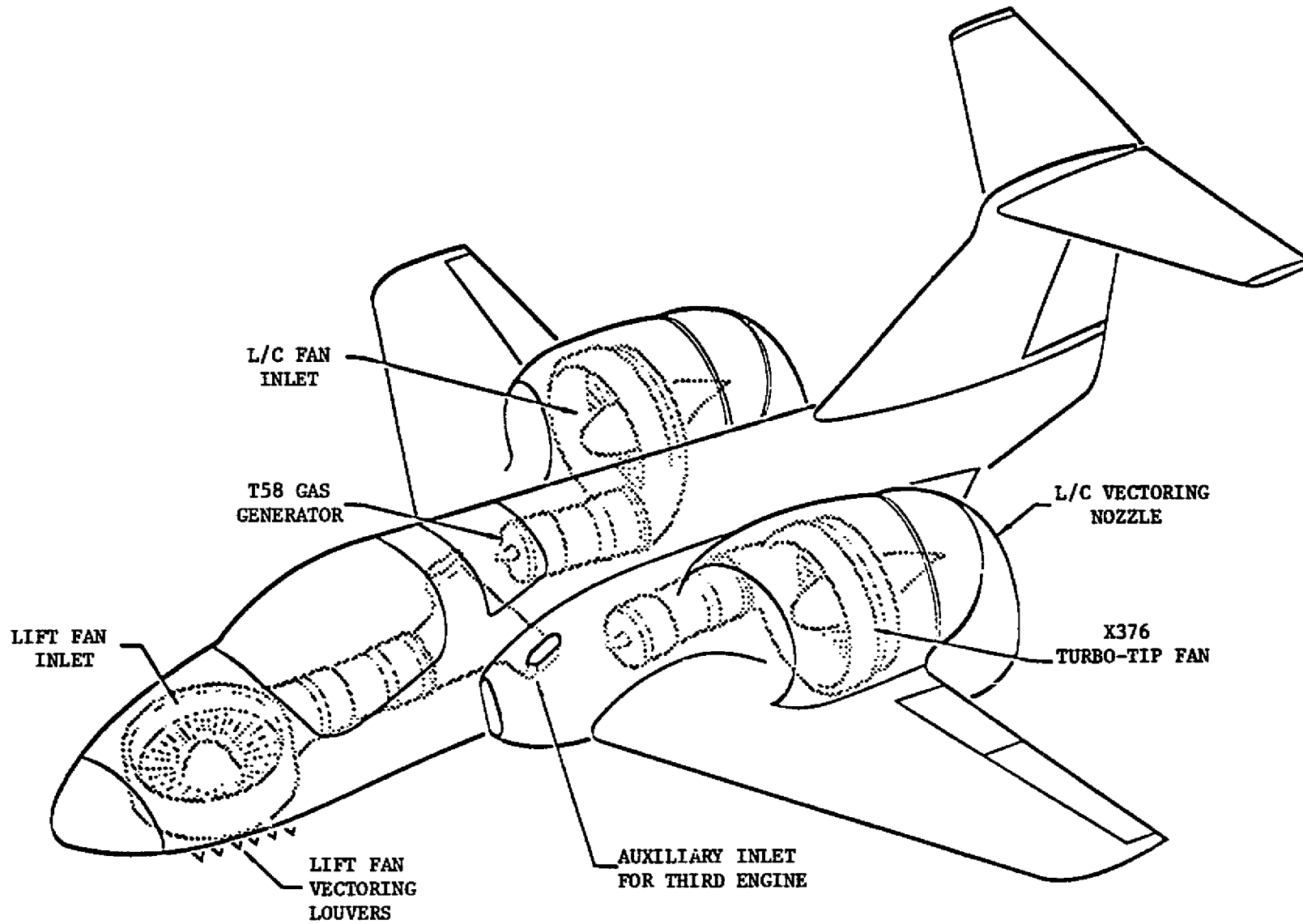
Figure 3.- Schematic of the model showing gas generator and turbo-tip fan
relationship.
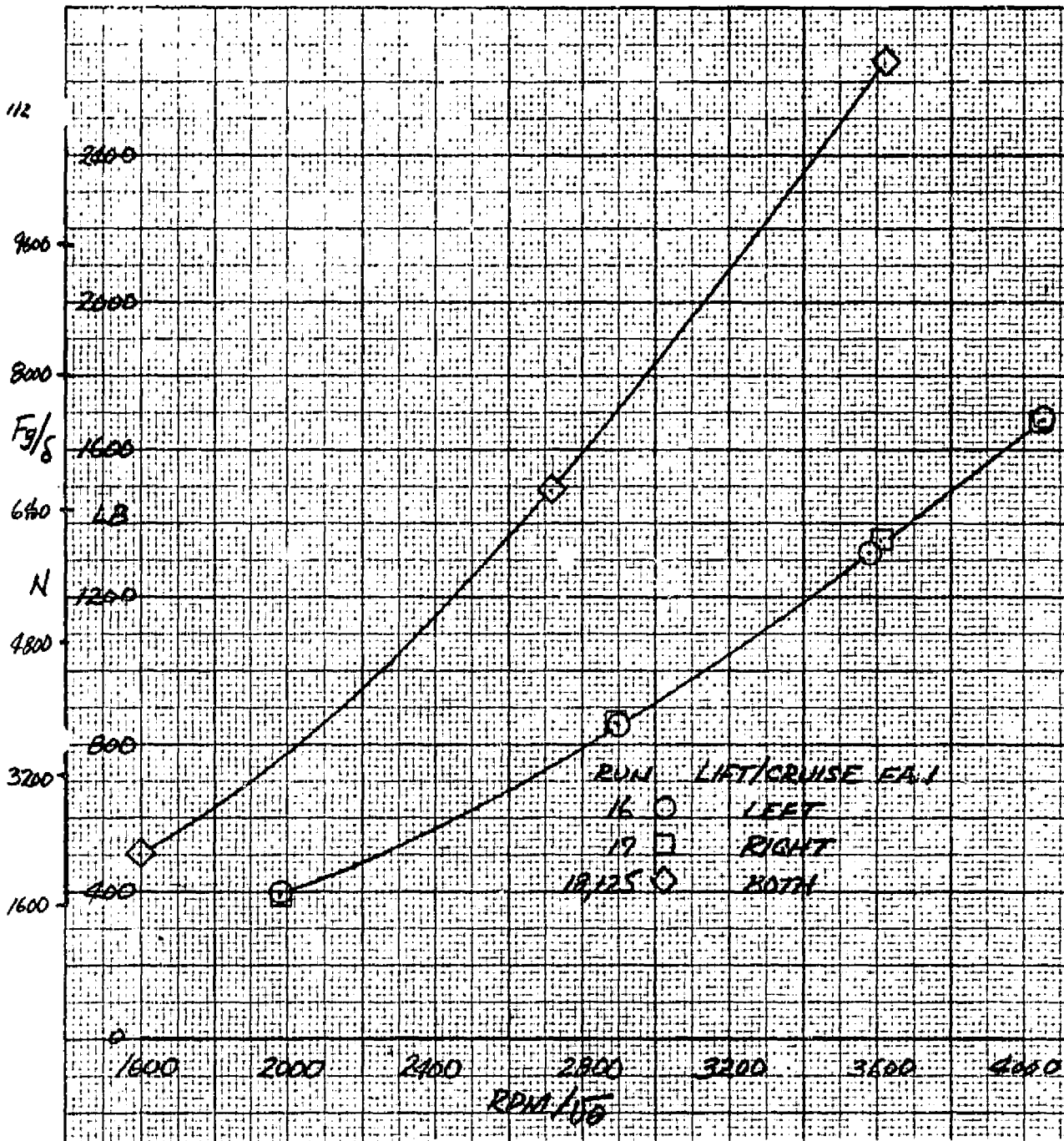
Figure 4.- Variation of static thrust with lift/cruise fan RPM; $\delta_{cn} = 0°$, $\alpha_u = 0°$, $q = 0$ N/m^2(psf).
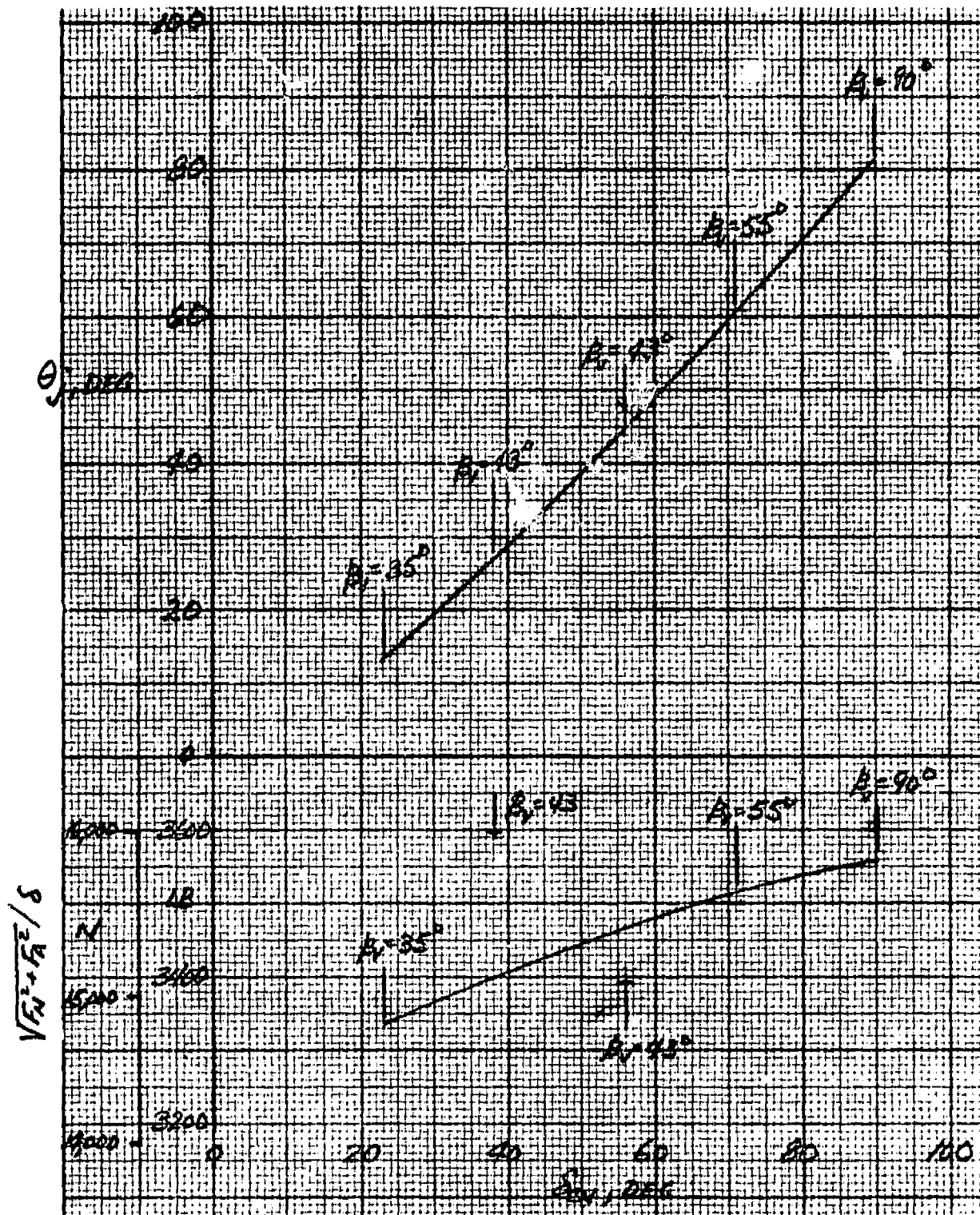
Figure 5.- Resultant static thrust and static turning angle with combined lift/cruise fan and forward fan operation; RPM/$\sqrt{\theta}$ = 3600, α_u = 0°, q = 0 N/m^2)psf).

24
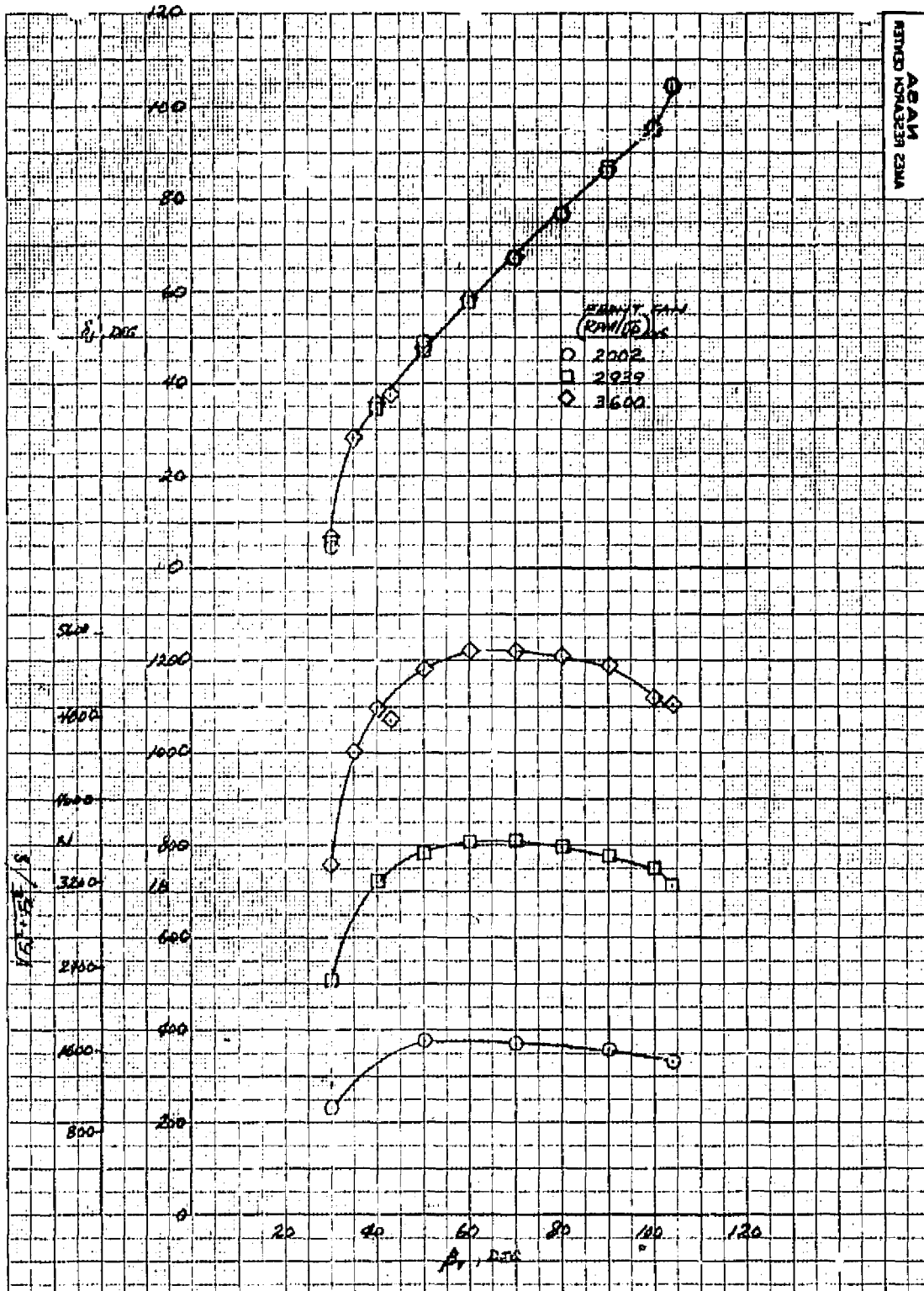
Figure 6.- Variation of resultant static thrust and static turning angle with β_v; $\alpha_u = 0°$, q = 0 psf.
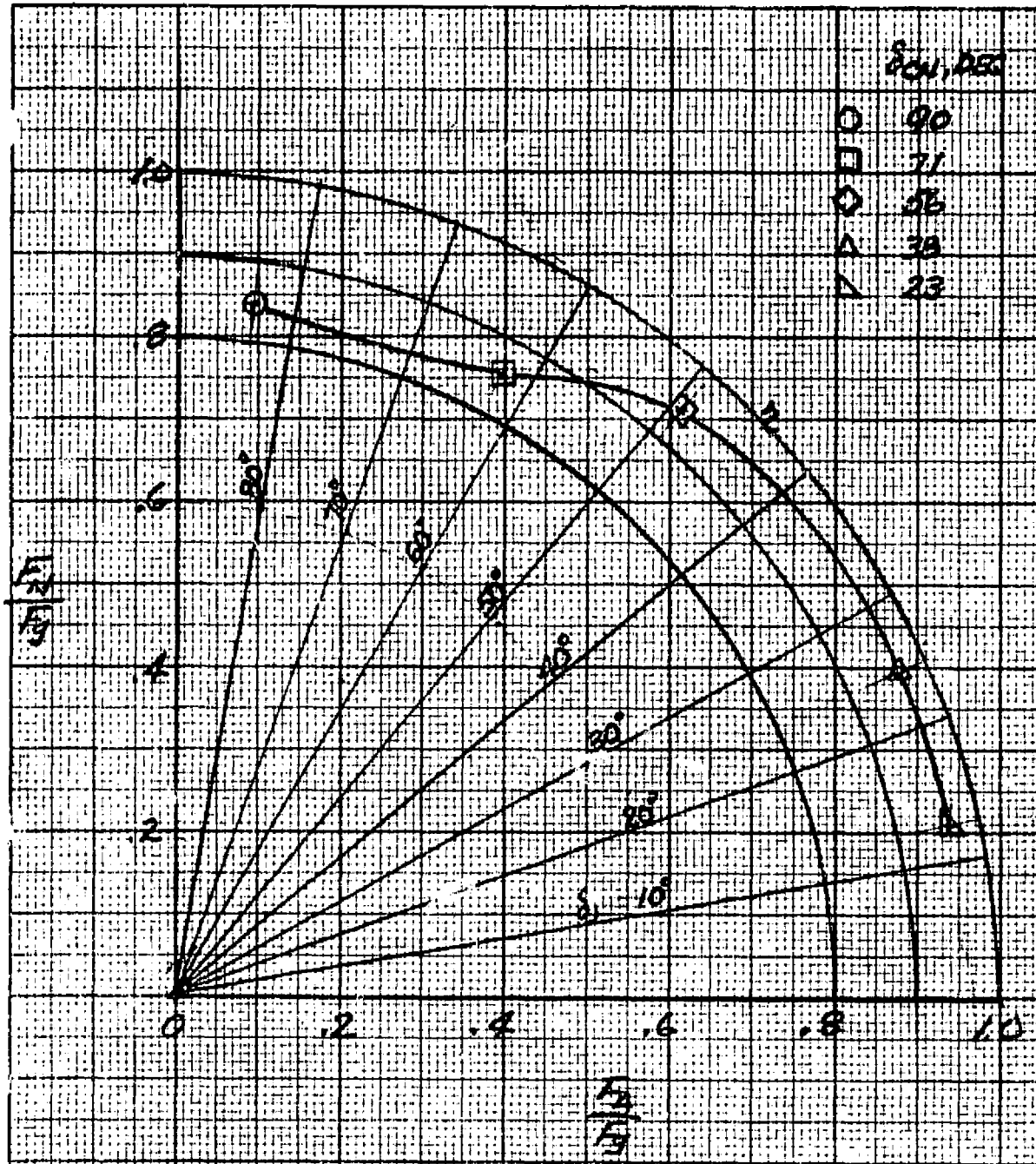
Figure 7.- Lift/cruise fan deflector static turning angle and turning
efficiency; $\alpha_u = 0°$.
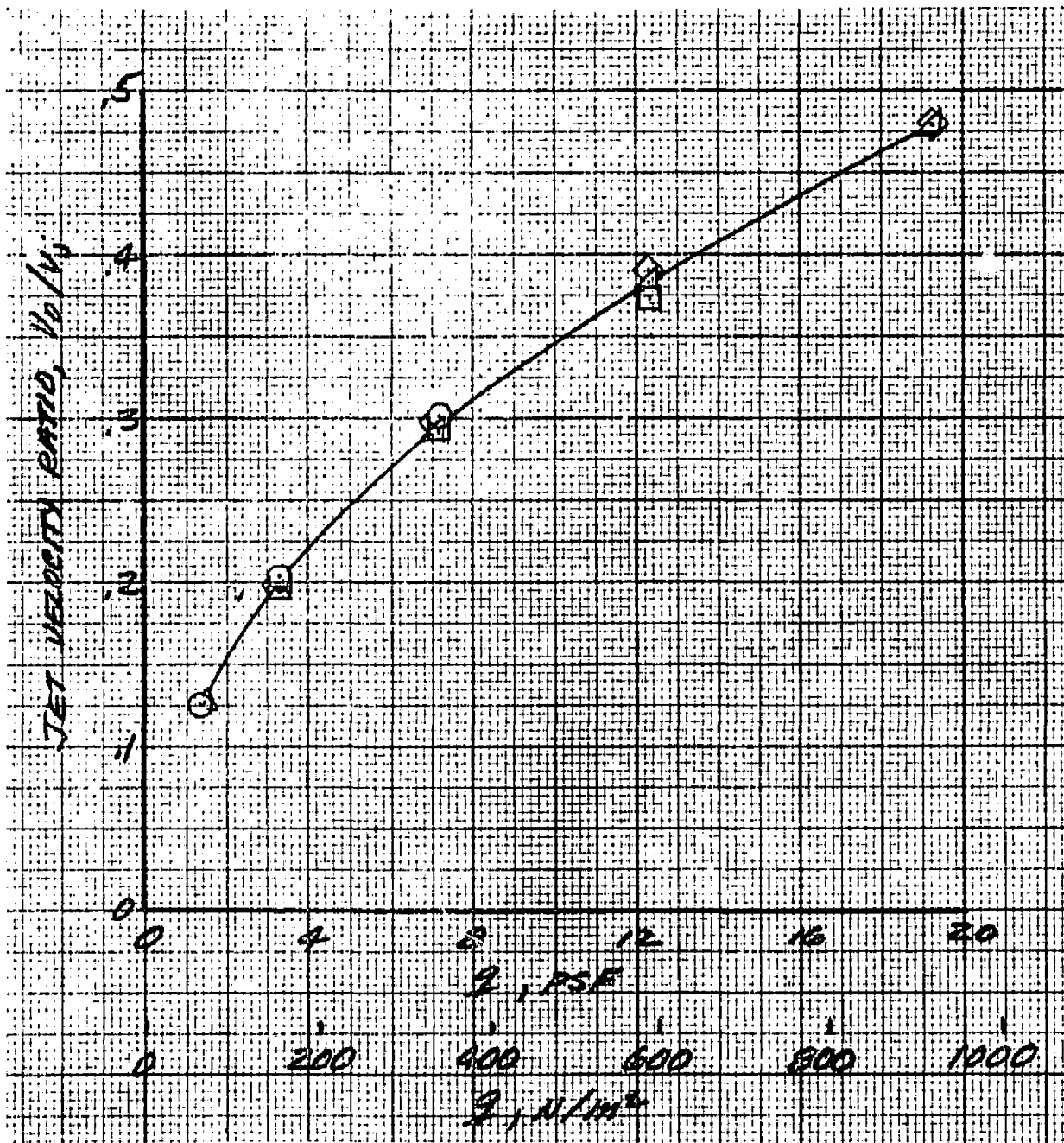
(a) Forward lift fan.

Figure 8.- The variation of jet velocity ratio with wind tunnel dynamic
pressure for the powered lift model configuration; nominal fan
RPM/$\sqrt{6}$ = 3600.
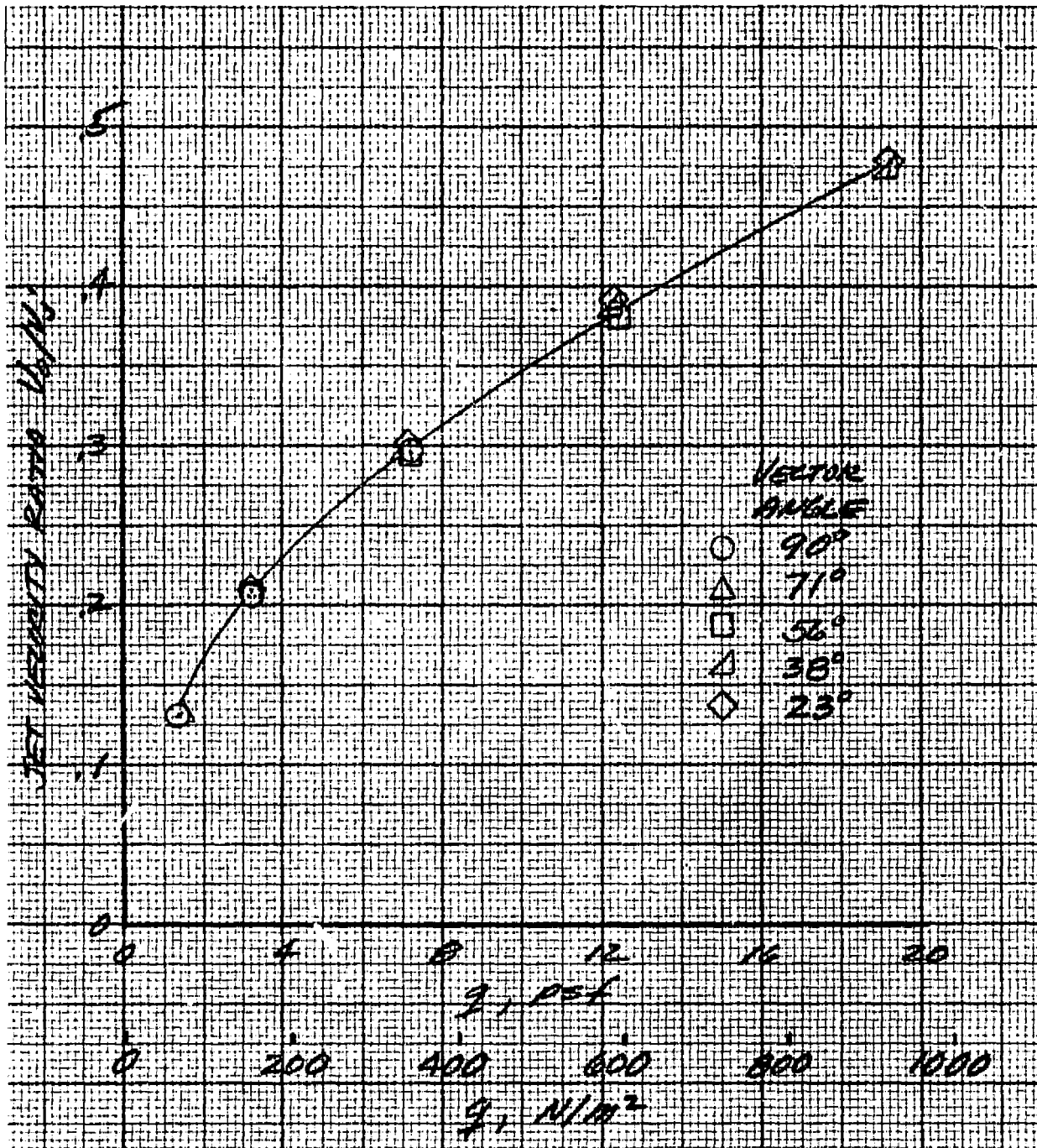
(b) L/H lift/cruise fan.

Figure 8.- Continued.
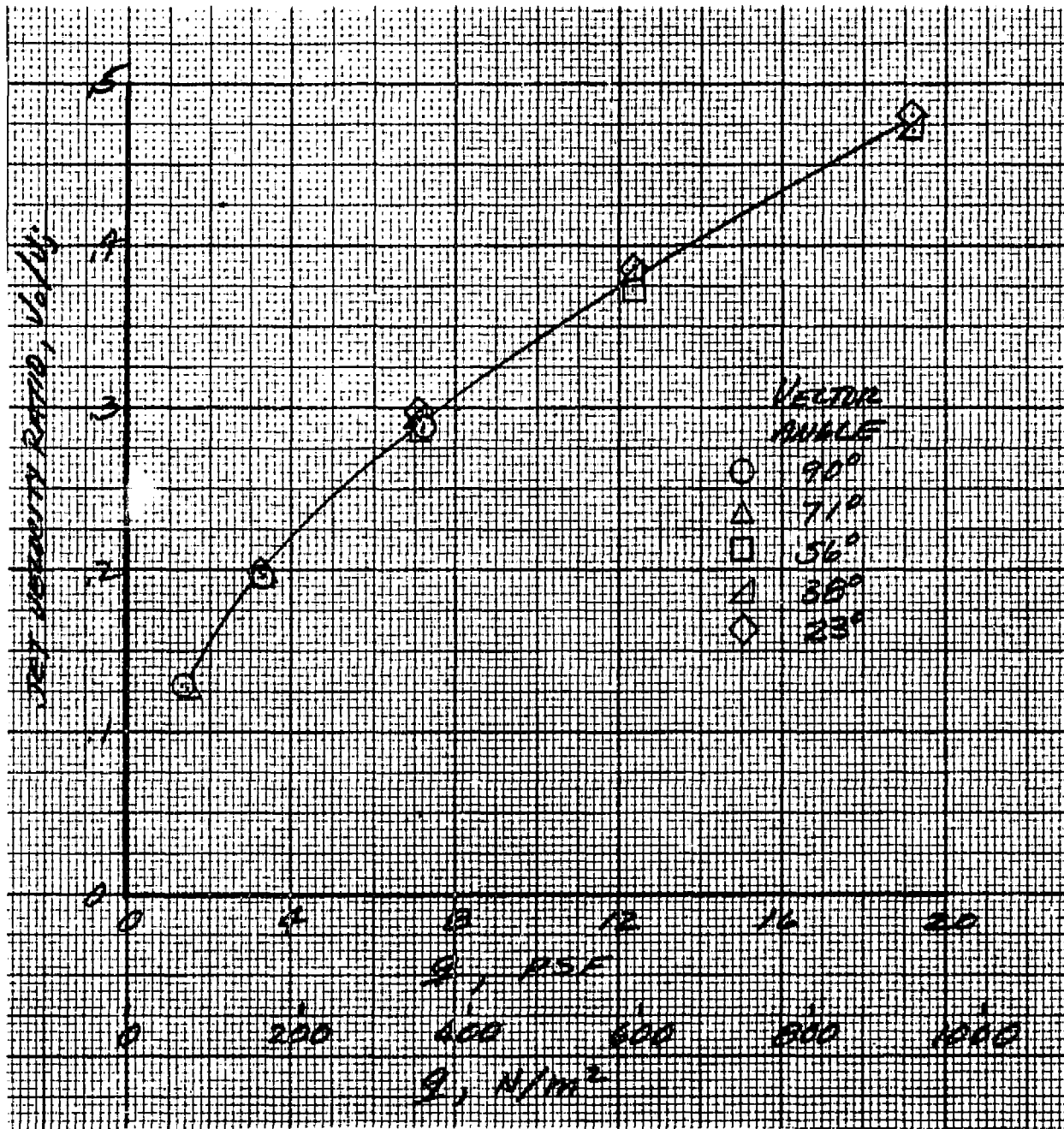
(c) R/H/ lift/cruise fan.

Figure 8.- Concluded.
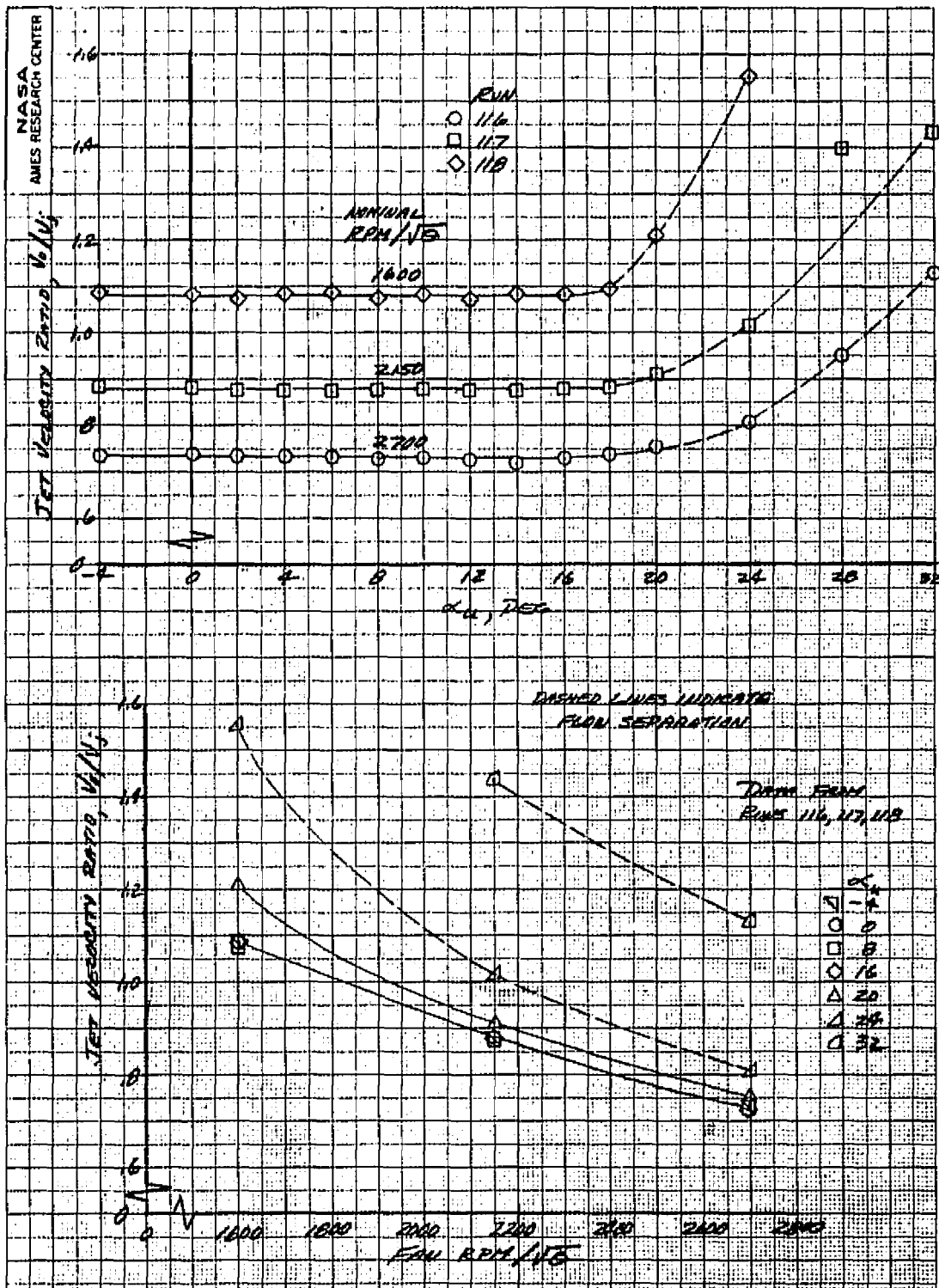
(a) L/H lift/cruise fan.

Figure 9.- Variation of jet velocity ratio with corrected fan RPM and model
angle of attack, cruise configuration, nominal q = 1699.7 N/m^2(35.5 psf),
β = 0°, δ$_{ail}$ = 0°, δ$_f$ = 0°.

30
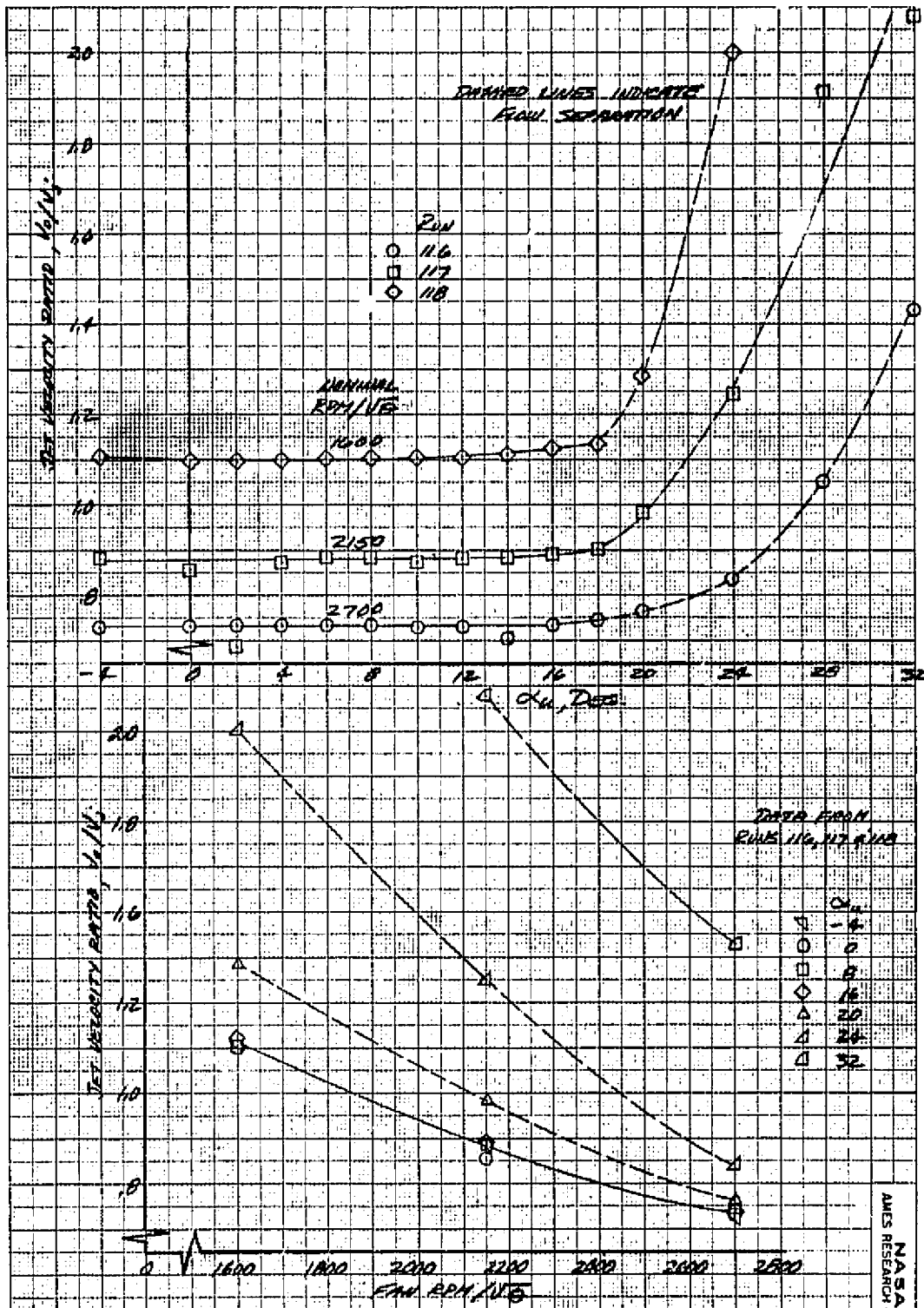
(b) R/H lift/cruise fan.

Figure 9.- Concluded.
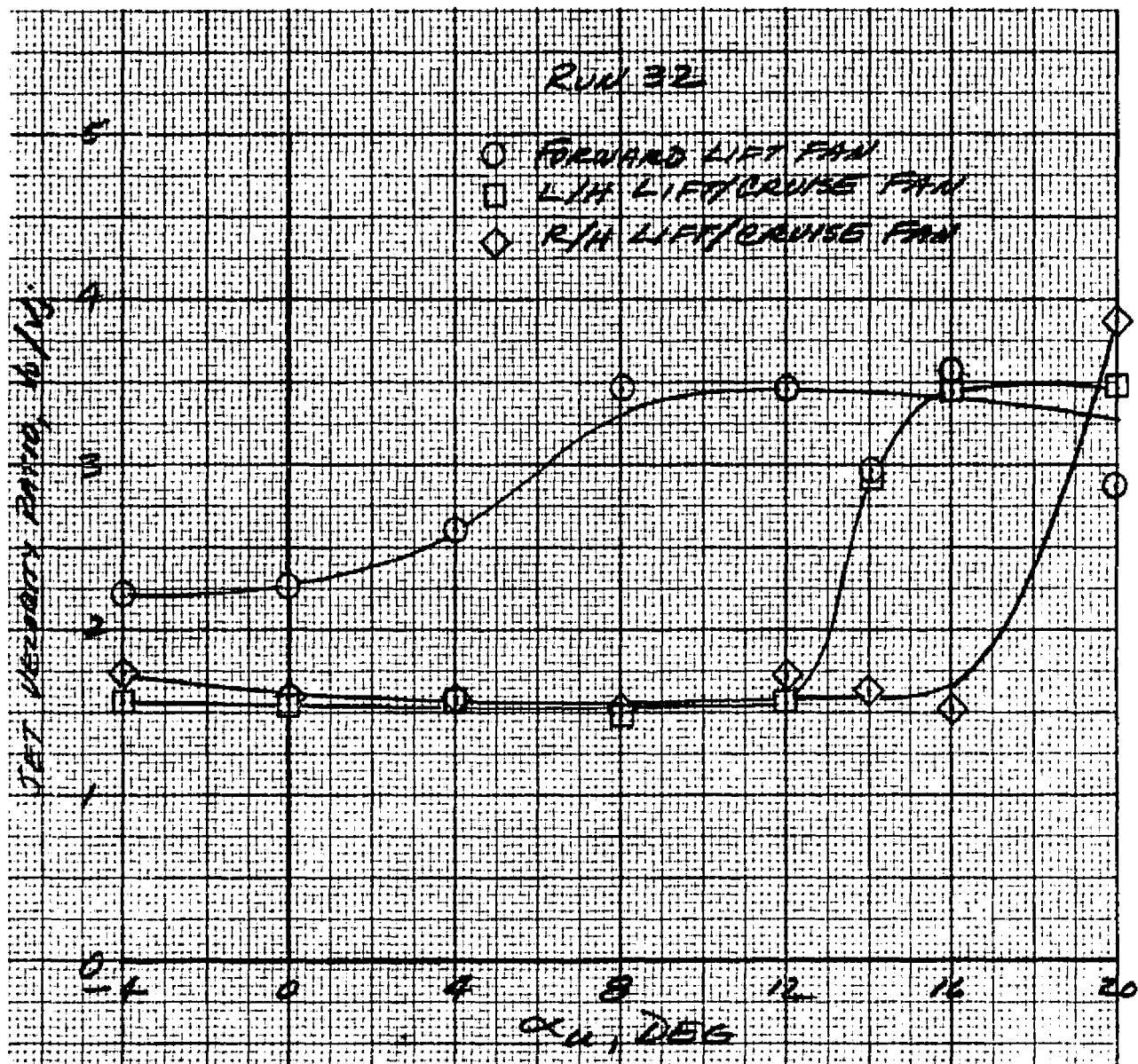
(a) $\delta_{cn} = 90°$, $\beta_v = 90°$, nominal q = 349.5 N/m^2(7.3 psf).

Figure 10.- Wind milling characterisitcs of the model fans.
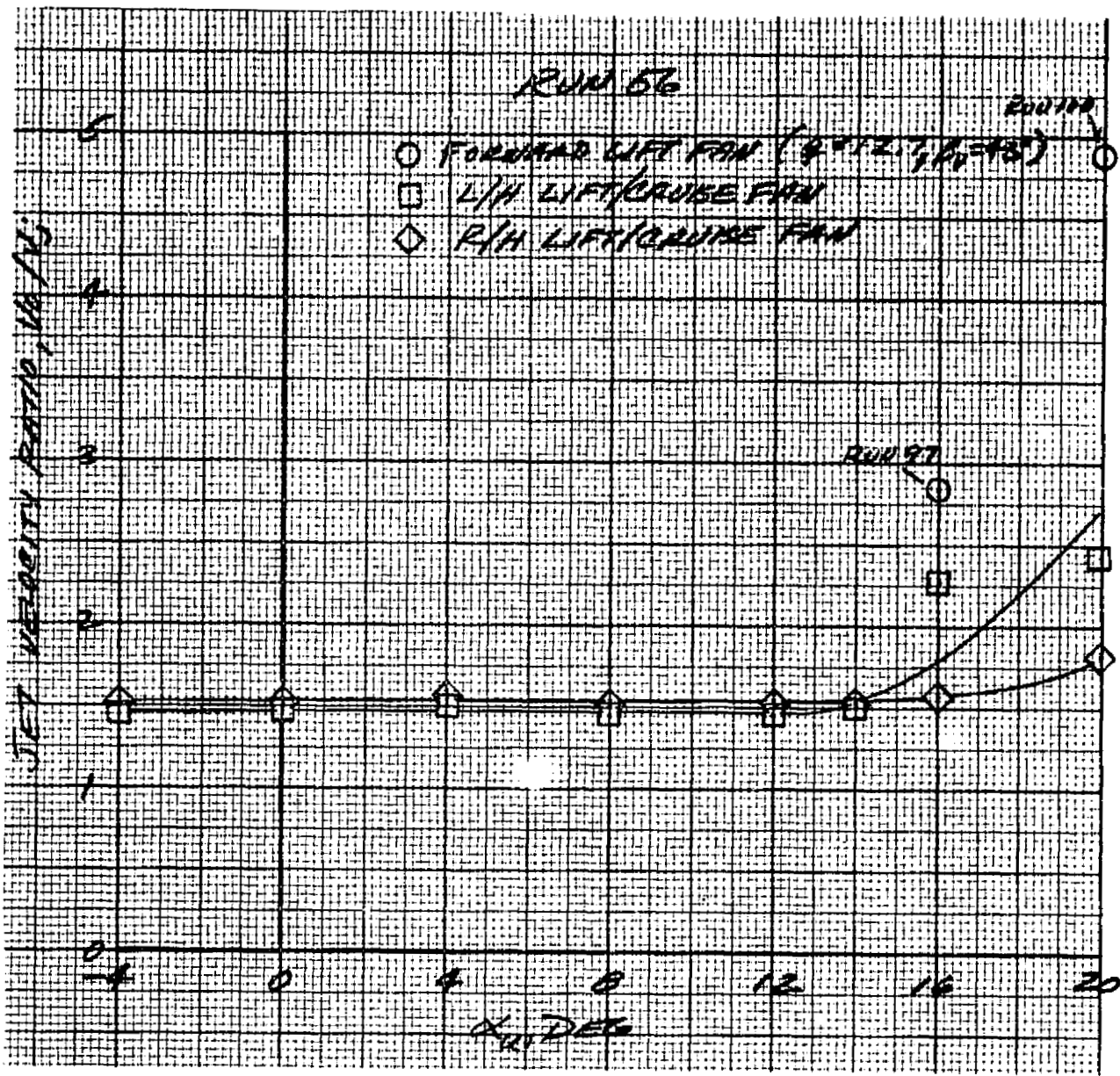
(b) $\delta_{cn} = 56°$, nominal q = 952.8 N/m^2(19.9 psf).

Figure 10.- Continued.

33
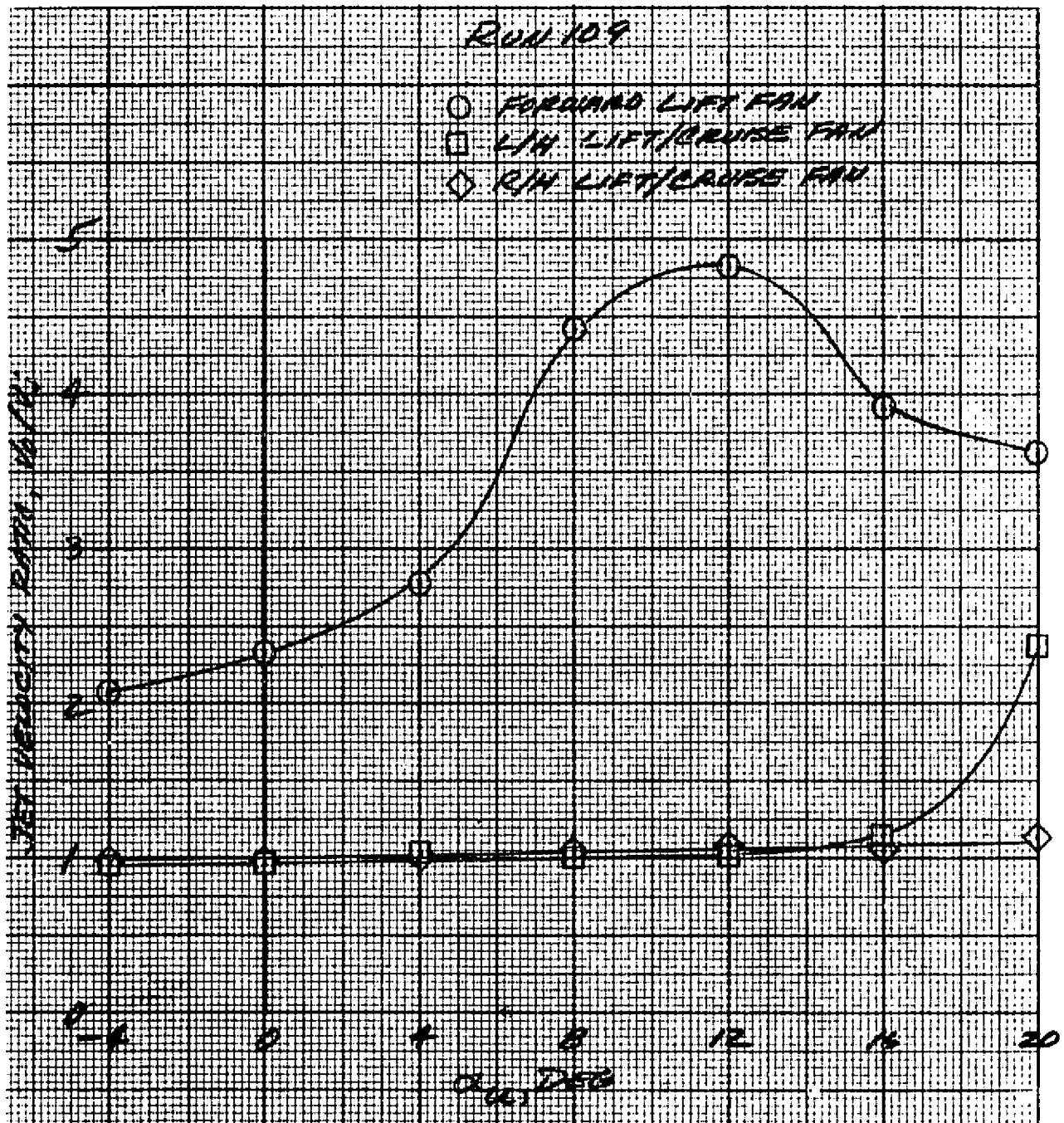
(c) $\delta_{cn} = 38°$, $\beta_v = 43°$, nominal $q = 952.8$ N/m^2(19.9 psf).

Figure 10.- Continued.
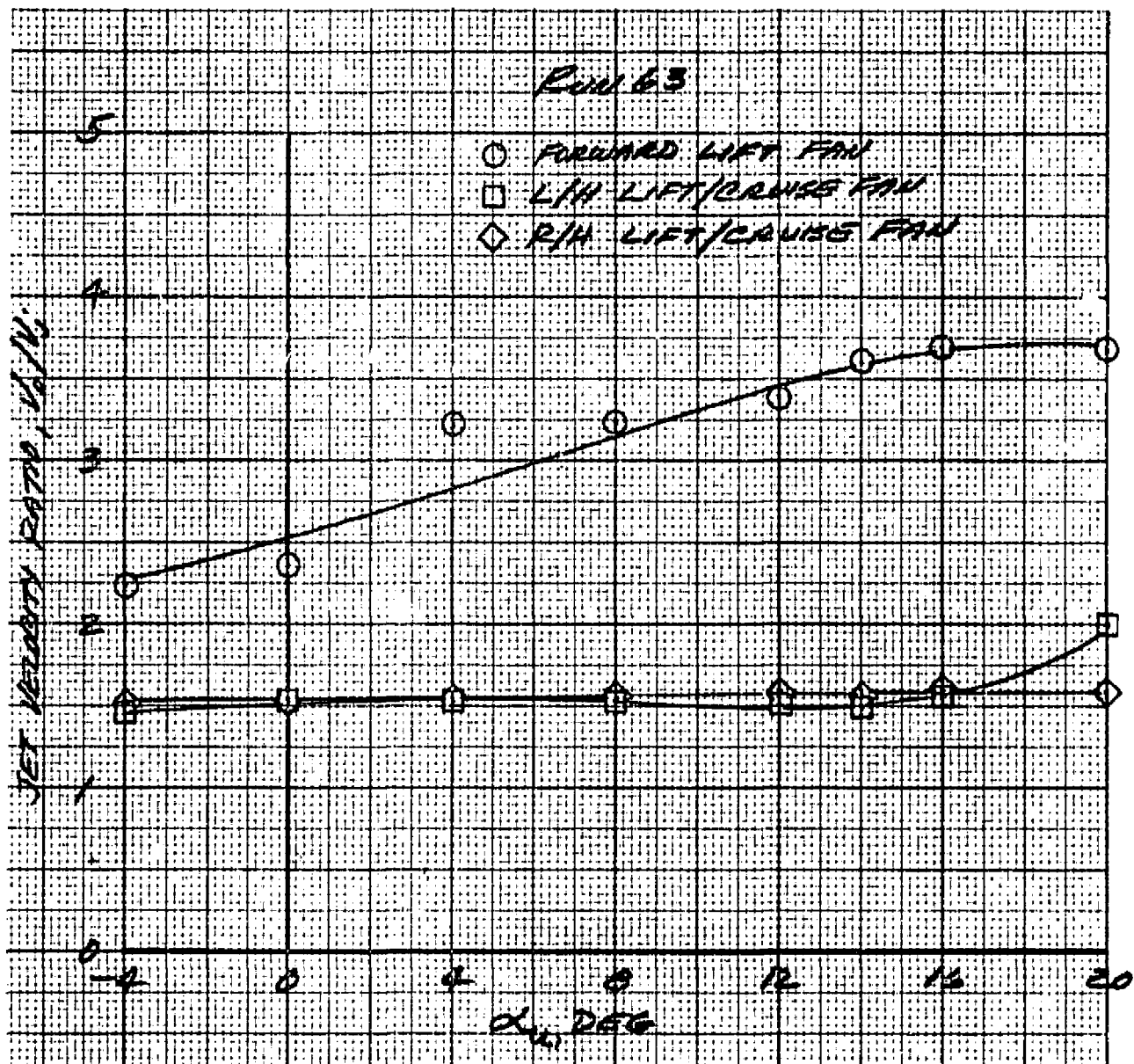
(d) $\delta_{cn} = 23°$, $\beta_v = 43°$, nominal q = 952.8 N/m^2(19.9 psf).

Figure 10.- Continued.

35
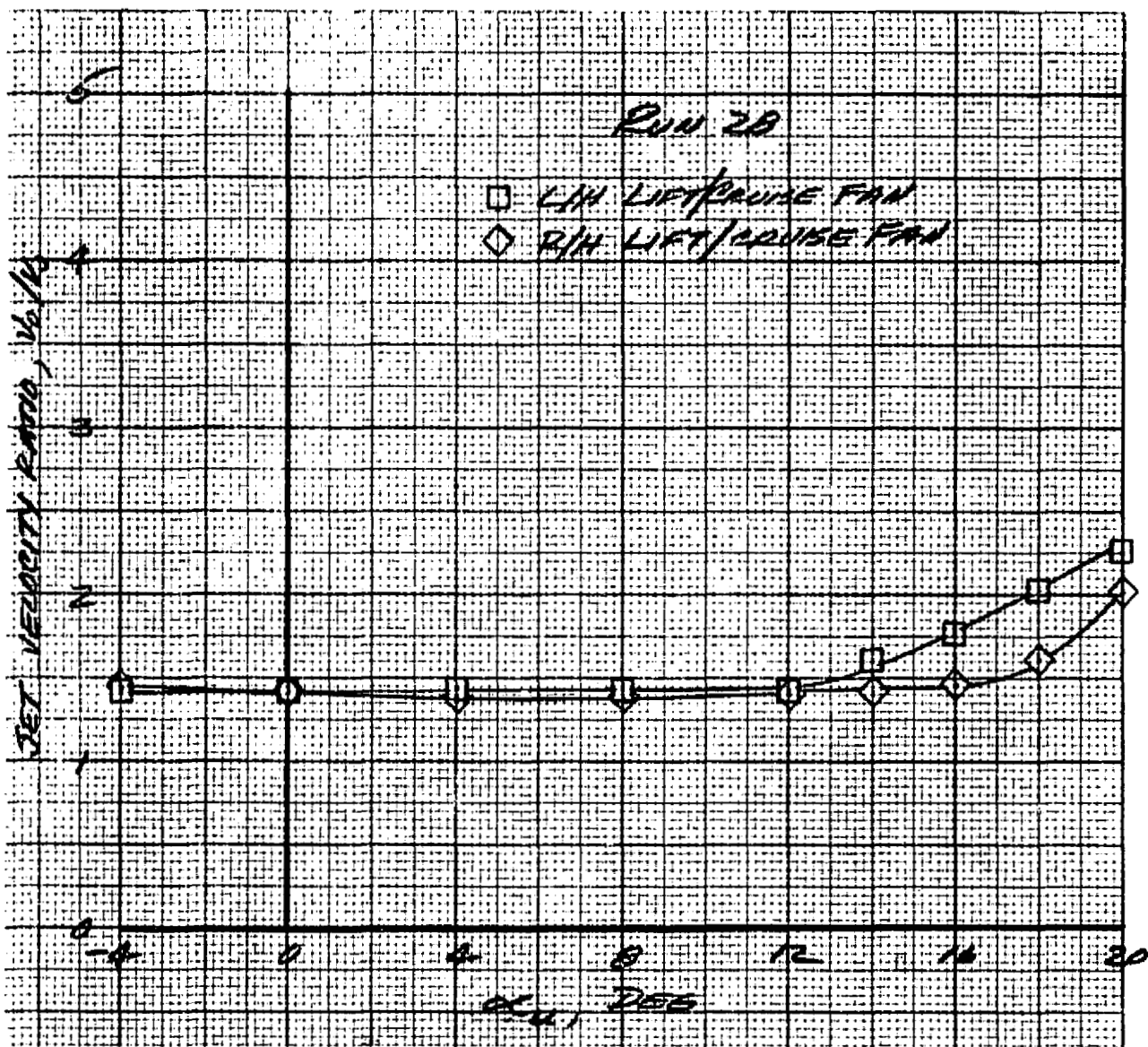
(e) $\delta_{cn} = 0°$, forward fan covered, nominal q = 1699.7 N/m^2(35.5psf).

Figure 10.- Concluded.
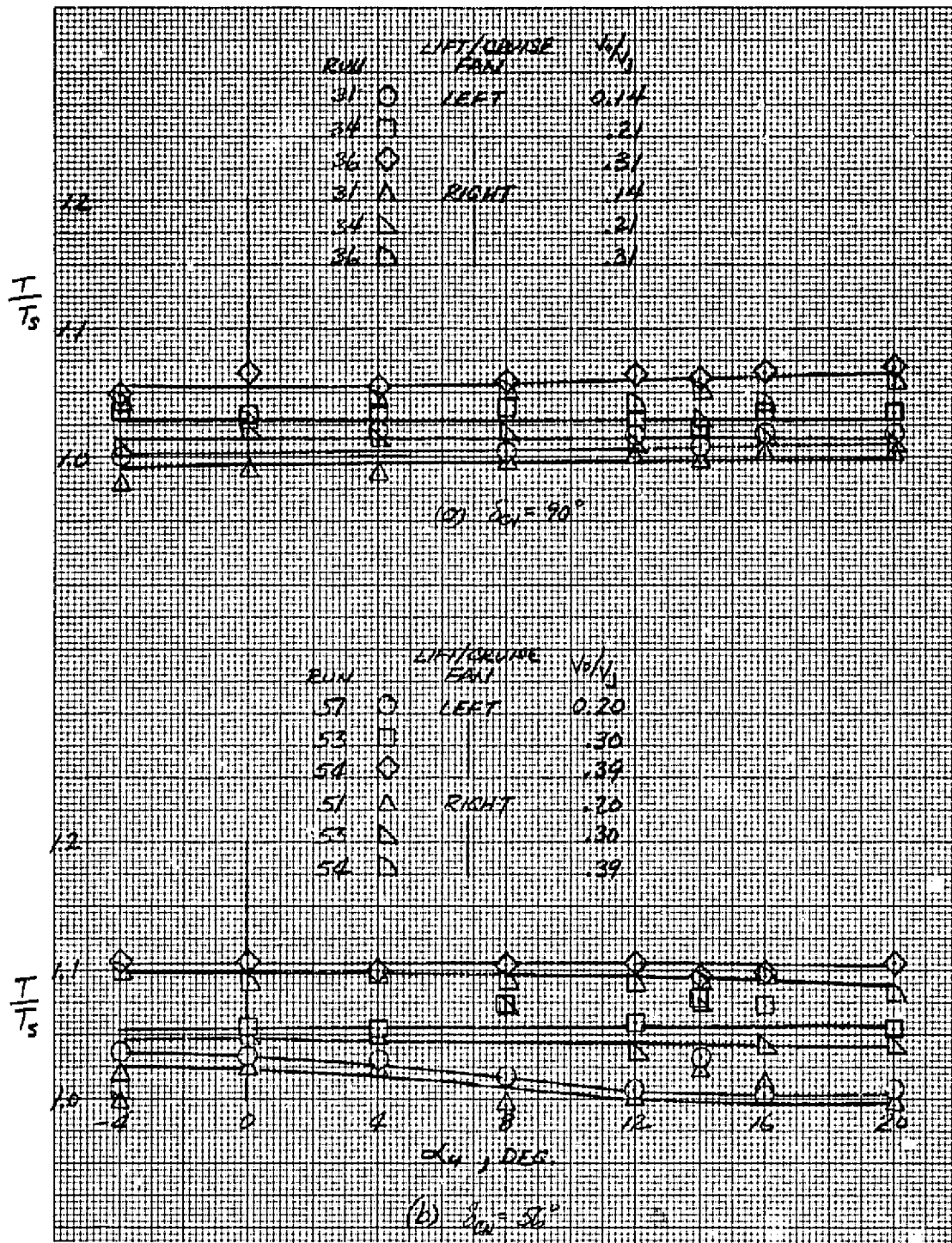
Figure 11.- Variation of fan resultant thrust to static resultant ratio with angle-of-attack.

37

(c) $\delta_{CN} = 38°$

(d) $\delta_{CN} = 23°$
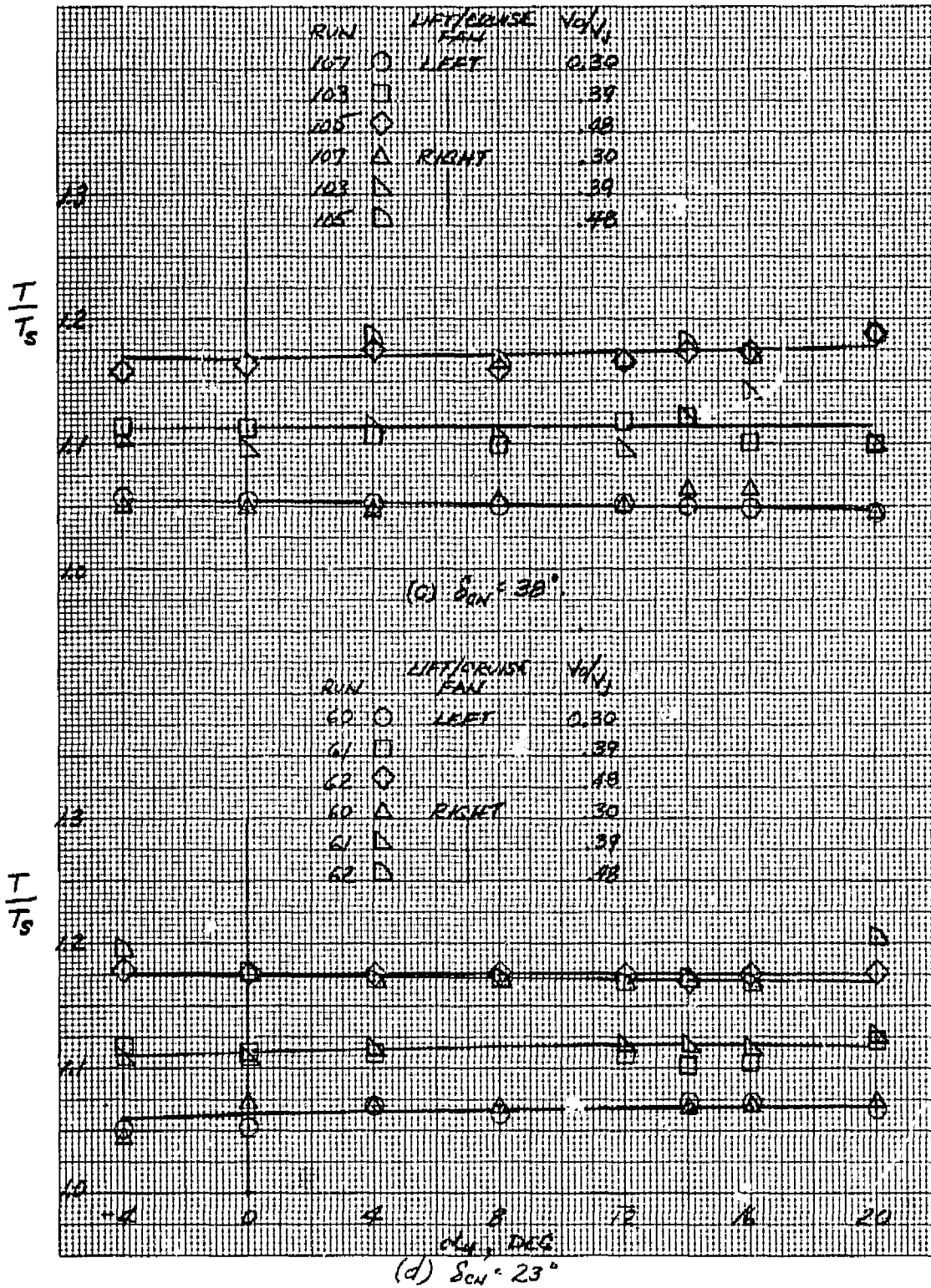
Figure 11.- Continued.
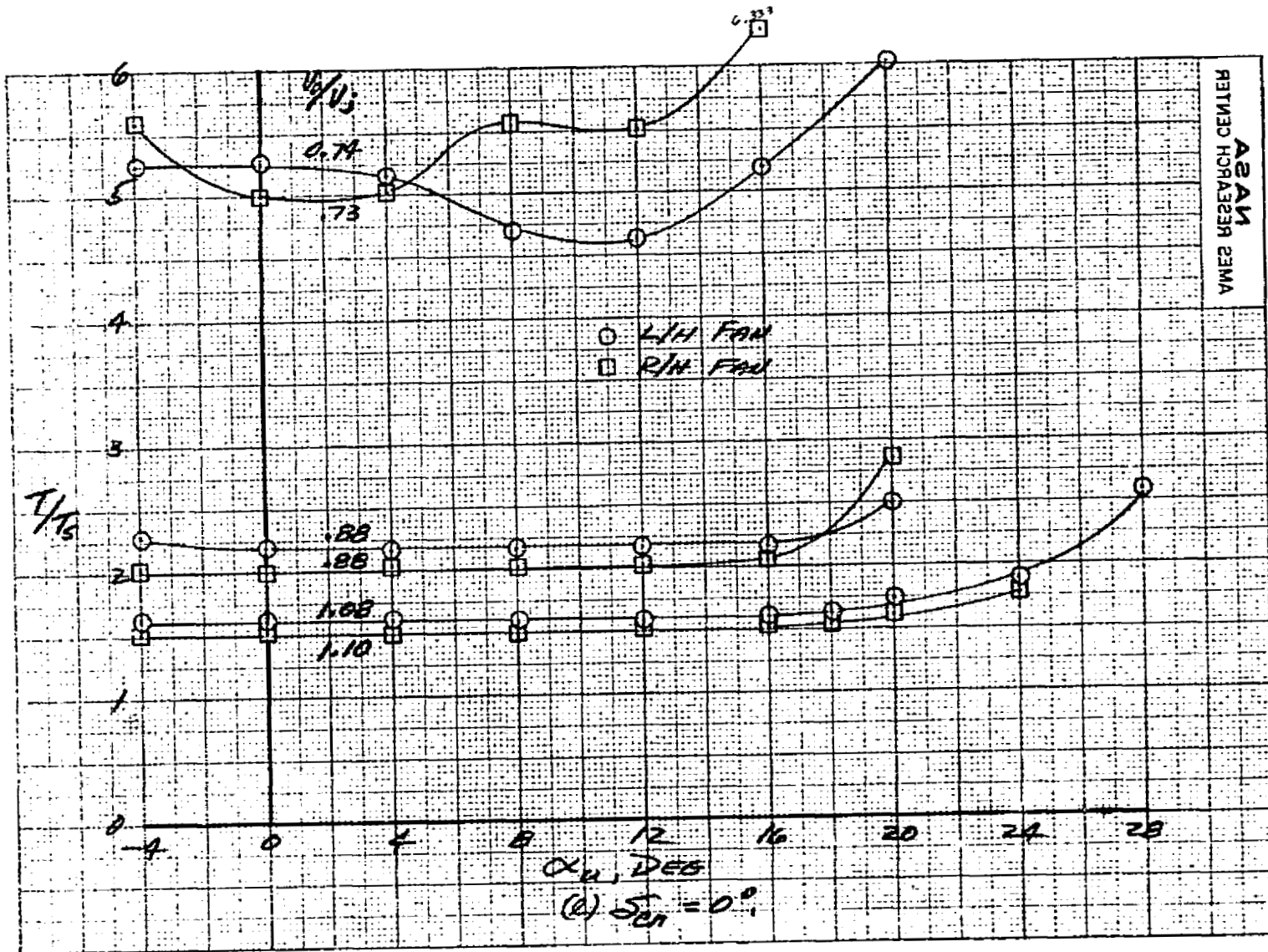
Figure 11.- Continued.
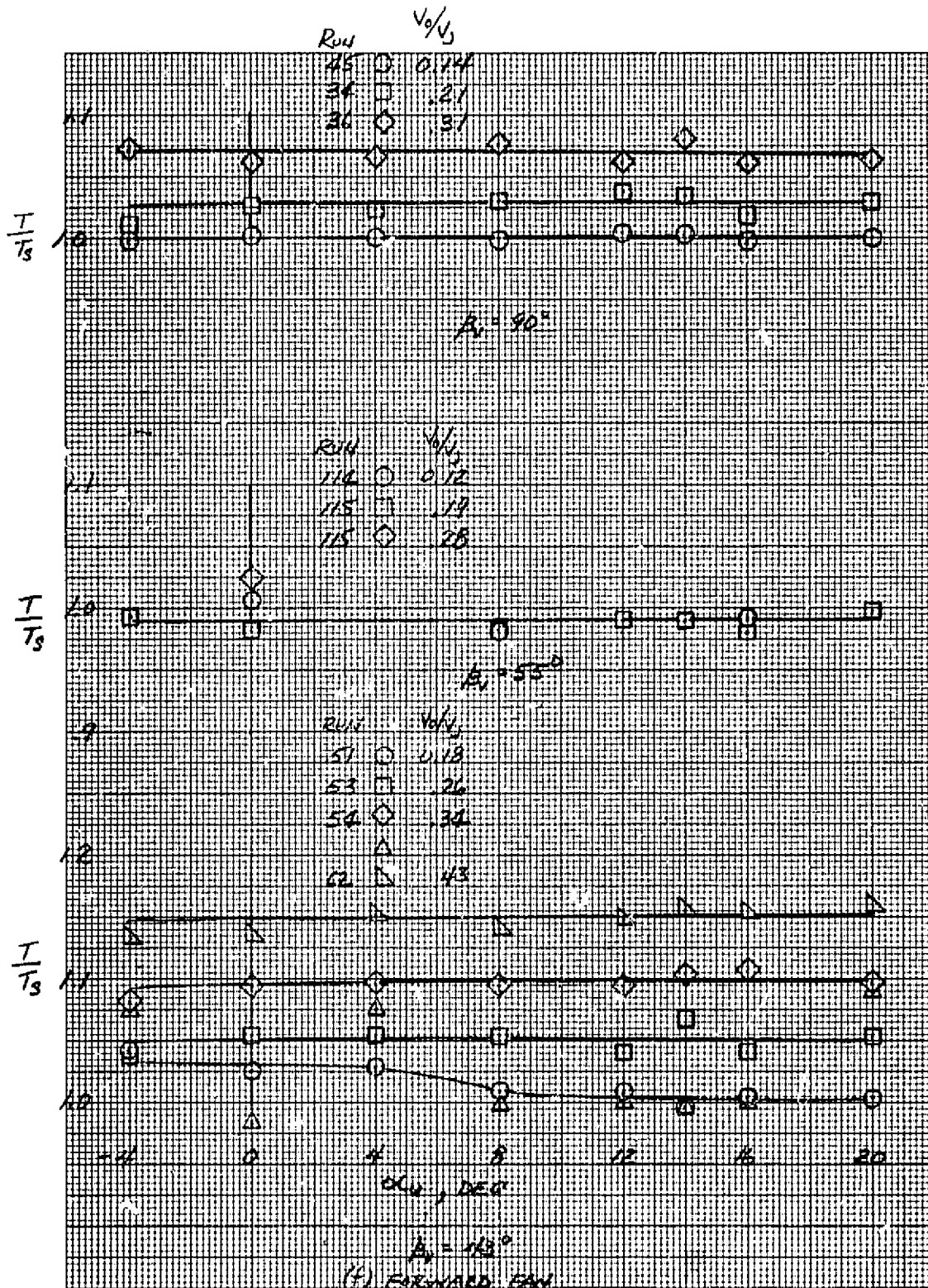
Figure 11.- Concluded.

40
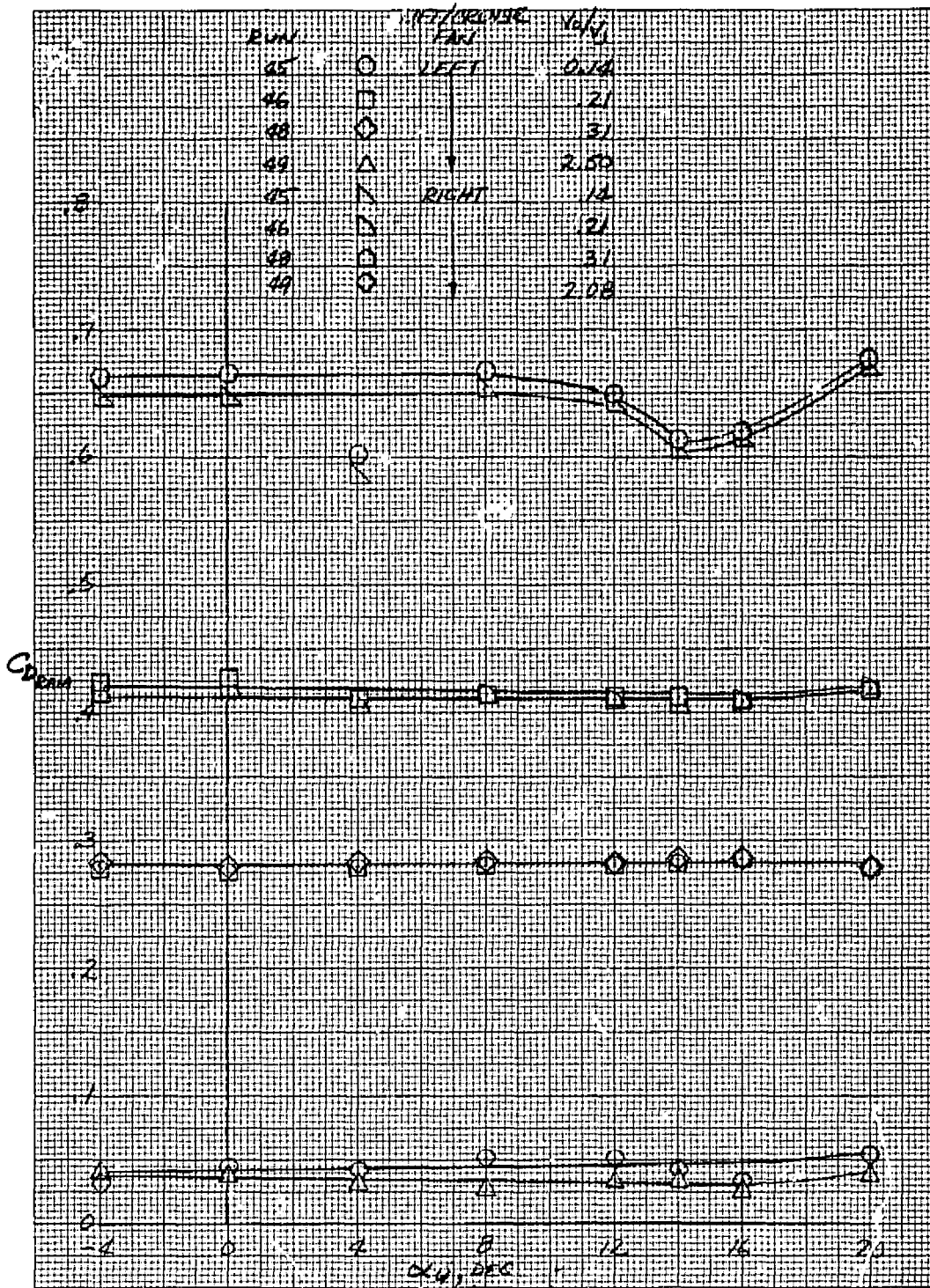
(a) $\delta_{cn} = 90°$.

Figure 12.- Variation of ram drag with angle-of-attack with forward fan
and lift/cruise fan operation.
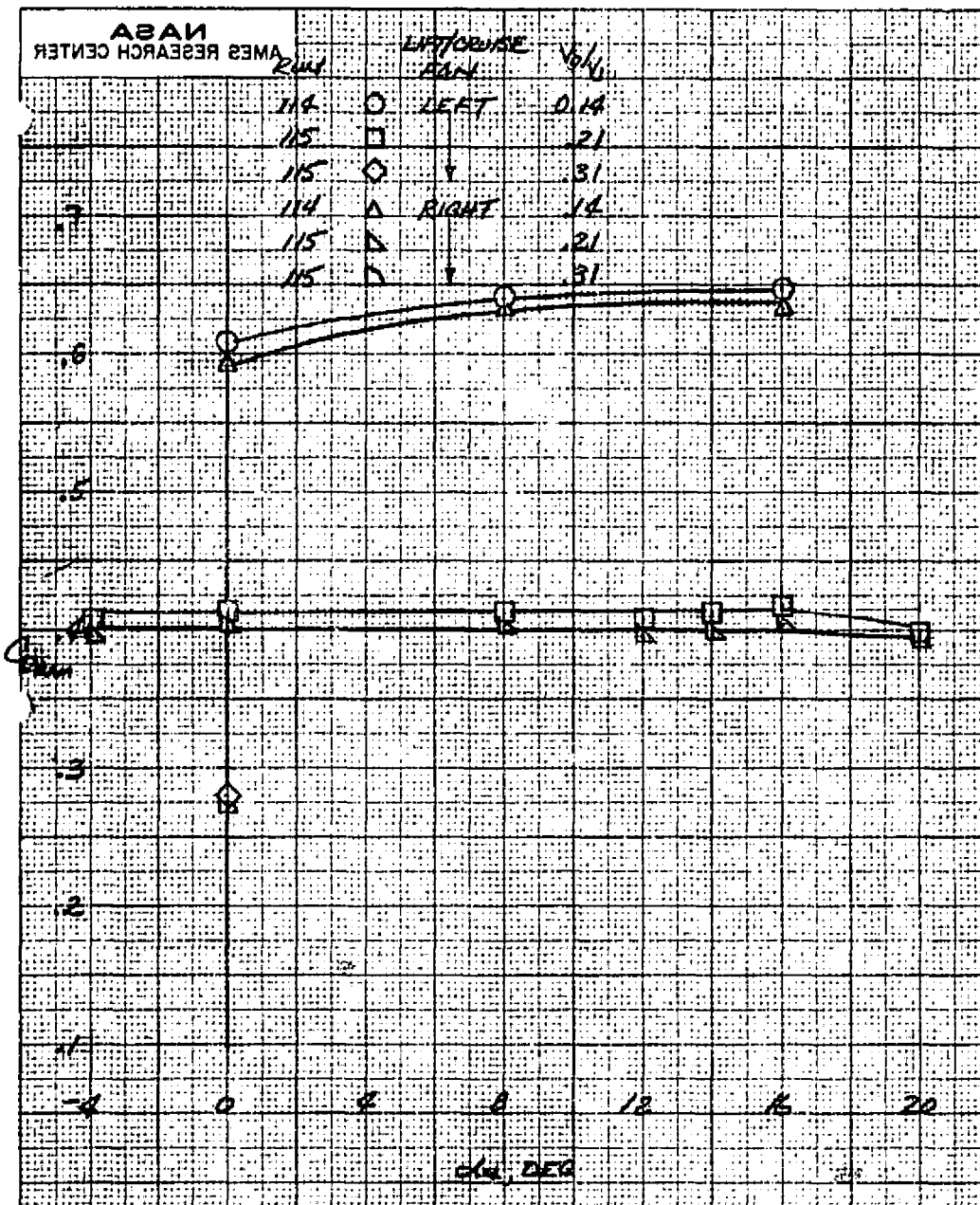
(b) $\delta_{cn} = 71°$.

Figure 12.- Continued.

42
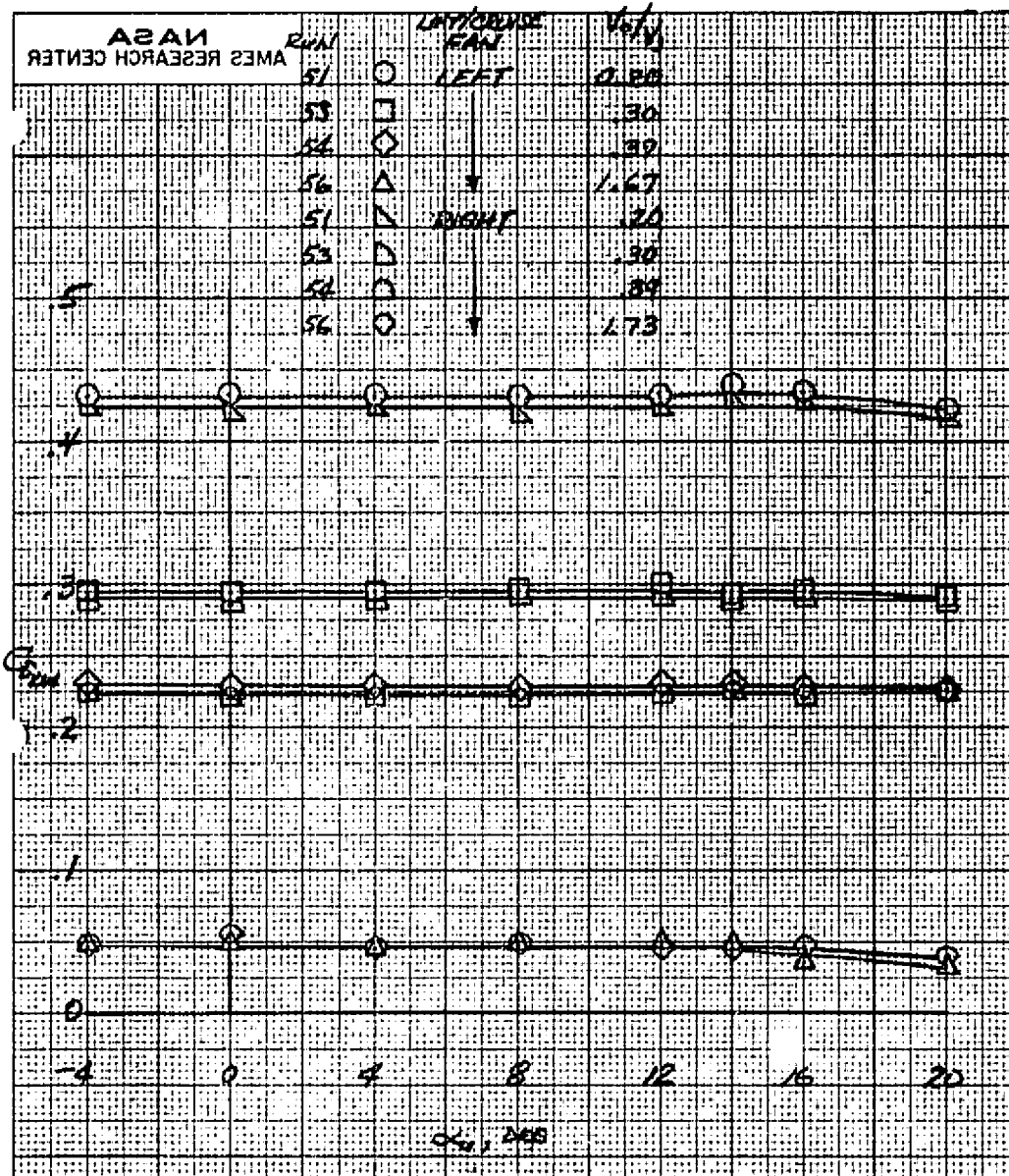
(c) $\delta_{cn} = 56°$

Figure 12.- Continued.
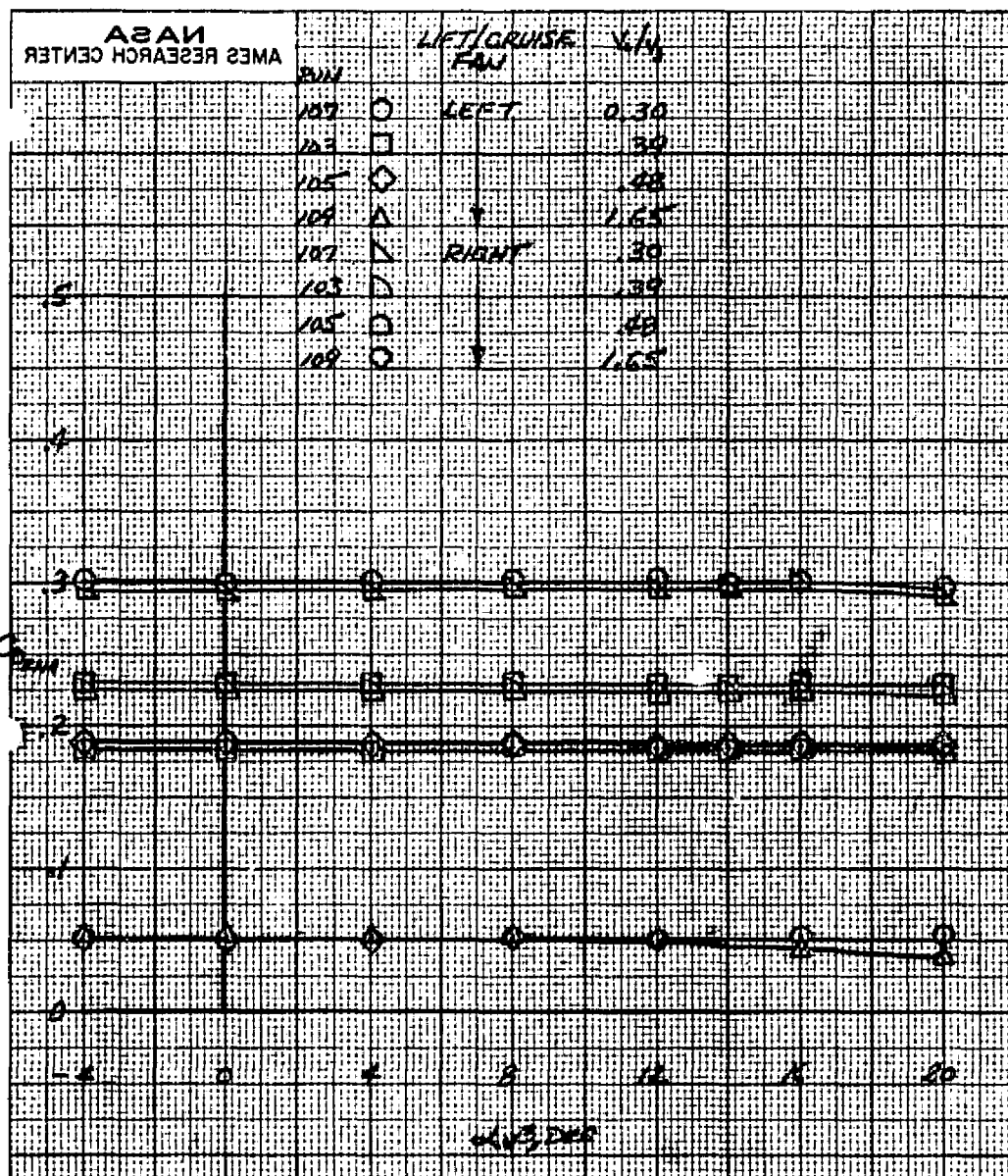
(d) $\delta_{cn} = 38°$.

Figure 12.- Continued.
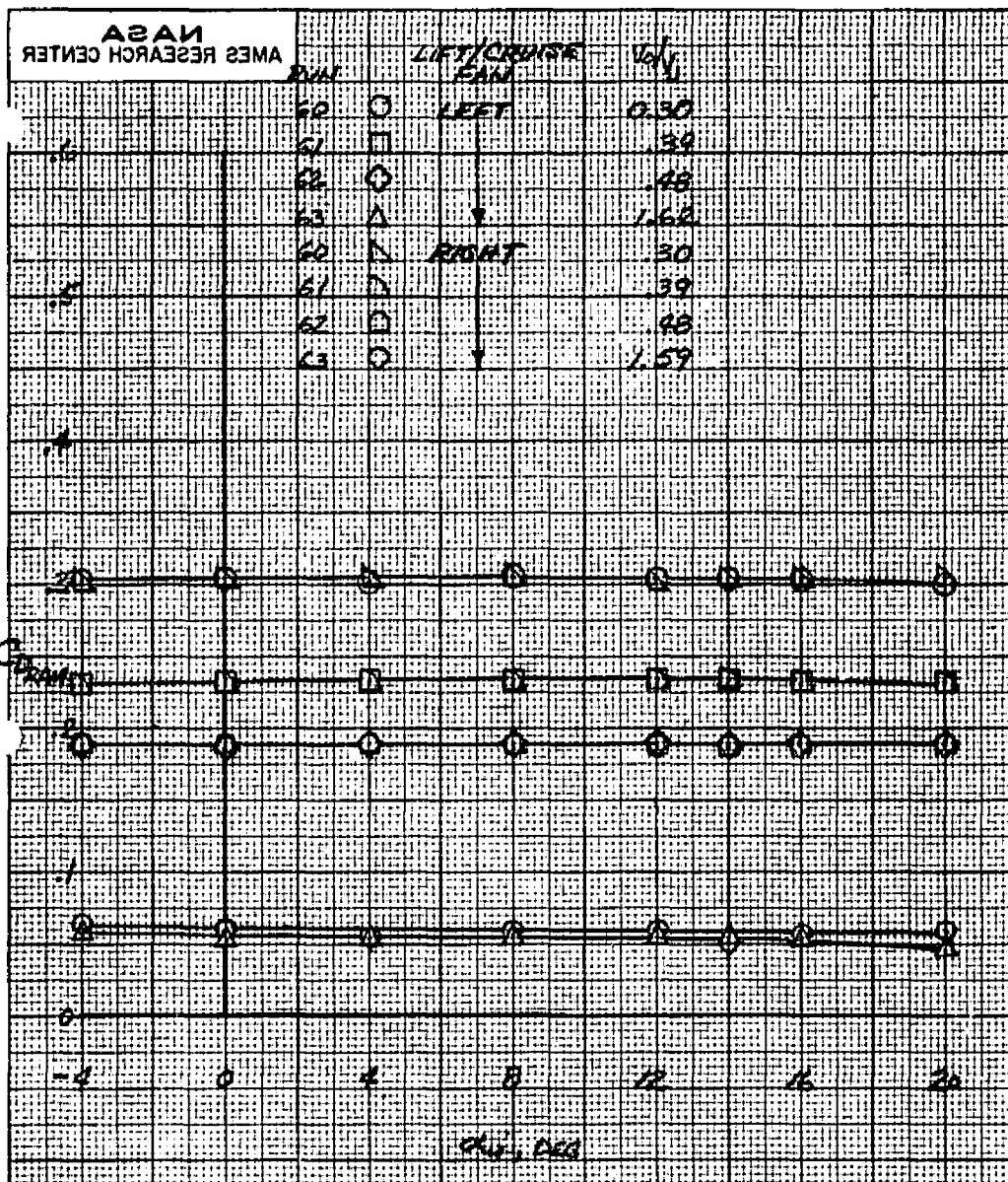
(e) $\delta_{cn} = 23°$.

Figure 12.- Continued.
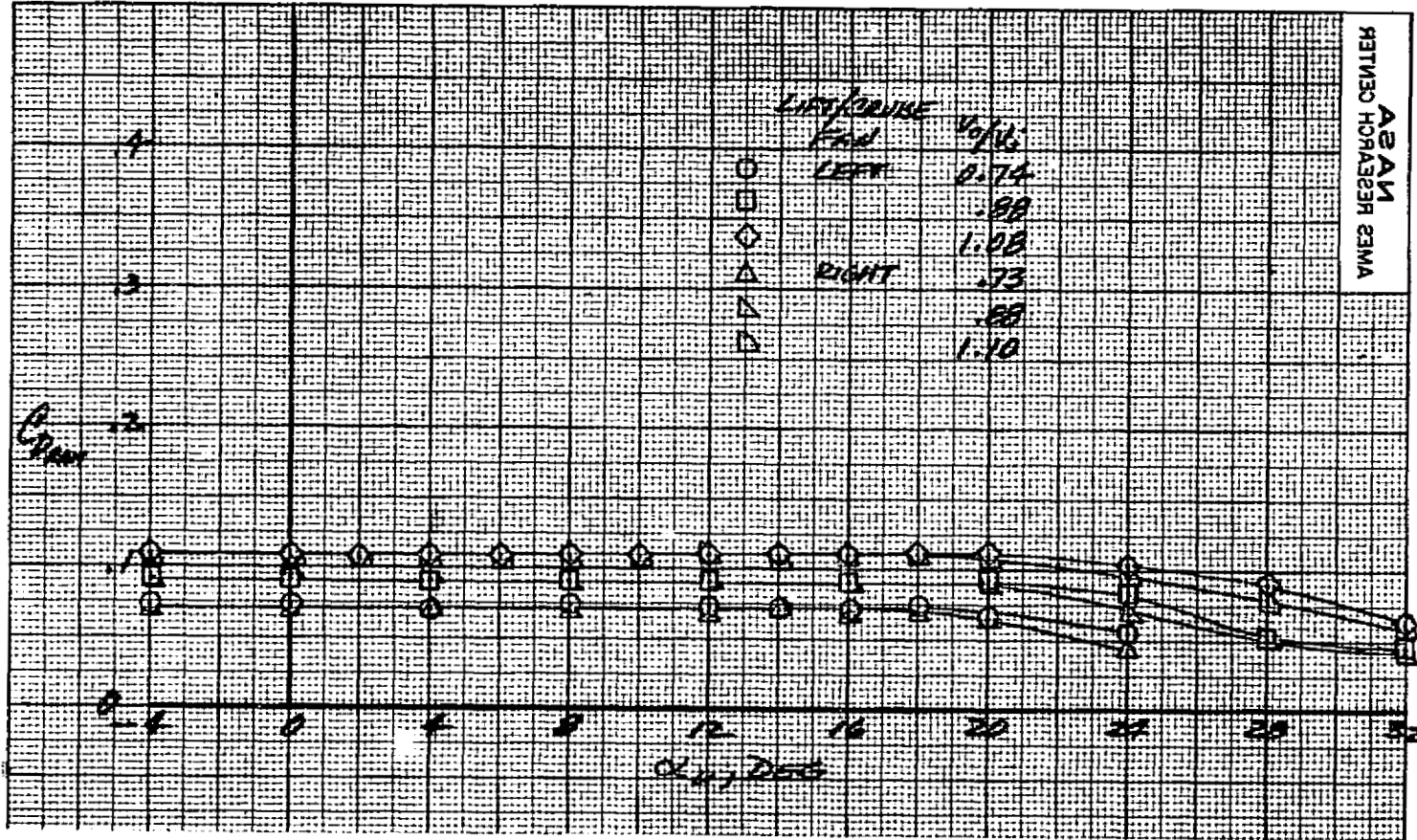
(f) $\delta_{cn} = 0°$.

Figure 12.- Continued.
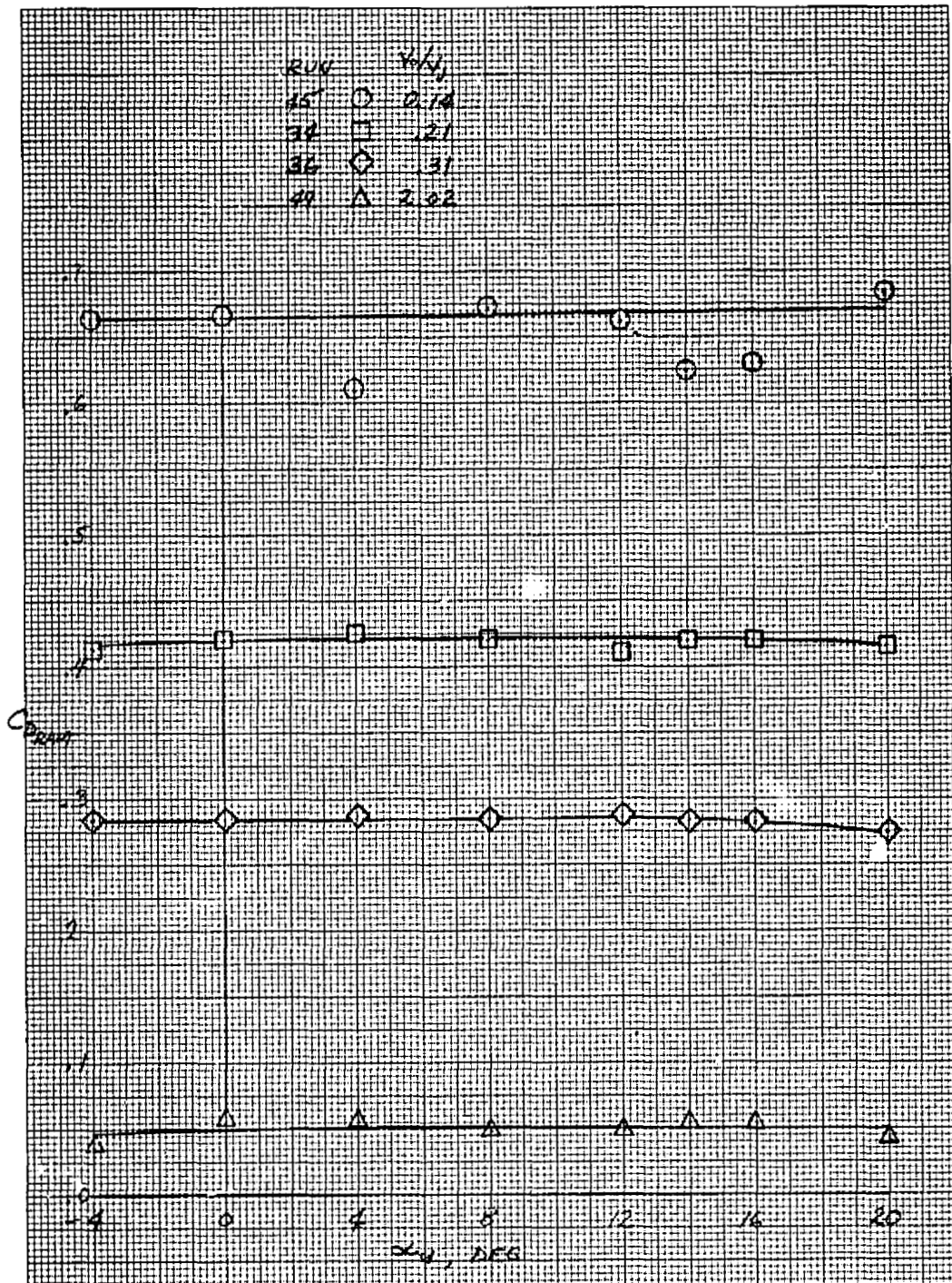
(g) Forward Fan, $\beta_v = 90°$.

Figure 12.- Continued.

47
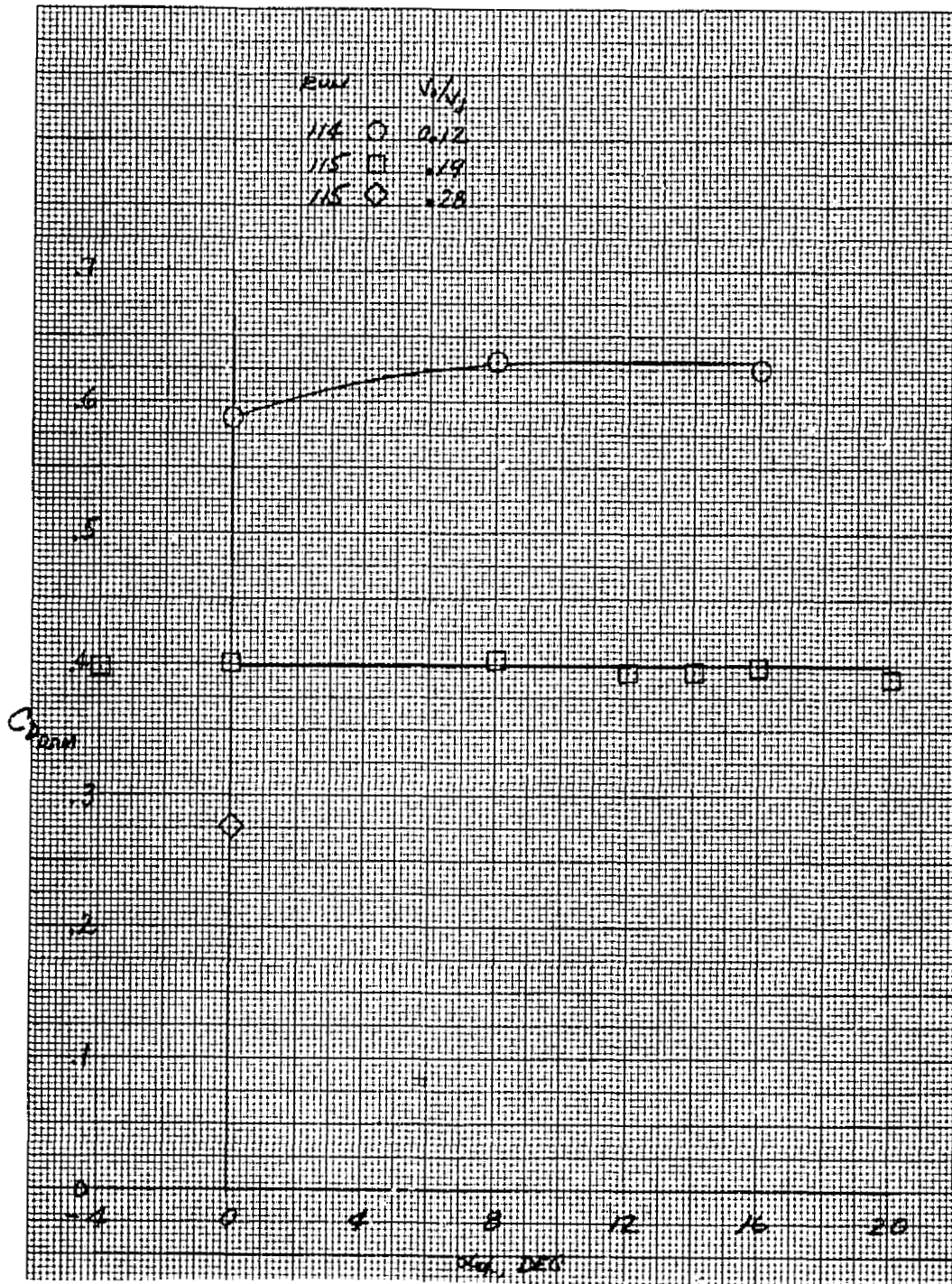
(h) Forward Fan, $\beta_v = 55°$.

Figure 12.- Continued.
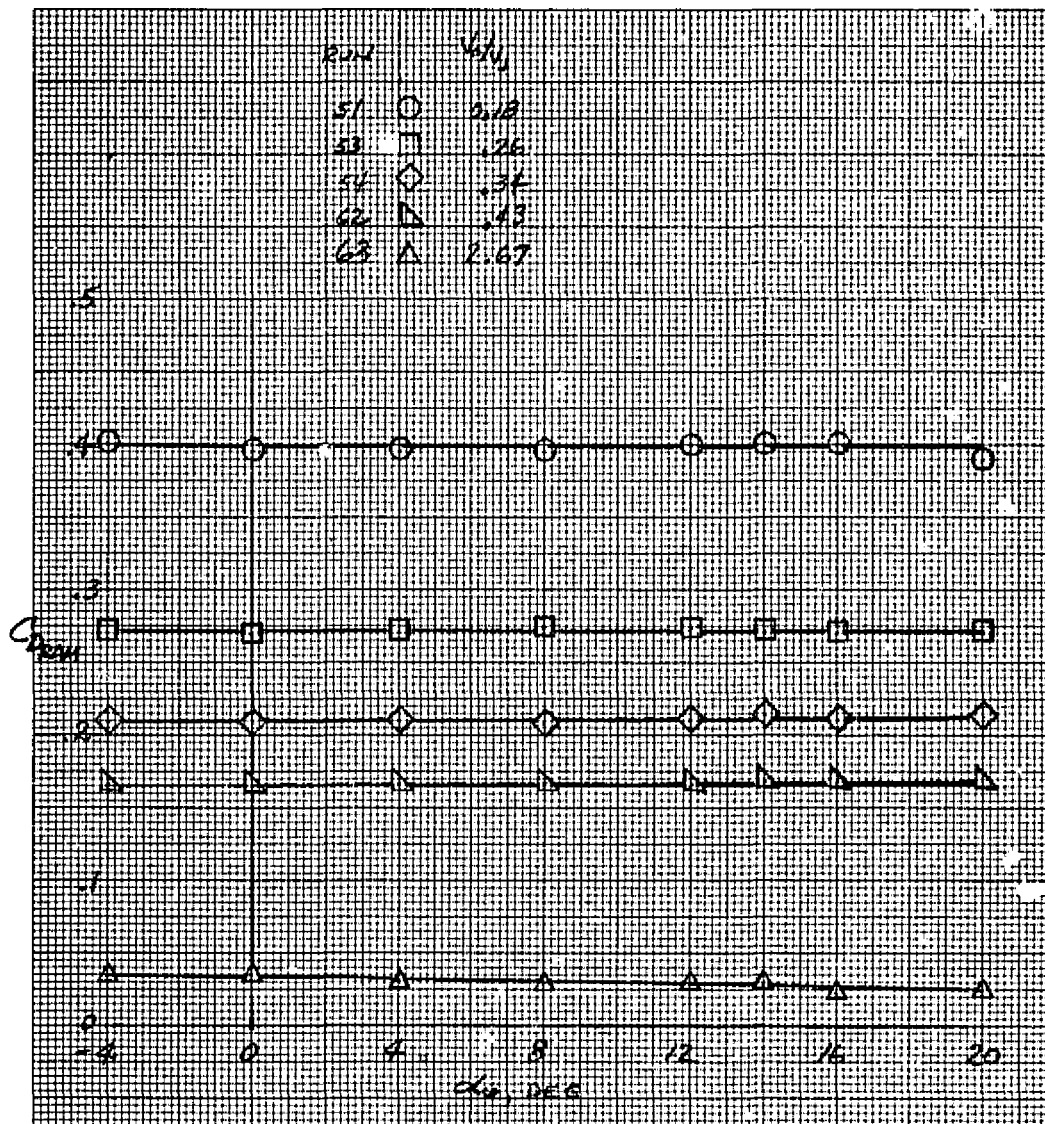
(i) Forward Fan, $\beta_v = 43°$.

Figure 12.- Concluded.
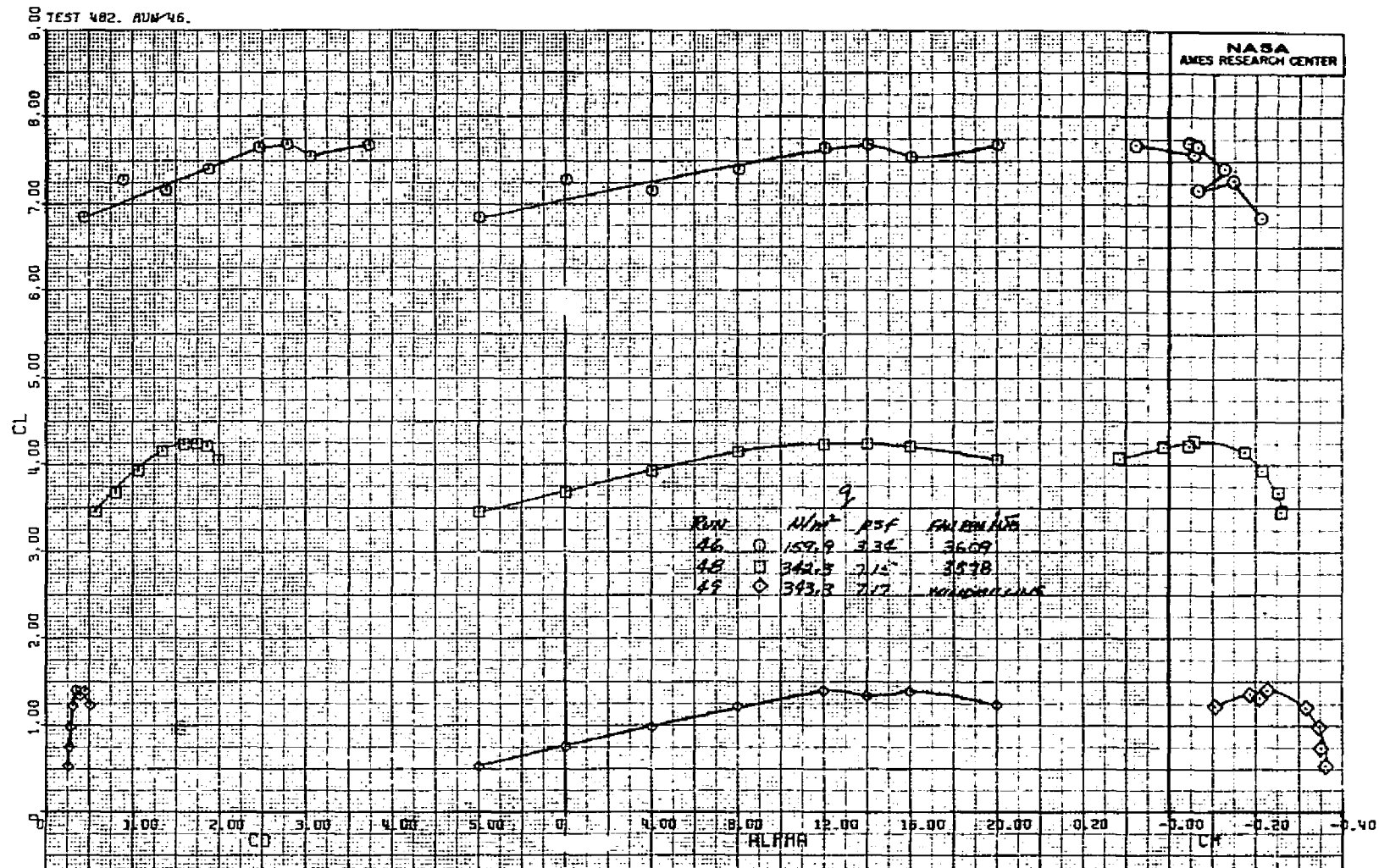
(a) $\delta_{cn} = 90°$, $\beta_v = 90°$.

Figure 13.– Longitudinal characteristics of the model with three fans operating; tail off, $\delta_f = 15°$, $\delta_{ail} = 10°$, $\delta_R = 0°$, $\beta = 0°$.
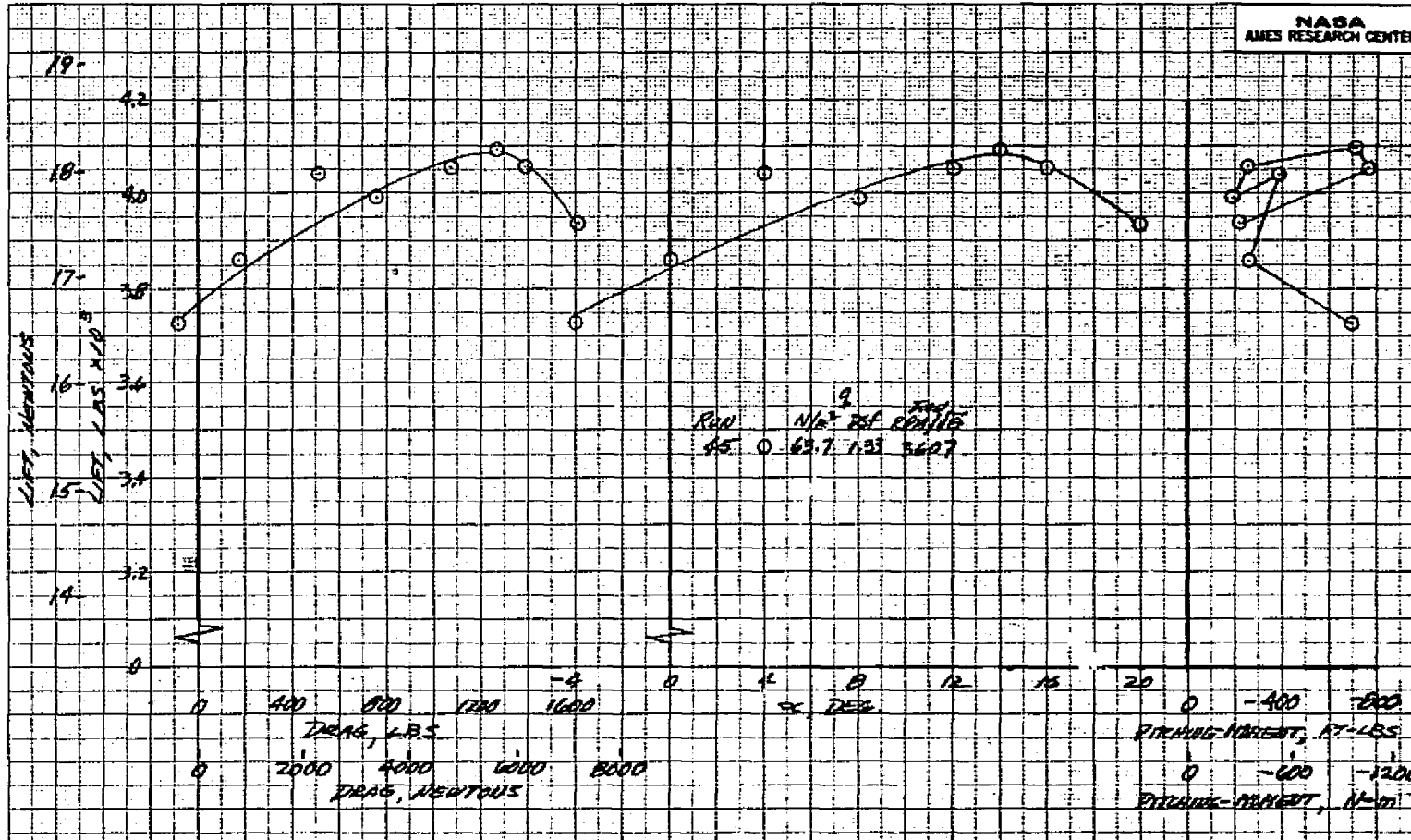
(b) $\delta_{cn} = 90°$, $\beta_v = 90°$.

Figure 13.- Continued.
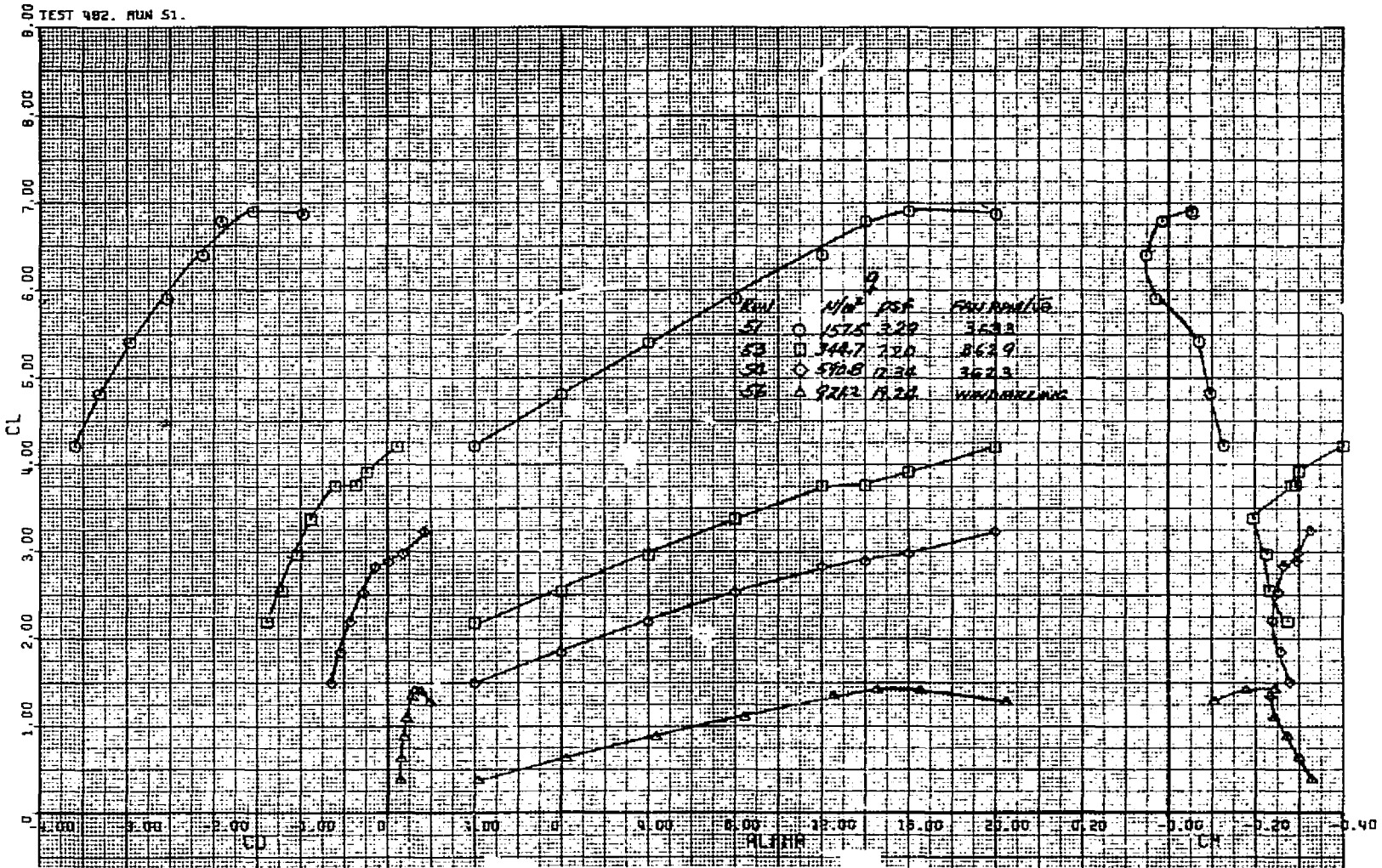
(c) $\delta_{cn} = 56°$, $\beta_v = 43°$.

Figure 13.– Continued.

52
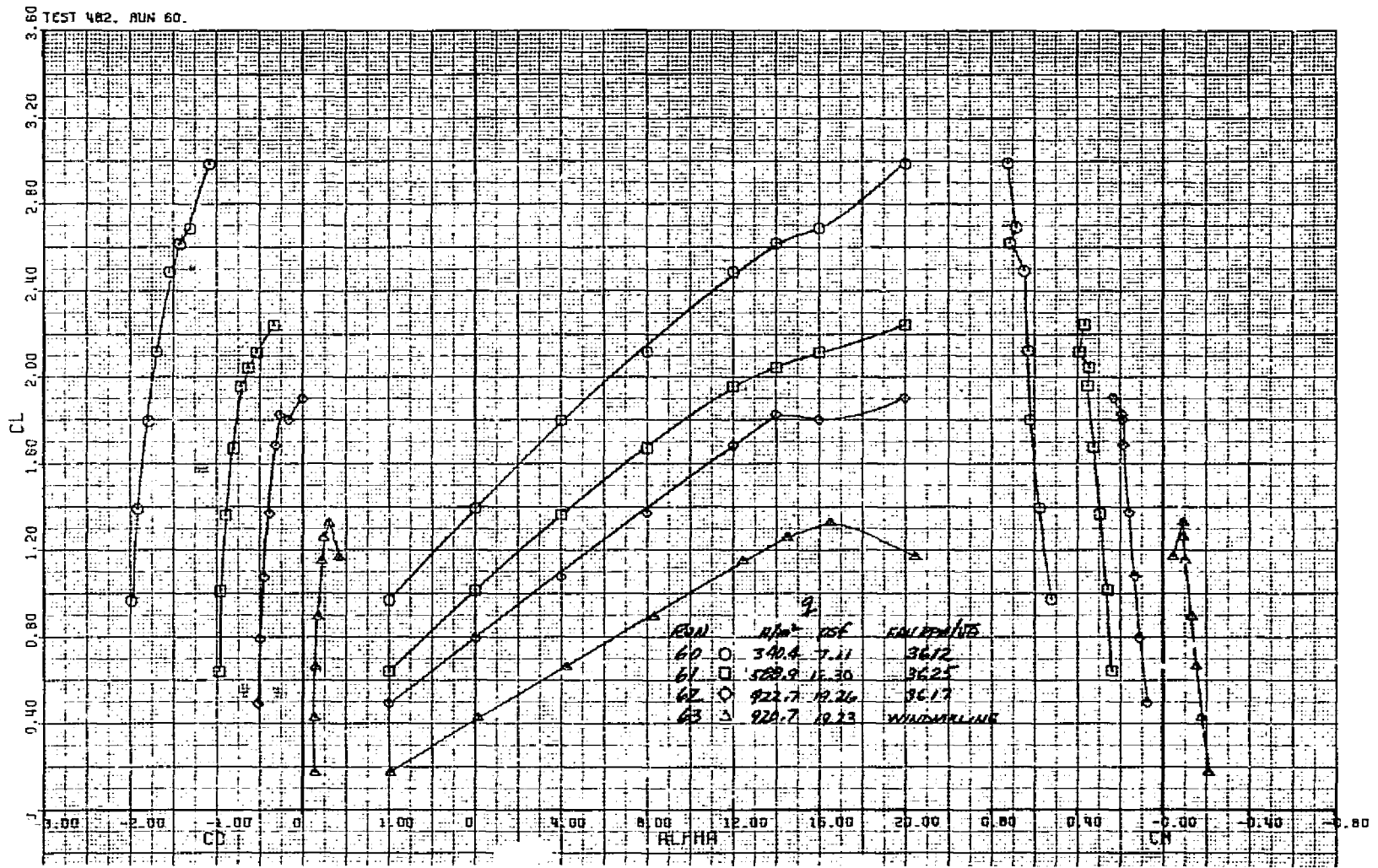
(d) $\delta_{cn} = 23°$, $\beta_v = 43°$.

Figure 13.- Concluded.
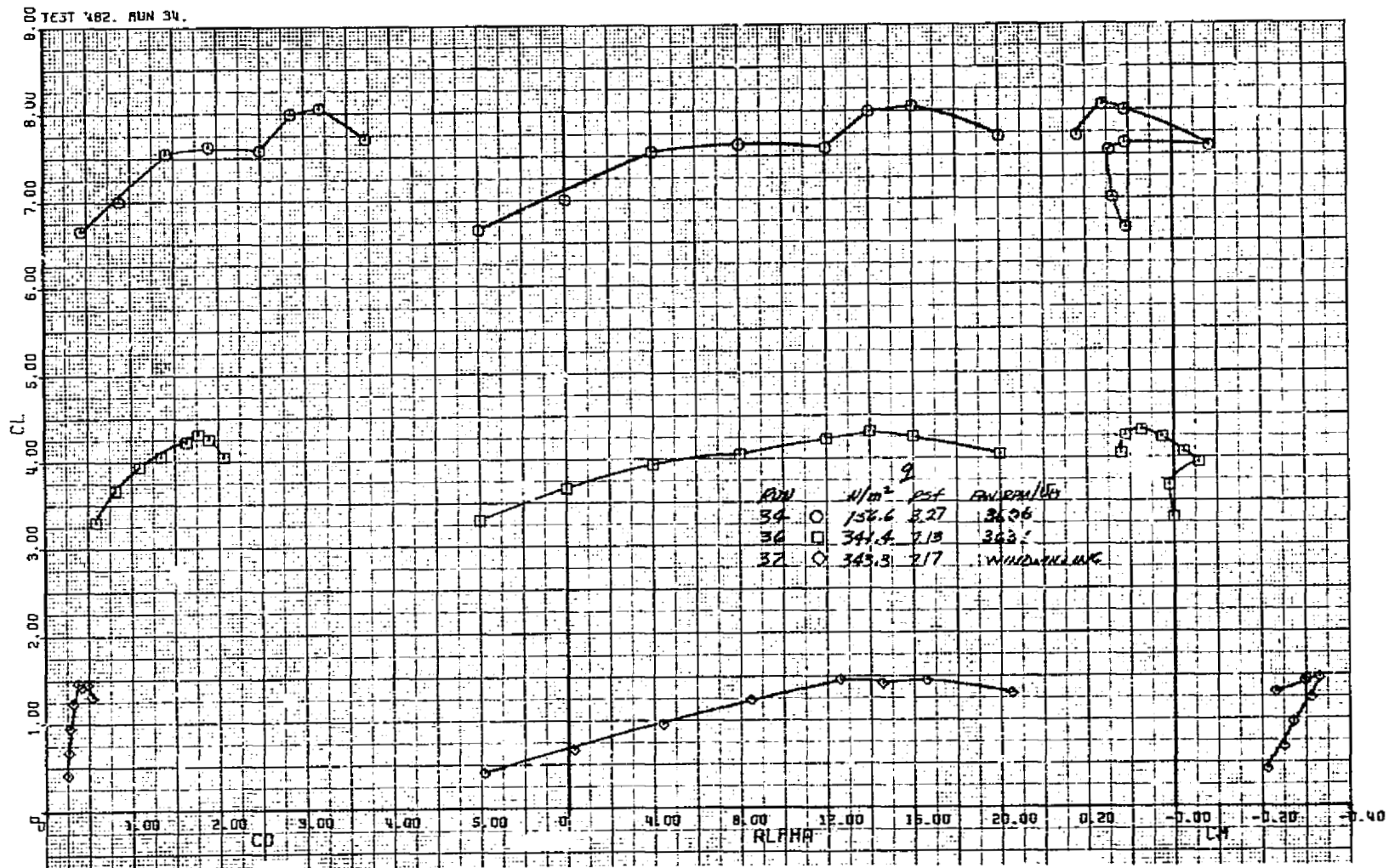
(a) $\delta_{cn} = 90°$, $\beta_v = 90°$.

Figure 14.- Longitudinal characteristics of the model with three fans operating and with the horizontal tail installed; $\delta_f = 15°$, $\delta_{ail} = 10°$, $i_t = 0°$, $\beta = 0°$, $\delta_R = 0°$.
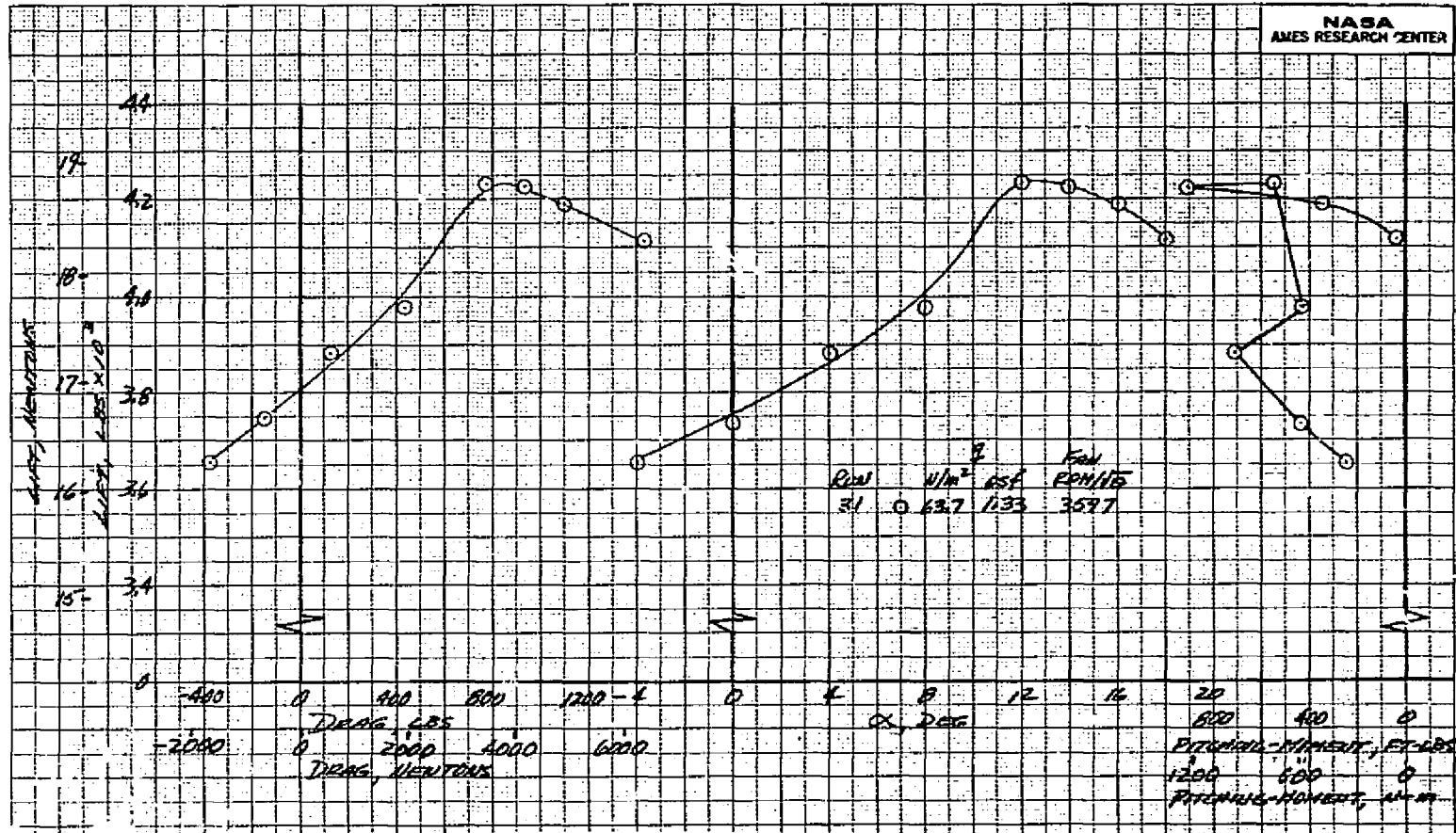
(b) $\delta_{cn} = 90°$, $\beta_v = 90°$.

Figure 14.- Continued.
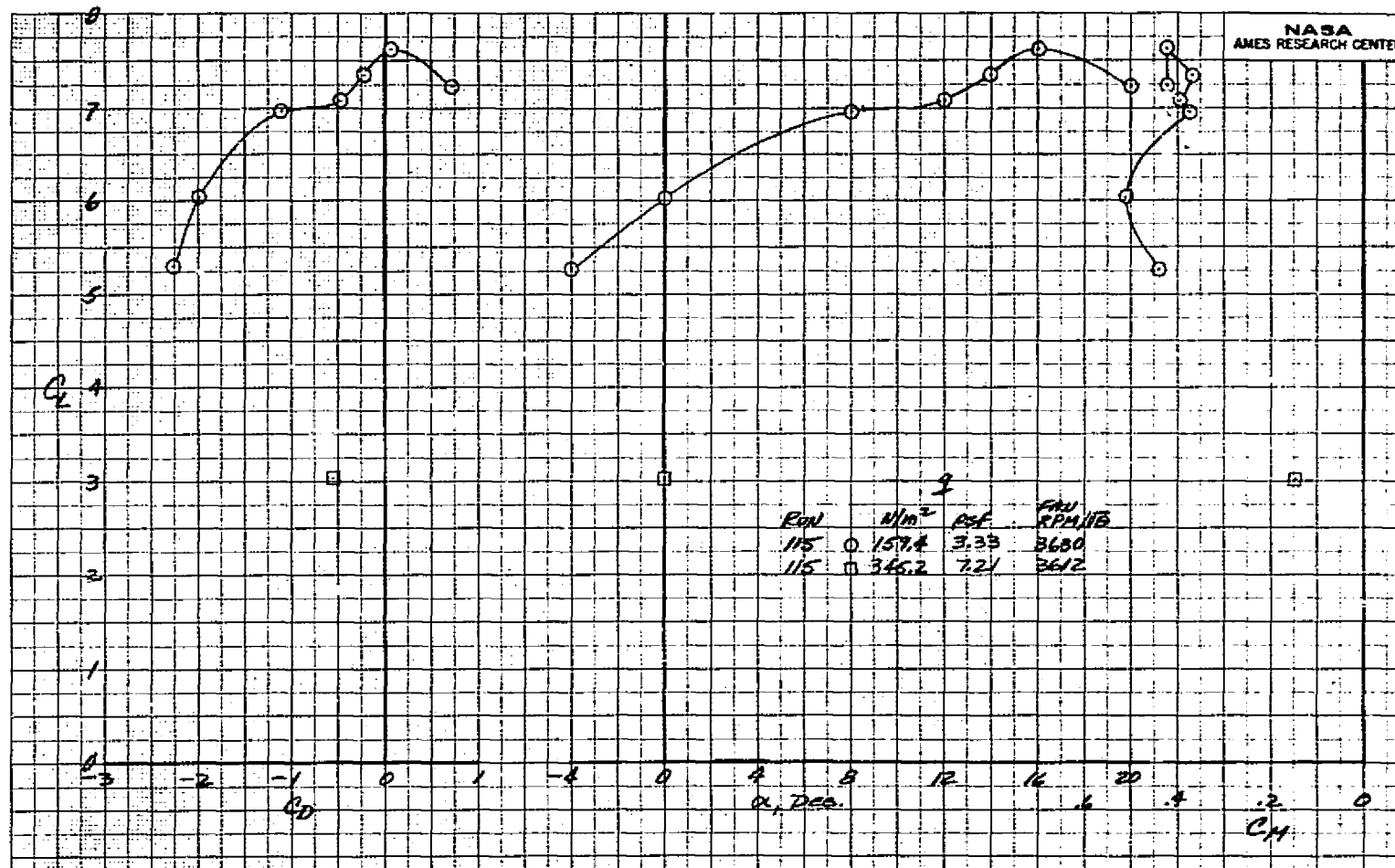
(c) $\delta_{cn} = 71°$, $\beta_v = 55°$.

Figure 14.- Continued.
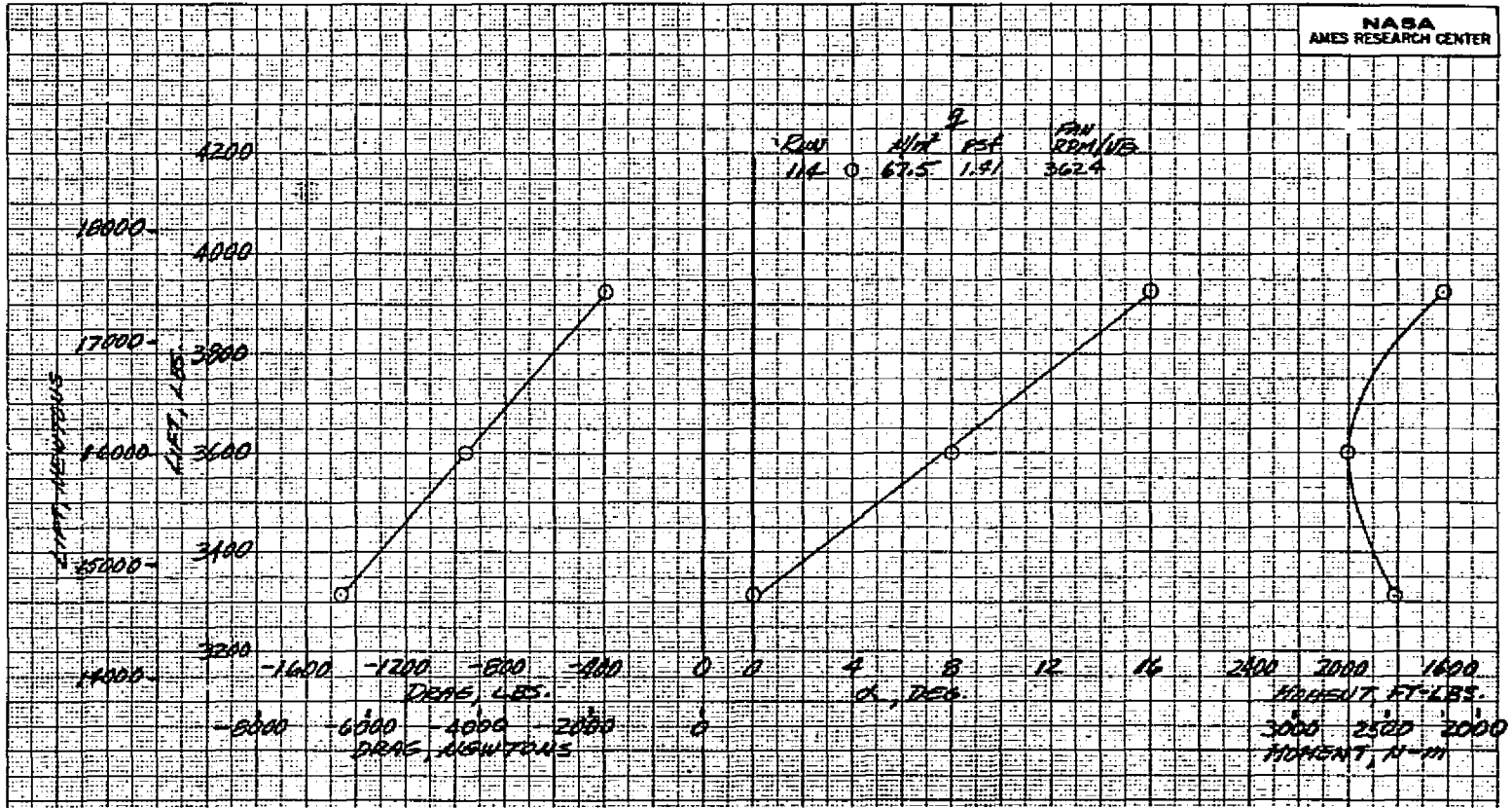
(d) $\delta_{cn} = 71°$, $\beta_v = 55°$.

Figure 14.- Continued.

(e) $\delta_{cn} = 56°$, $\beta_v = 43°$.

Figure 14.- Continued.

58

TEST 482. RUN 107.

CL

CD ALFHA CM

RUN		N/m²	PSF	GALLROM/HR
107	○	344.1	7.13	3627
103	□	590.8	12.34	3628
105	◇	920.7	19.23	3636
109	△	922.2	18.26	WINDMILLING
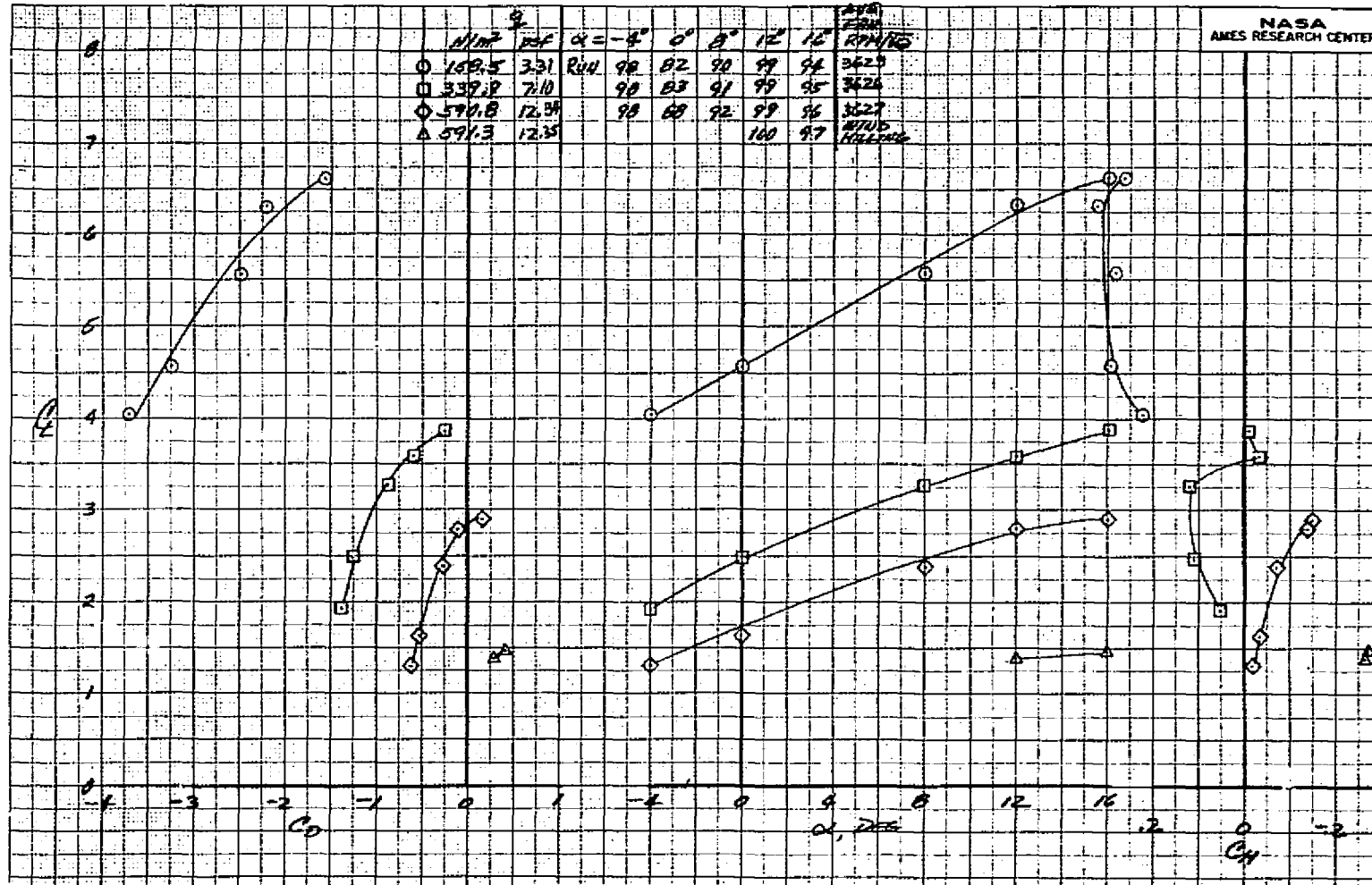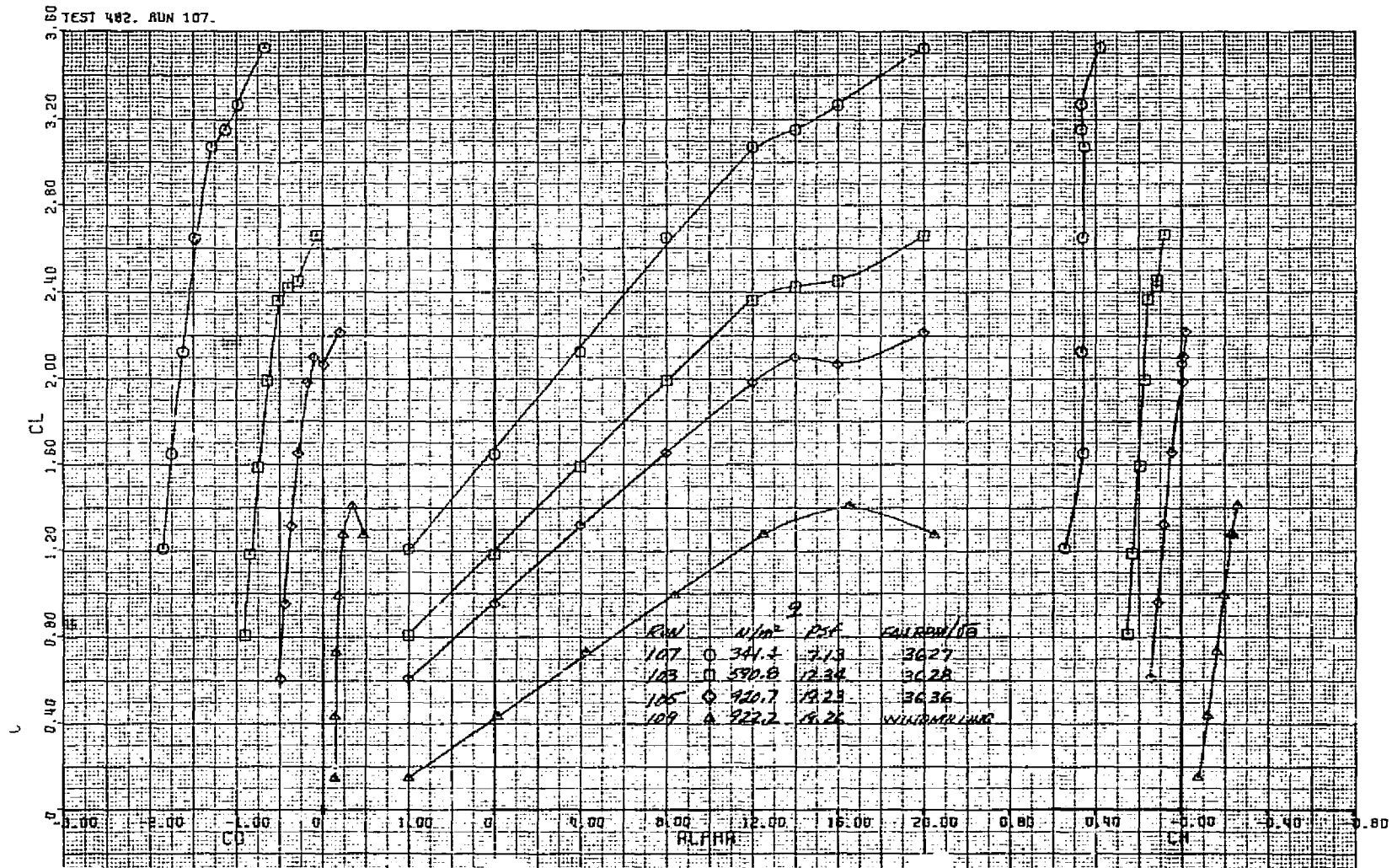
(f) $\delta_{cn} = 38°$, $\beta_v = 43°$.

Figure 14.— Continued.
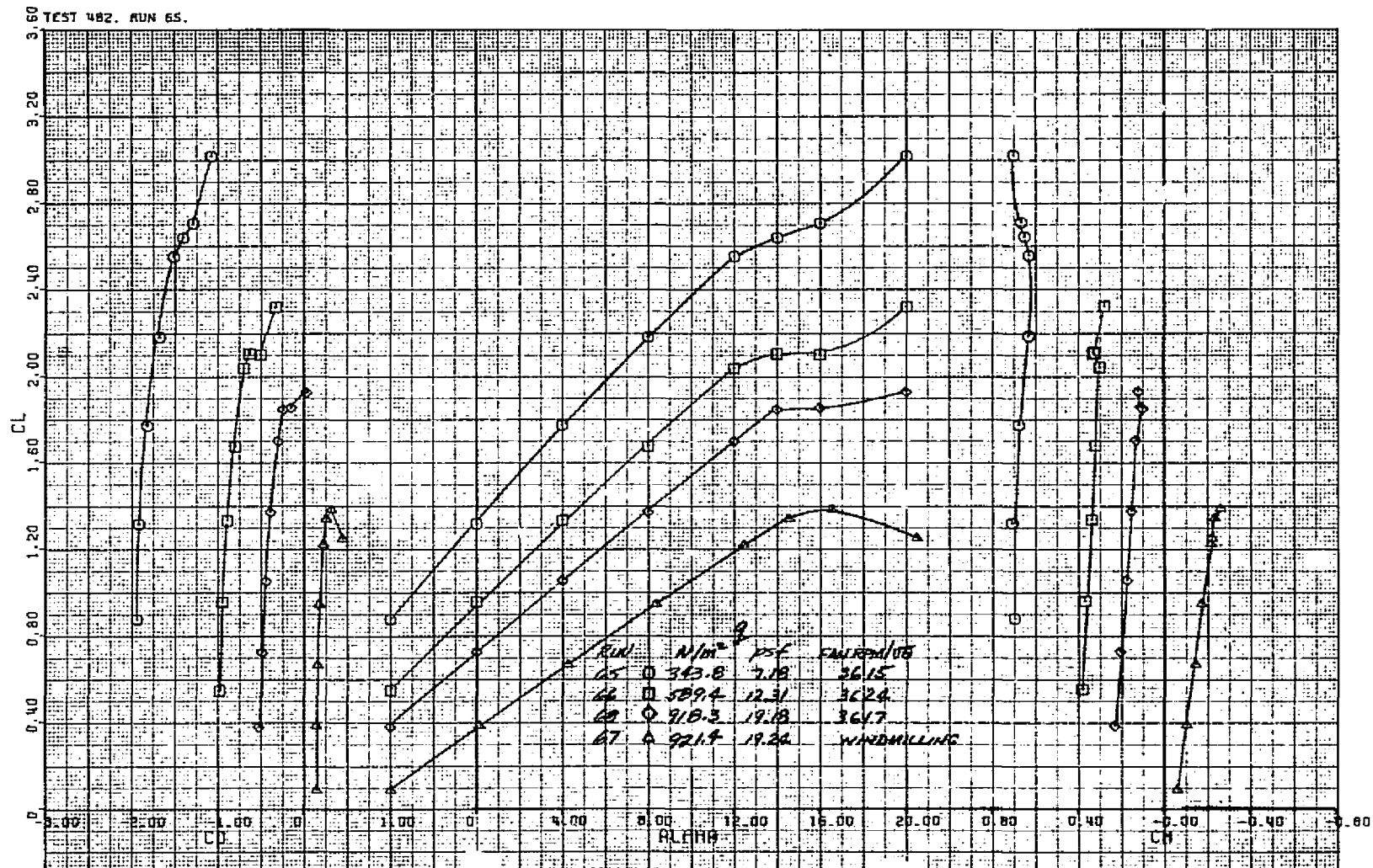
(g) $\delta_{cn} = 23°$, $\beta_v = 43°$.

Figure 14.- Concluded.
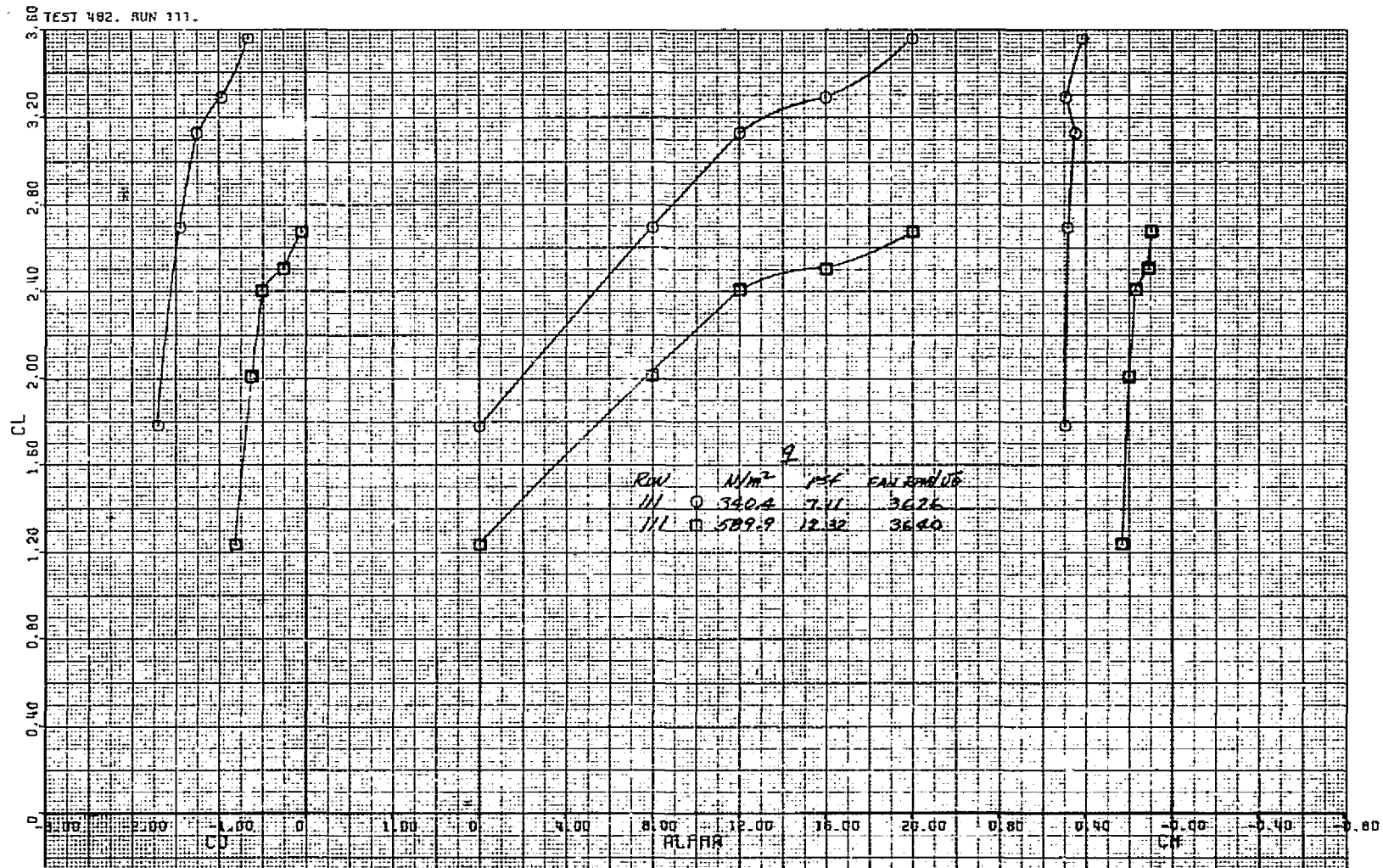
(a) Longitudinal characteristics.

Figure 15.- Longitudinal and laterial characteristics of the model with three fans operating and the rudder deflected; $\delta_r = 23°$, $\delta_{cn} = 38°$, $\beta_v = 43°$, $\delta_f = 15°$, $\delta_{ail} = 10°$, $\beta = 0°$, $i_t = 0°$.

(b) Lateral characteristics.

Figure 15.- Concluded.
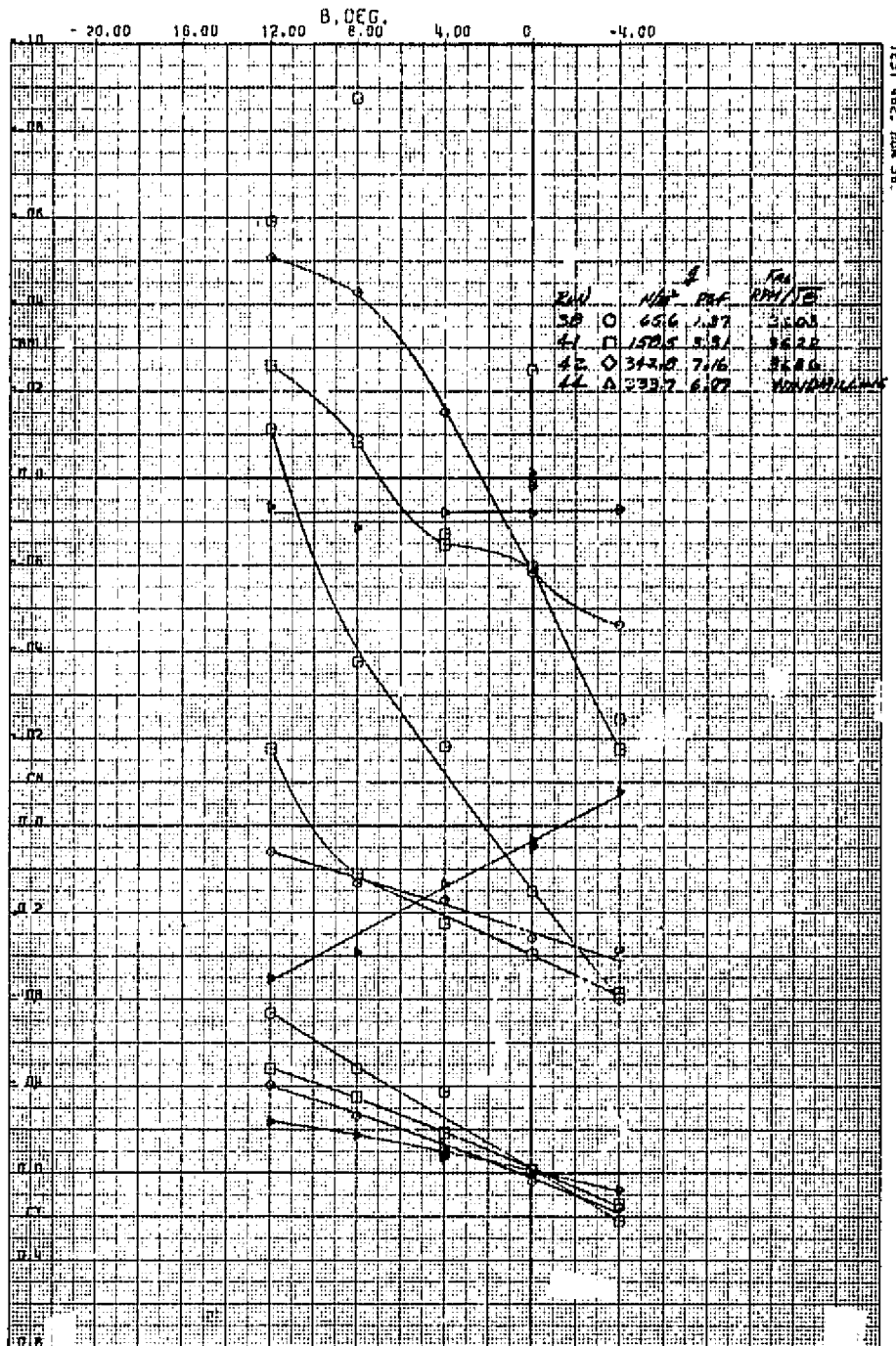
(a) $\delta_{cn} = 90°$, $\beta_v = 90°$, $\alpha_u = 0°$.

Figure 16.- Variation of side force, yawing-moment, and rolling moment coefficients with sideslip and with three fans operating; $\delta_f = 15°$, $\delta_{ail} = 10°$, $i_t = 0°$, $\delta_R = 0°$.
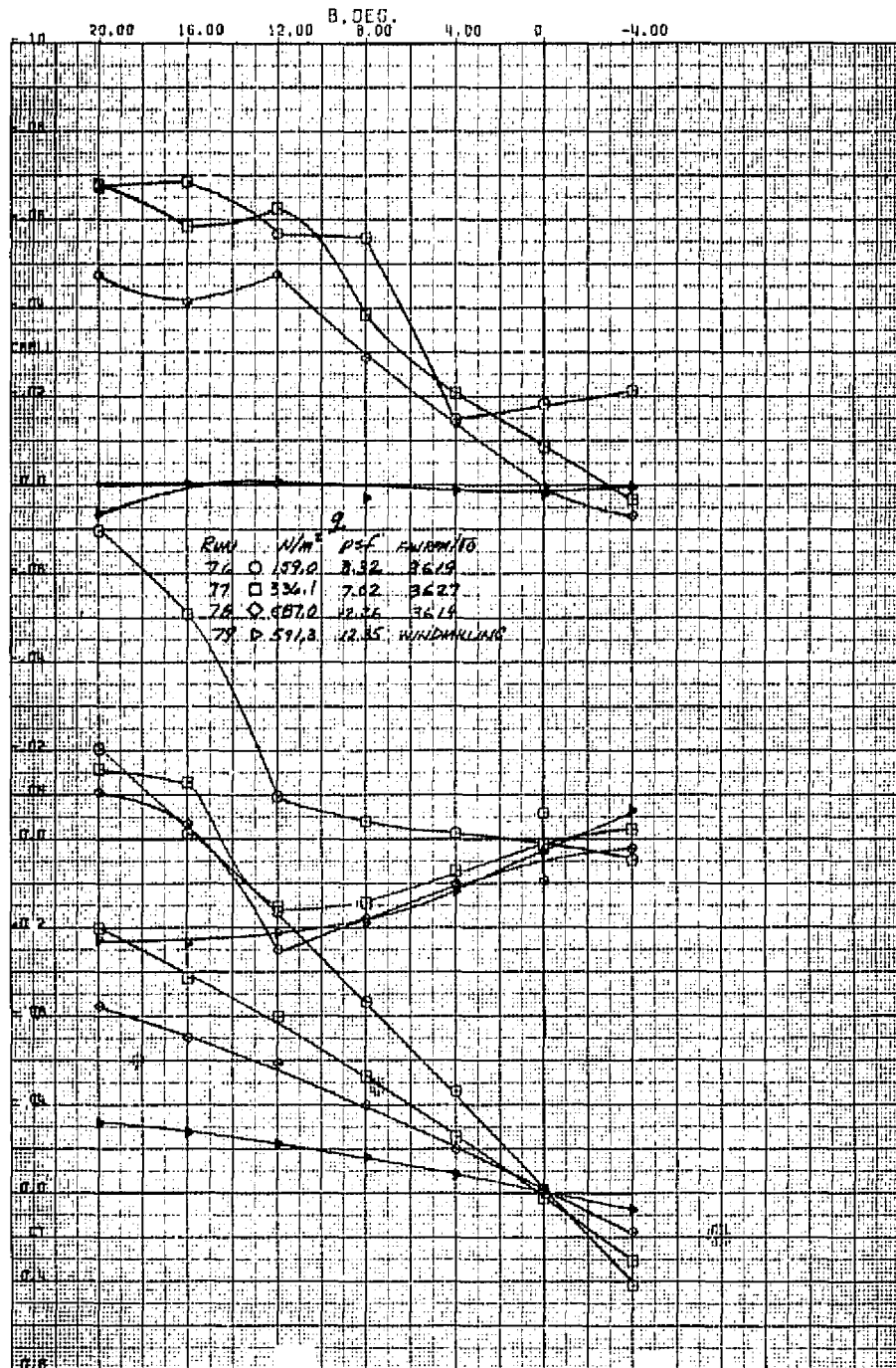
(b) $\delta_{cn} = 56°$, $\beta_v = 43P$, $\alpha_u = 0°$.

Figure 16.- Continued.
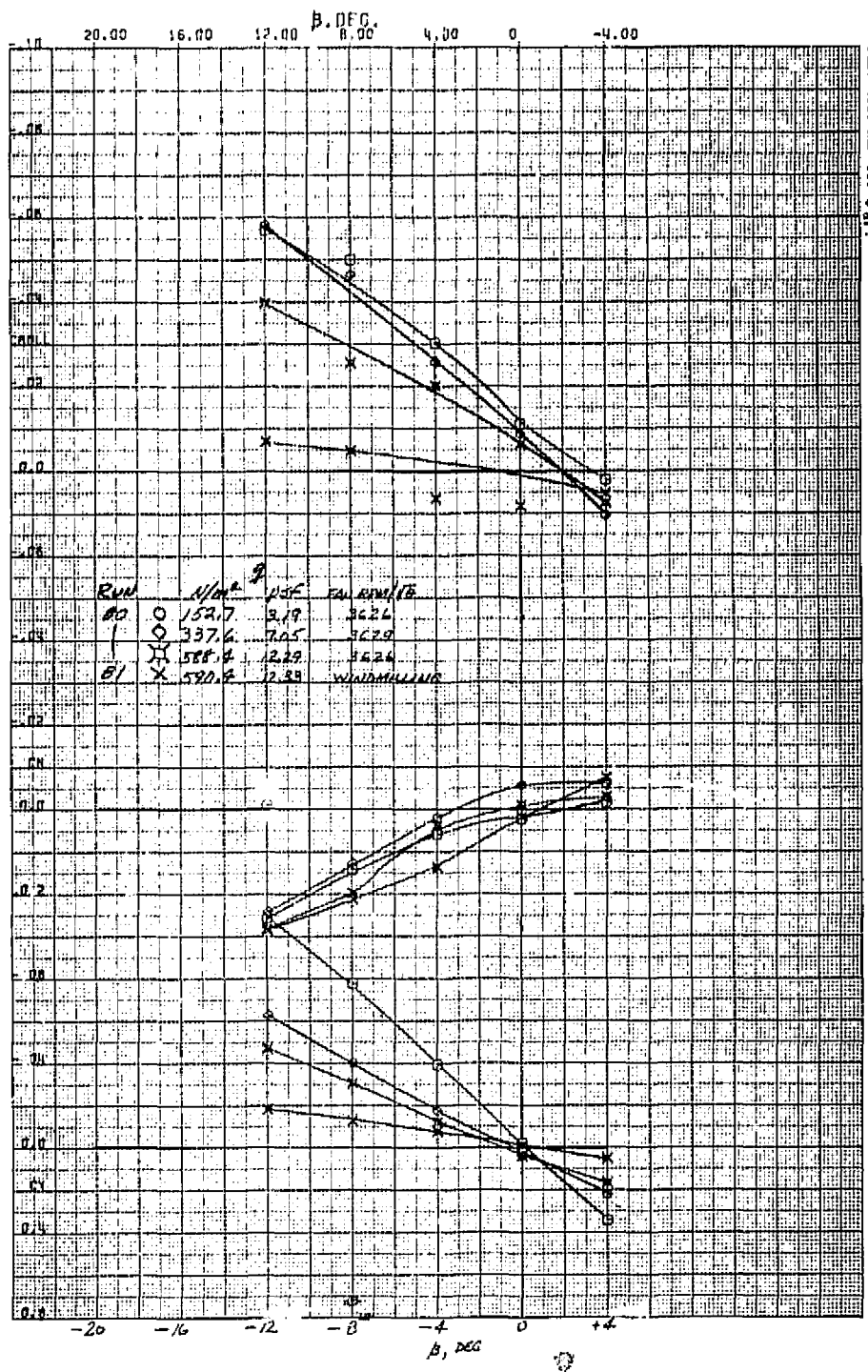
(c) $\delta_{cn} = 56°$, $\beta_v = 43°$, $\alpha_u = 8°$.

Figure 16.- Continued.
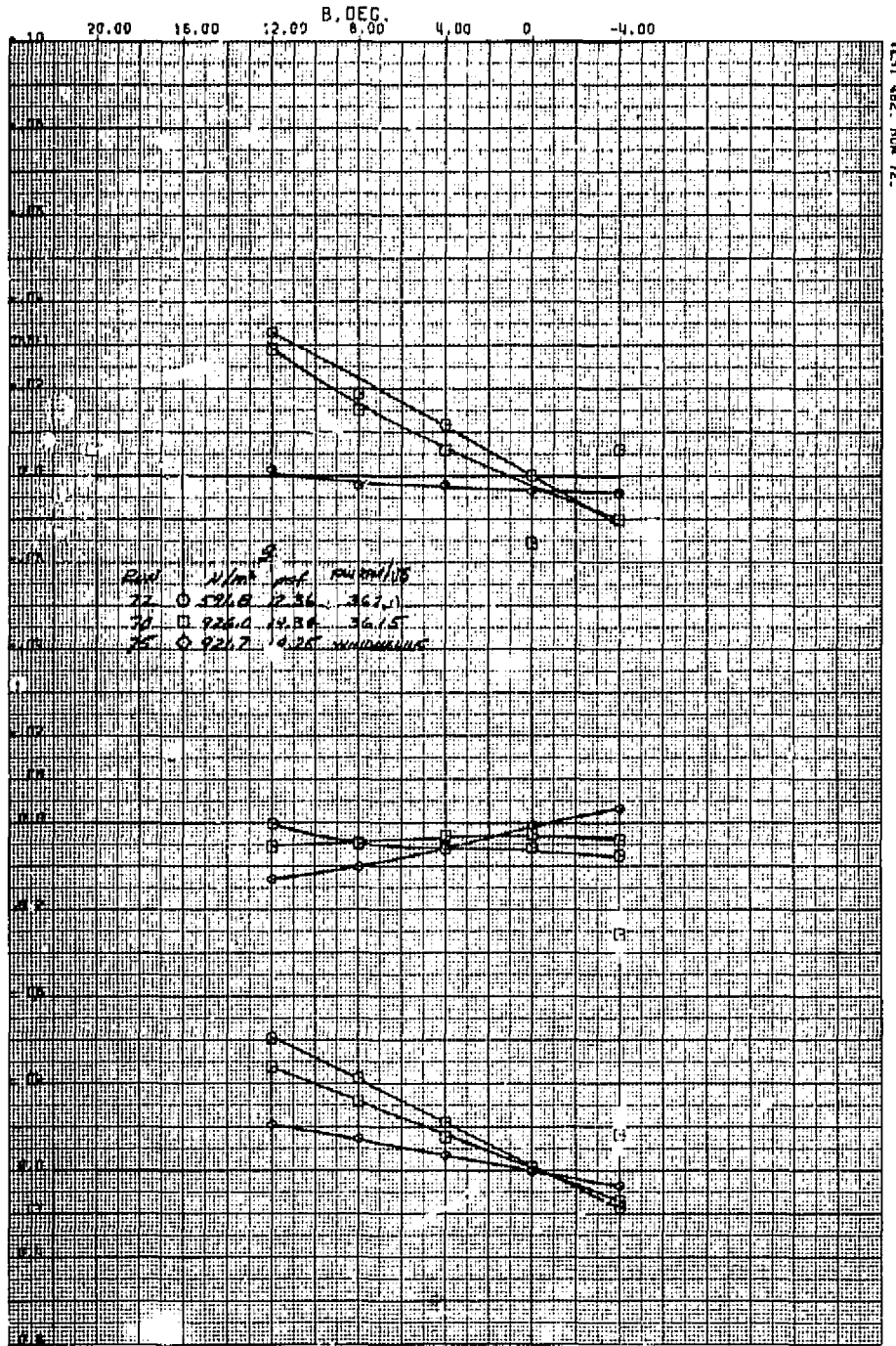
(d) $\delta_{cn} = 23°$, $\beta_v = 43°$, $\alpha_u = 0°$.

Figure 16.- Concluded.
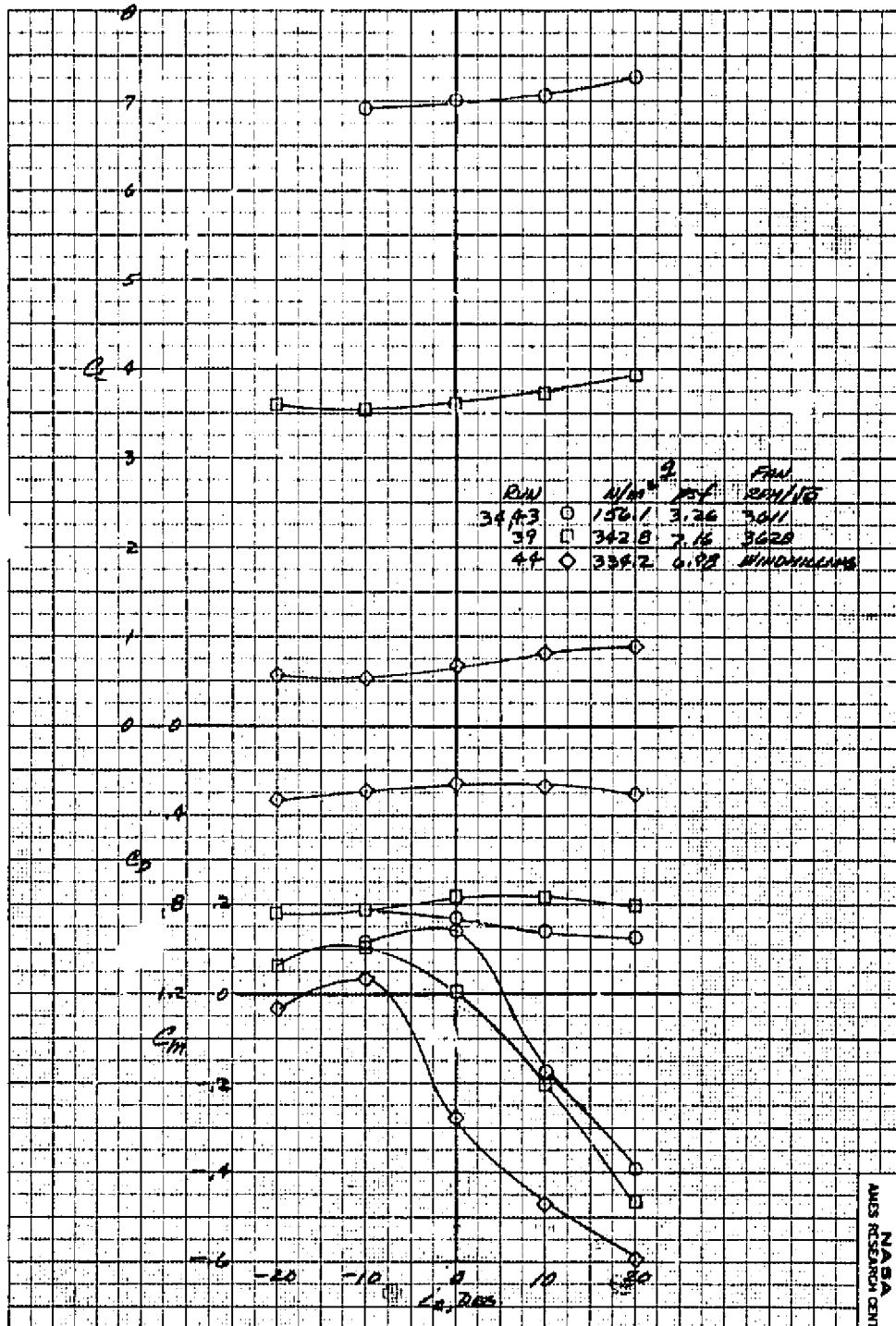
(a) $\alpha_u = 0°$.

Figure 17.- The effect of tail incidence on longitudinal aerodynamic characteristics with three fans operating; $\delta_{cn} = 90°$, $\beta_v = 90°$, $\delta_f = 15°$, $\delta_{ail} = 10°$, $\beta = 0°$, $\delta_R = 0°$.

67
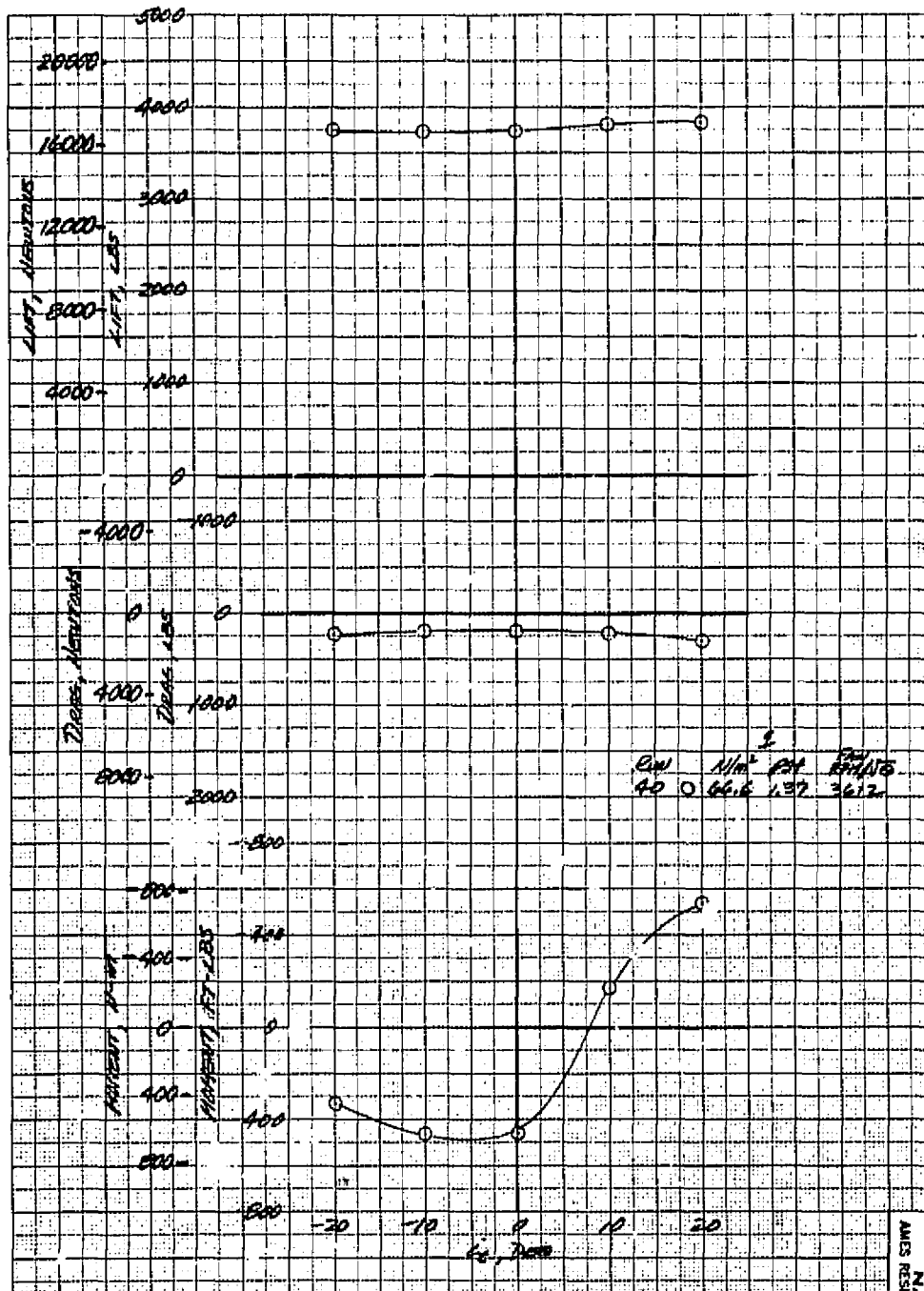
(b) $\alpha_u = 0°$.

Figure 17.- Continued.
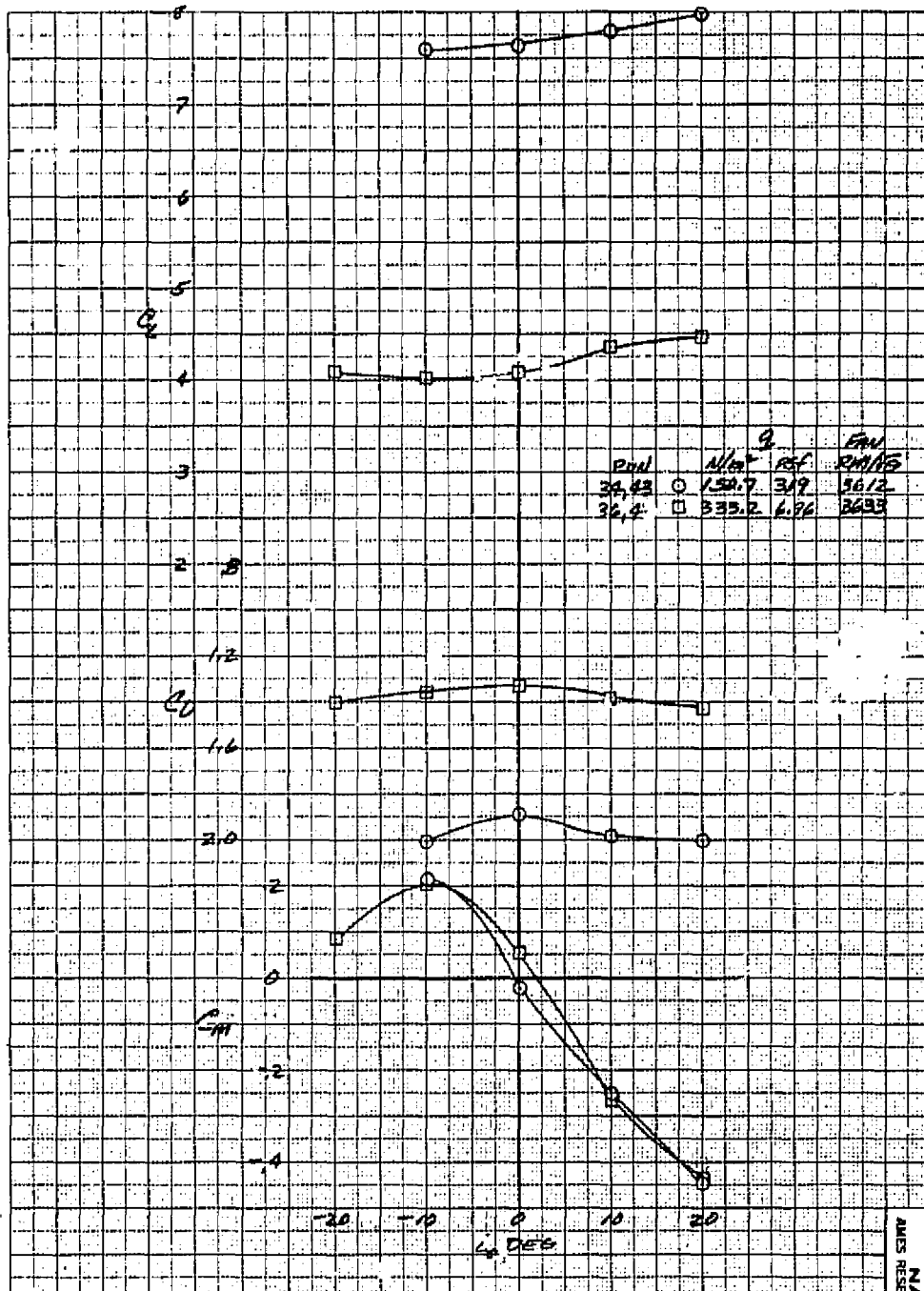
(c) $\alpha_u = 8°$.

Figure 17.- Continued.

69
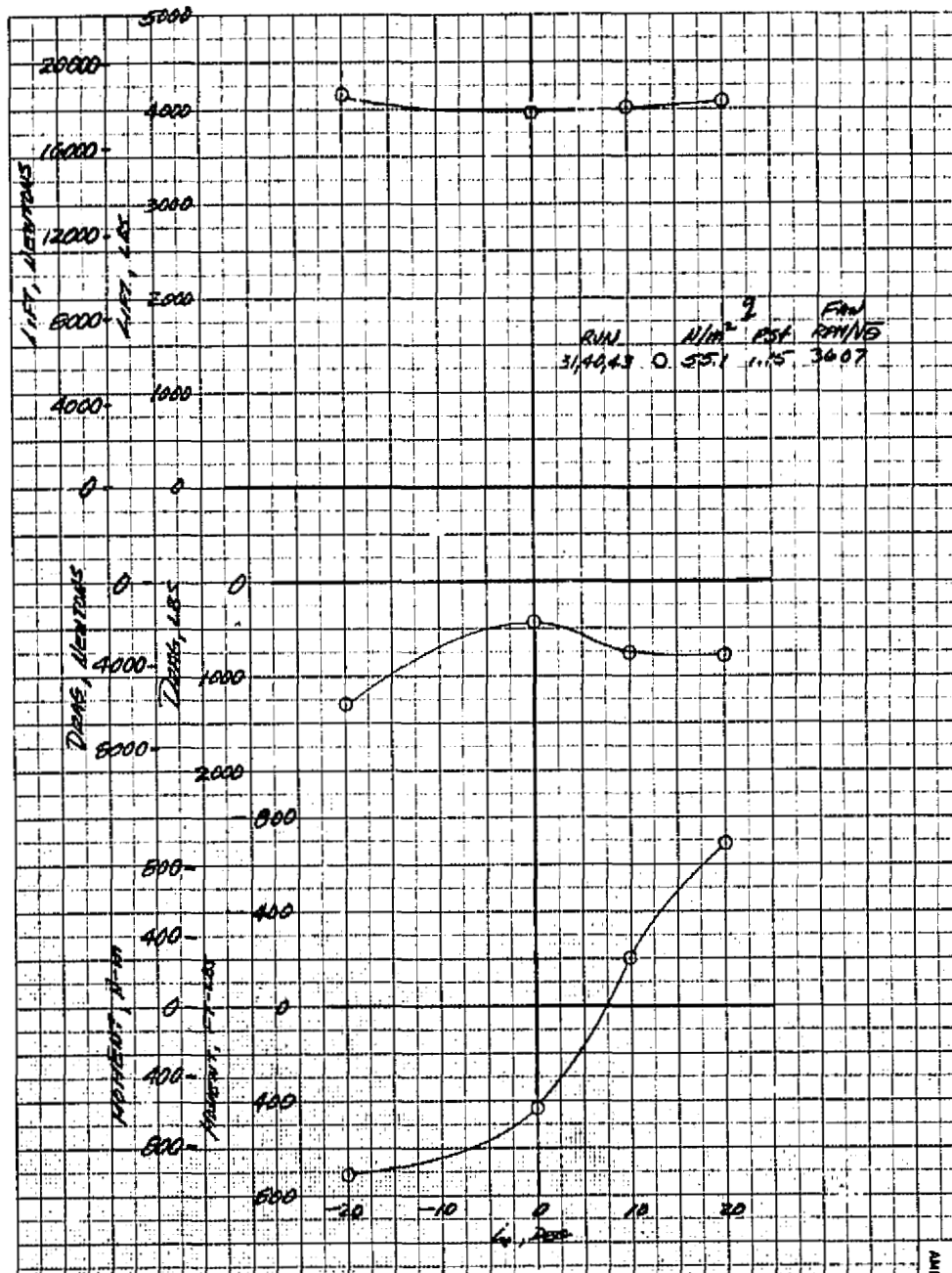
(d) $\alpha_u = 8°$.

Figure 17.- Continued.

70
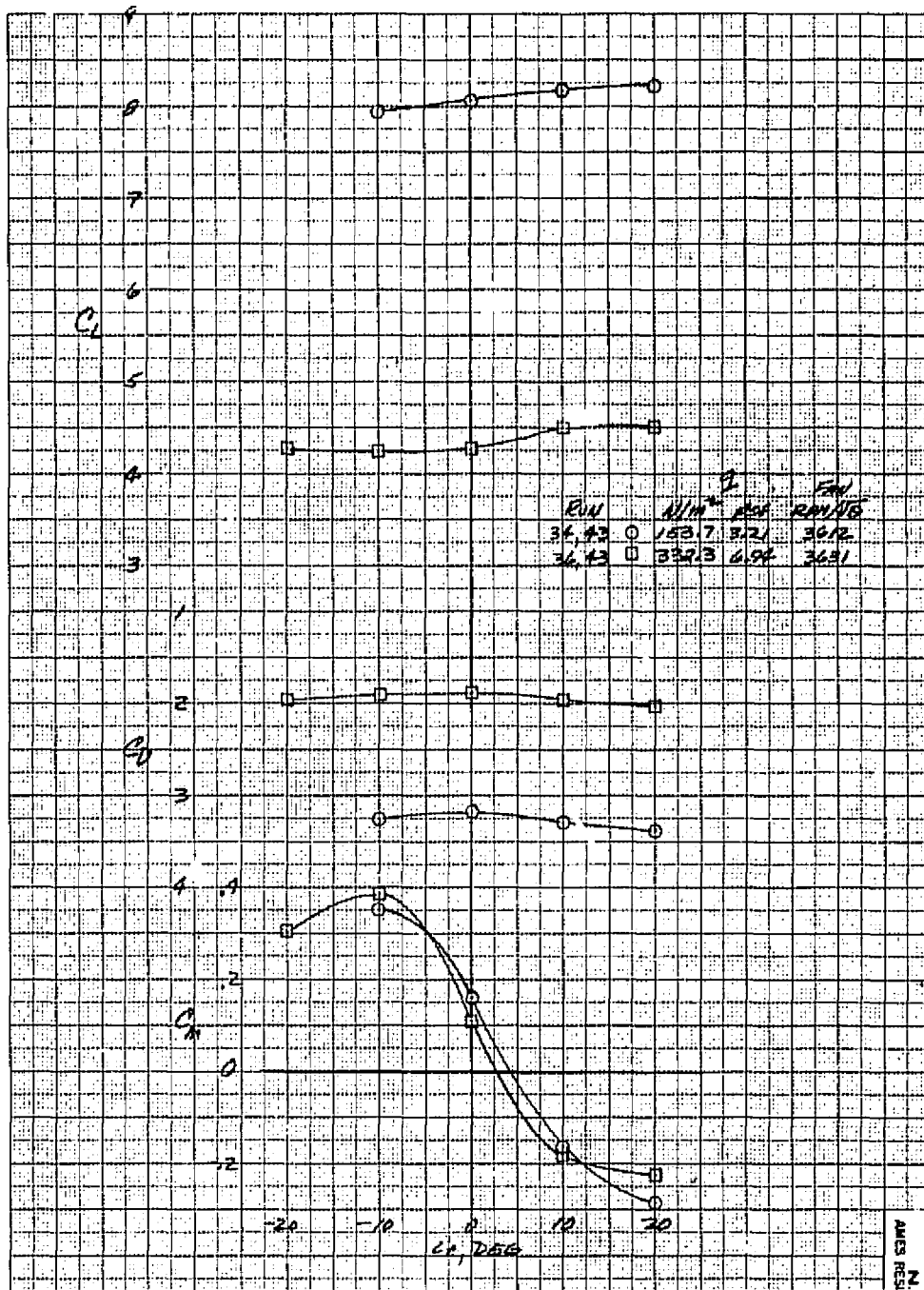
(e) $\alpha_u = 16°$.

Figure 17.- Continued.

71
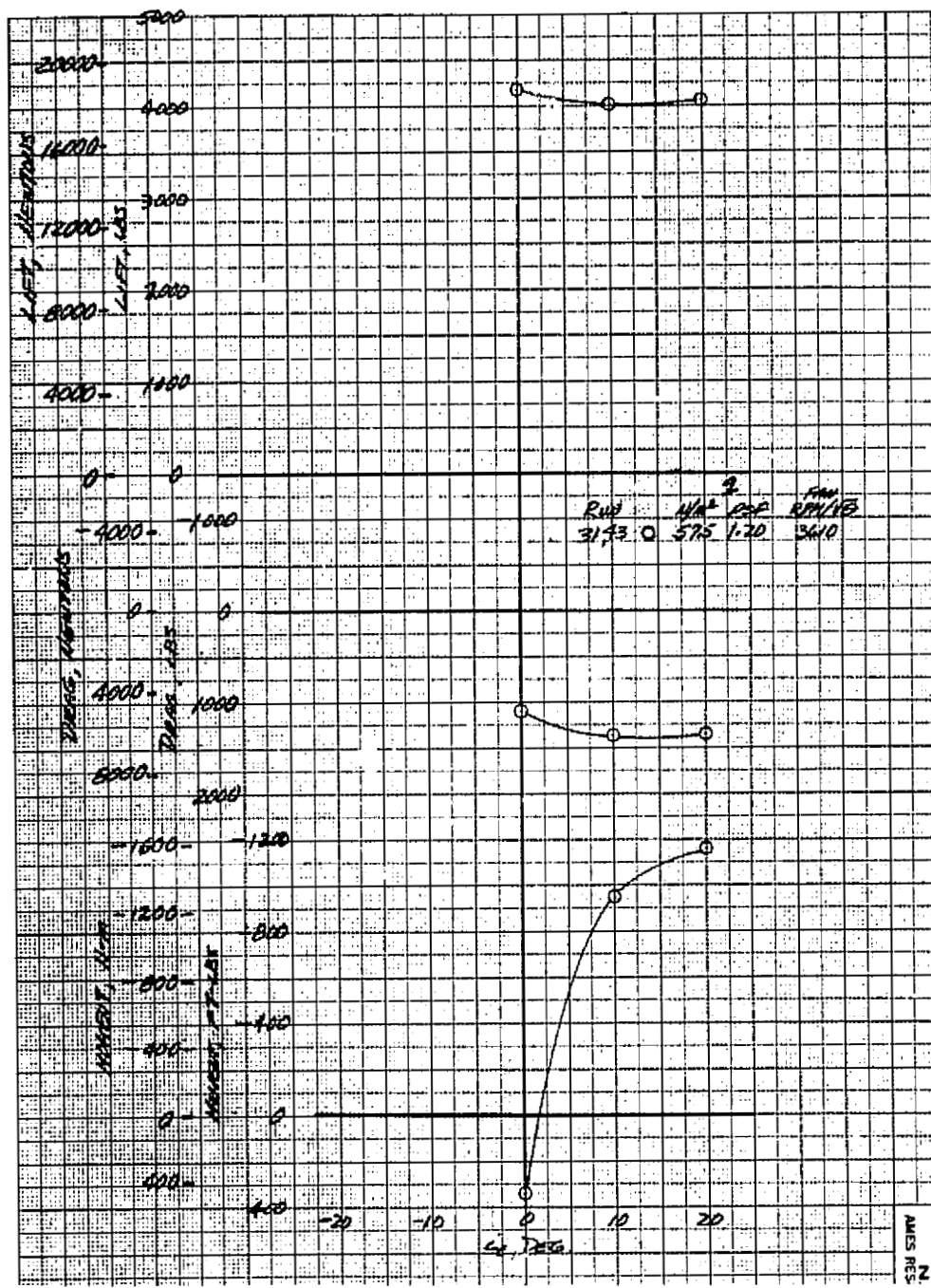
(f) $\alpha_u = 16°$.

Figure 17.- Concluded.
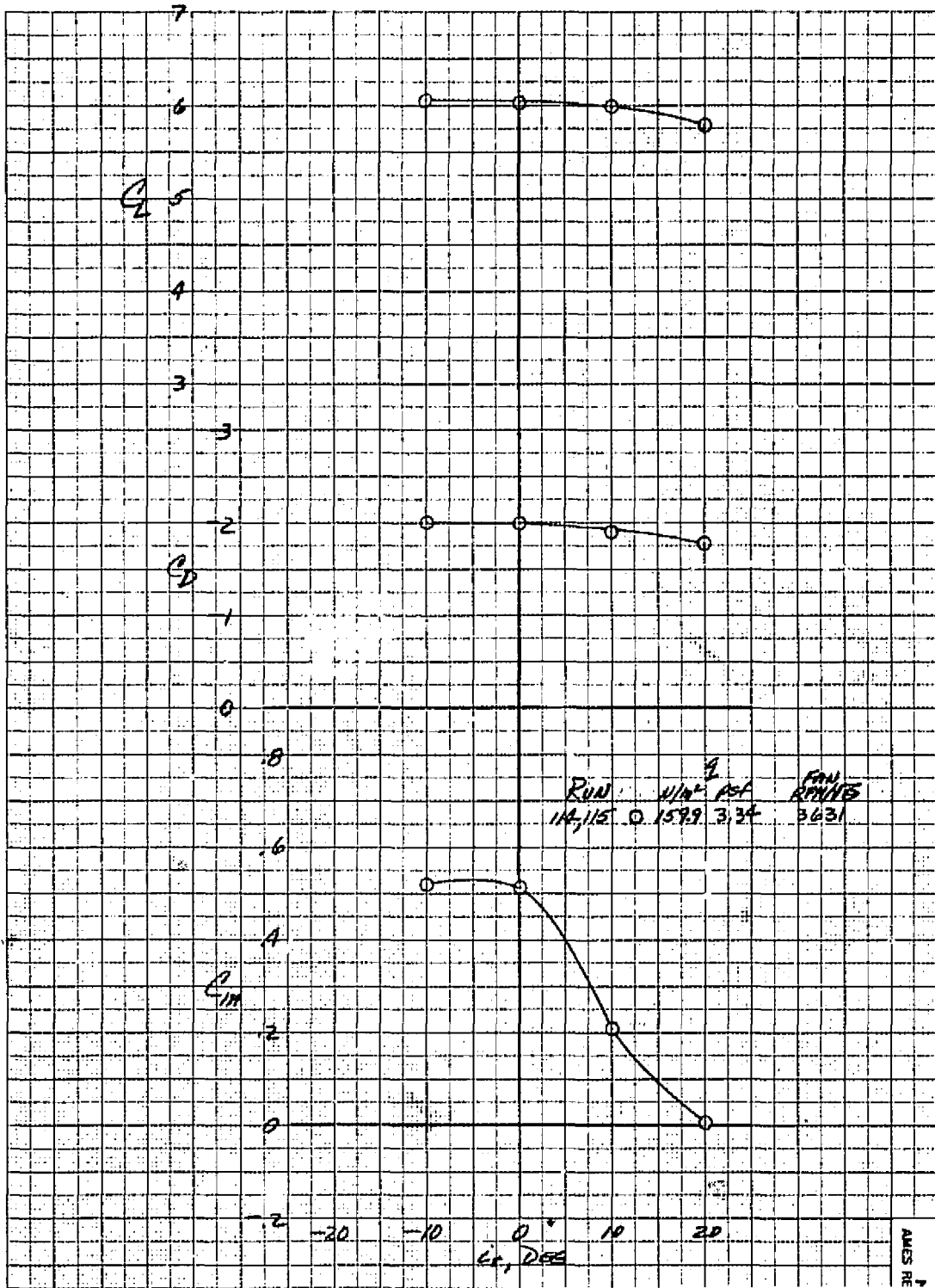
Figure 18.- The effect of tail incidence on longitudinal aerodynamic characteristics with three fans operating; $\delta_{cn} = 71°$, $\beta_v = 55°$, $\delta_f = 15°$, $\delta_{ail} = 10°$, $\alpha_u = 0°$, $\beta = 0°$, $\delta_R = 0°$.
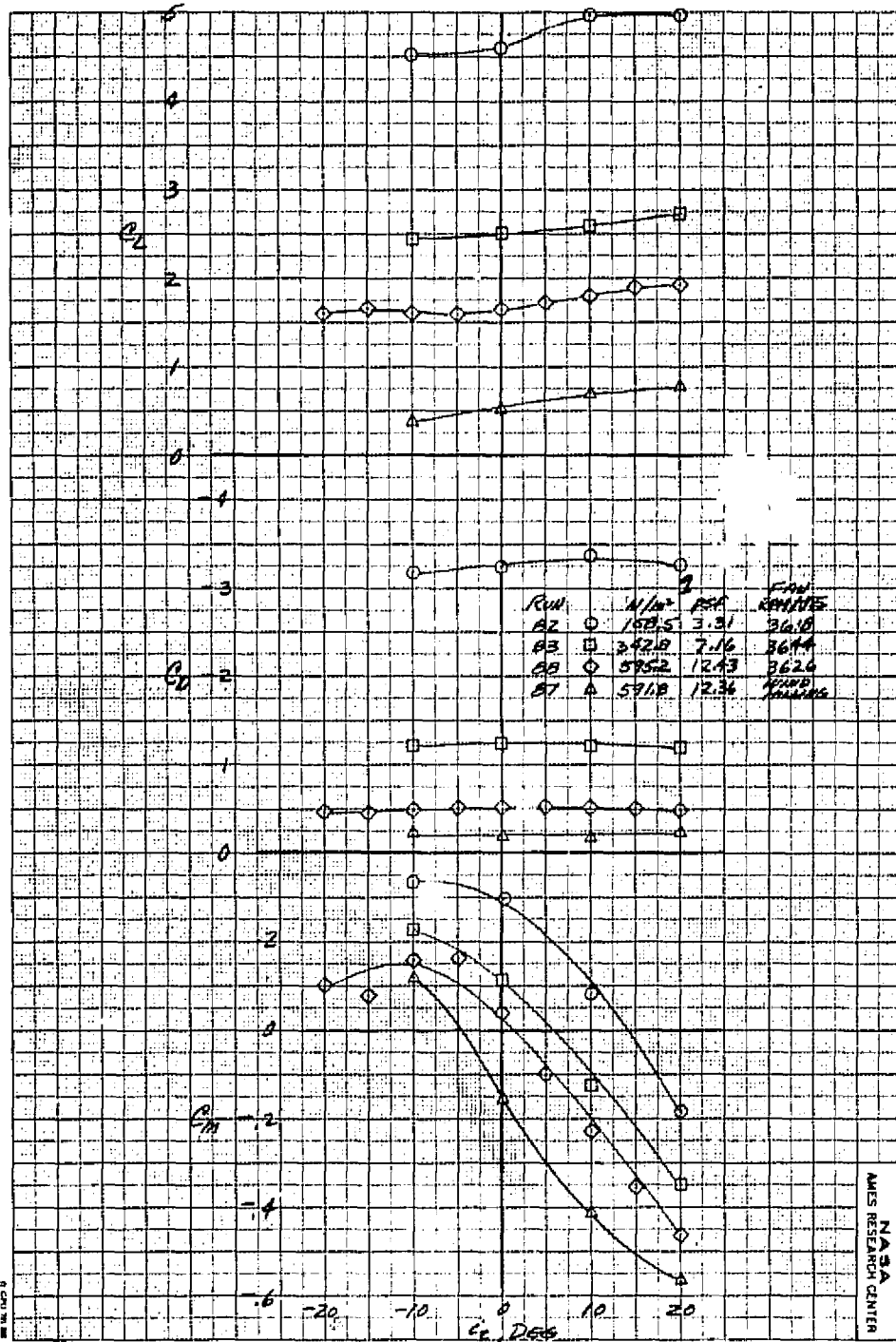
(a) $\alpha_u = 0°$.

Figure 19.- The effect of tail incidence on longitudinal aerodynamic characteristics with three fans operating; $\delta_{cn} = 56°$, $\beta_v = 43°$, $\delta_f = 15°$, $\delta_{ail} = 10°$, $\beta = 0°$, $\delta_R = 0°$.
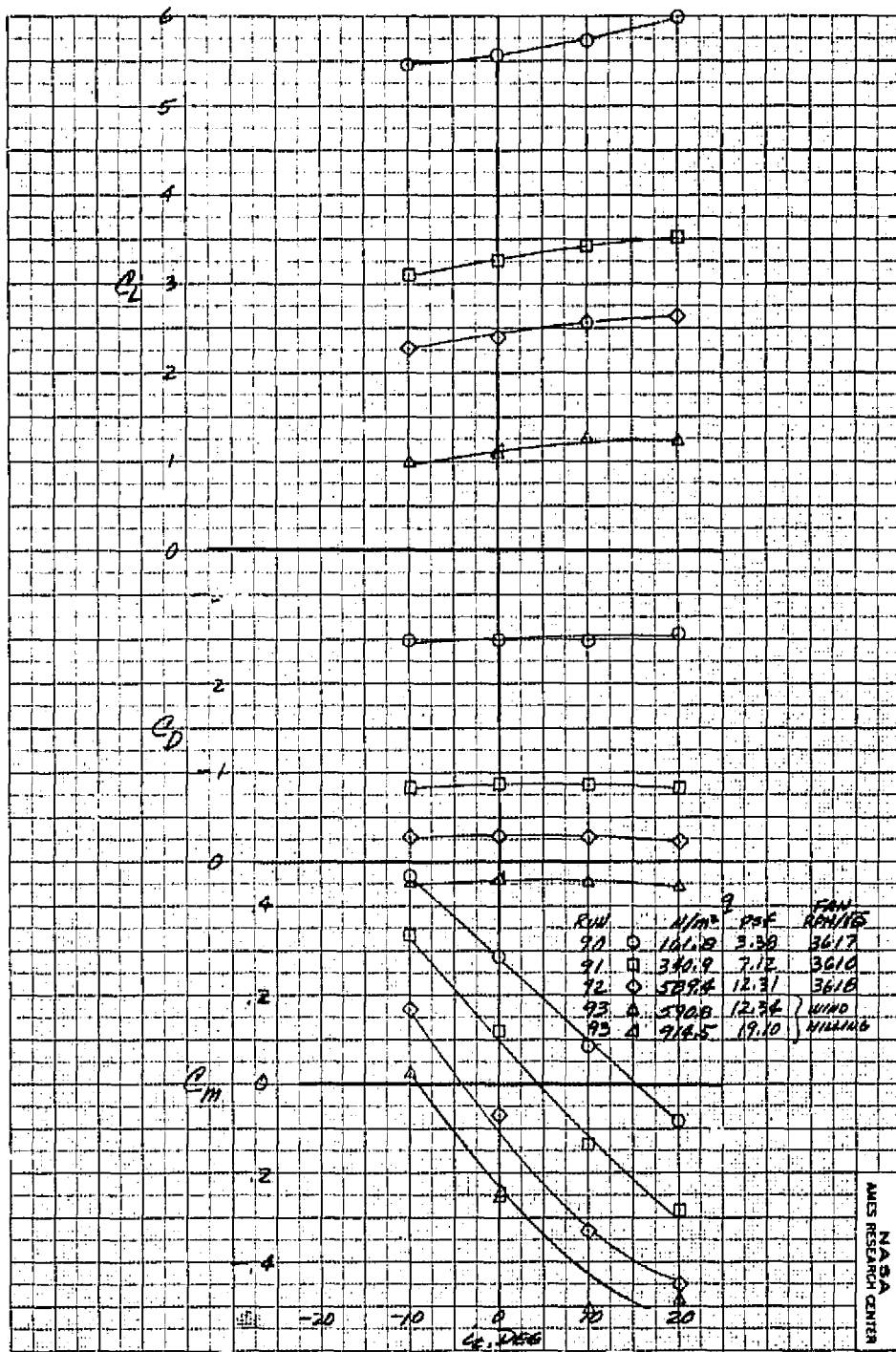
(b) $\alpha_u = 8°$.

Figure 19.- Continued.
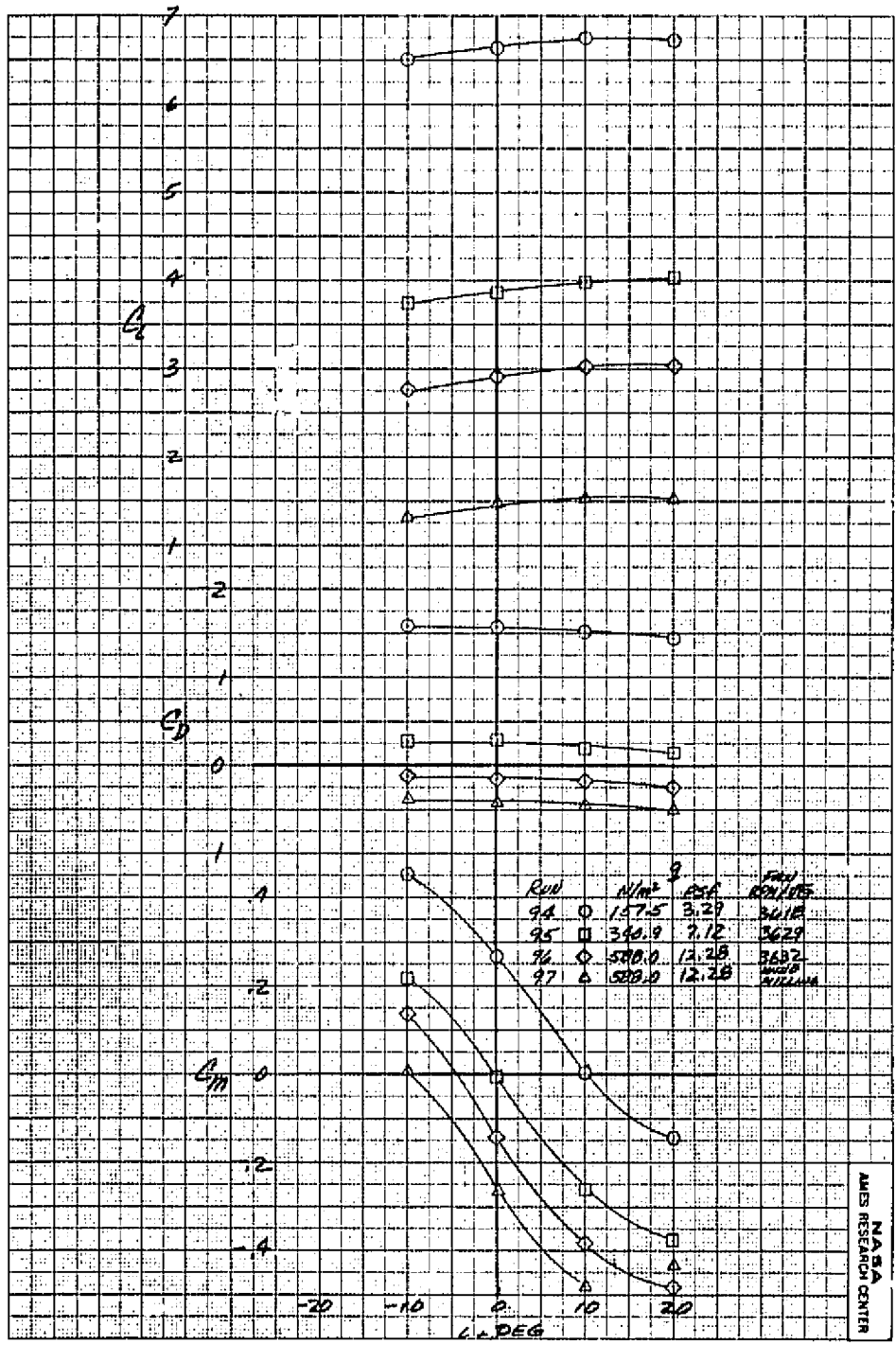
(c) $\alpha_u = 16°$.

Figure 19.- Concluded.
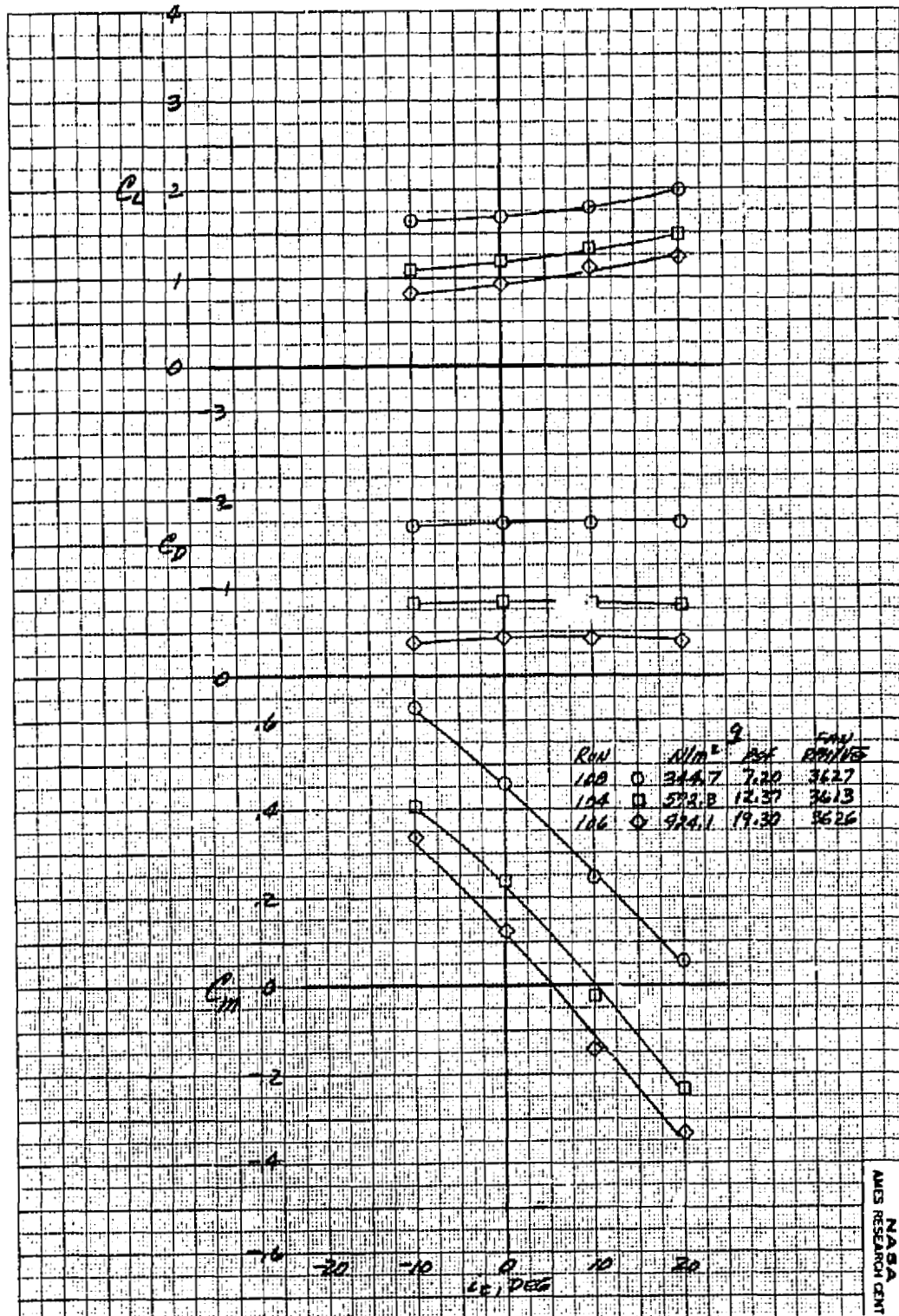
Figure 20.- The effect of tail incidence on longitudinal aerodynamic characteristics with three fans operating; $\delta_{cn} = 38°$, $\beta_v = 43°$, $\delta_f = 15°$, $\delta_{ail} = 10°$, $\beta = 0°$, $\alpha_u = 0°$, $\delta_R = 0°$.
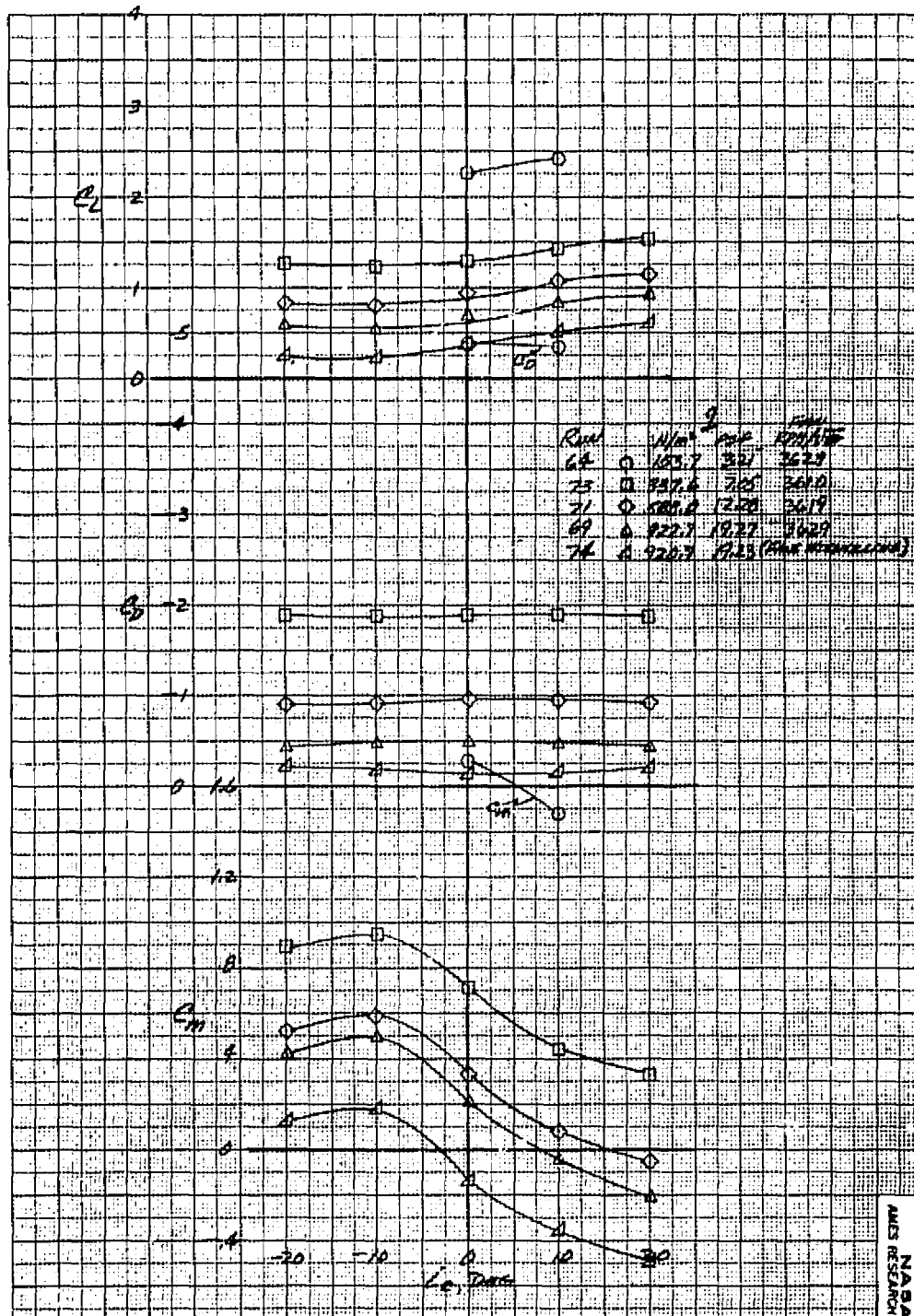
(a) $\alpha_u = 0°$.

Figure 21.- The effect of tail incidence on longitudinal aerodynamic
characteristics with three fans operating; $\delta_{cn} = 23°$, $\beta_v = 43°$,
$\delta_f = 15°$, $\delta_{ail} = 10°$, $\beta = 0°$, $\delta_R = 0°$.
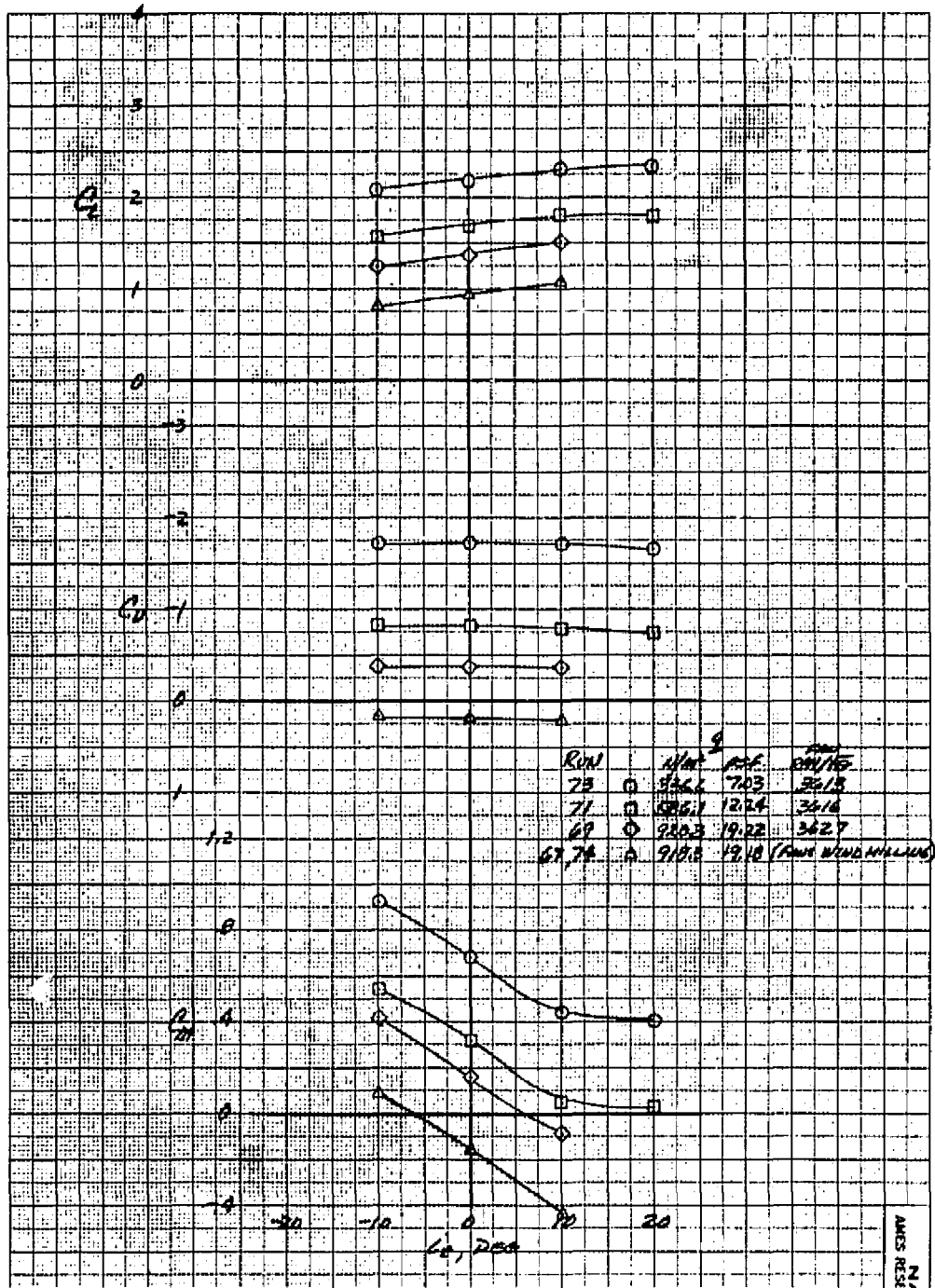
(b) $\alpha_u = 8°$.

Figure 21.- Continued.
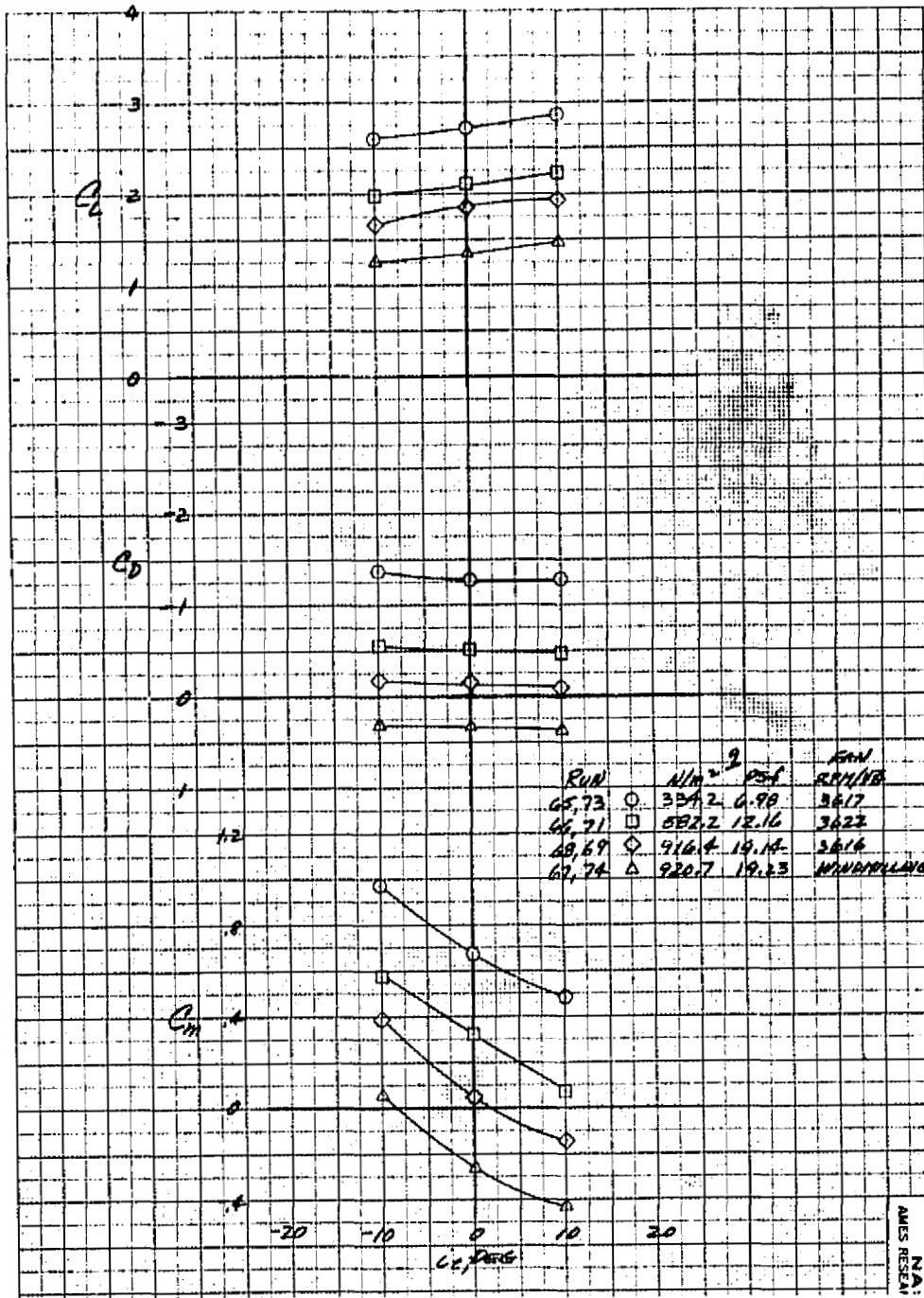
(c) $\alpha_u = 16°$.

Figure 21.- Concluded.
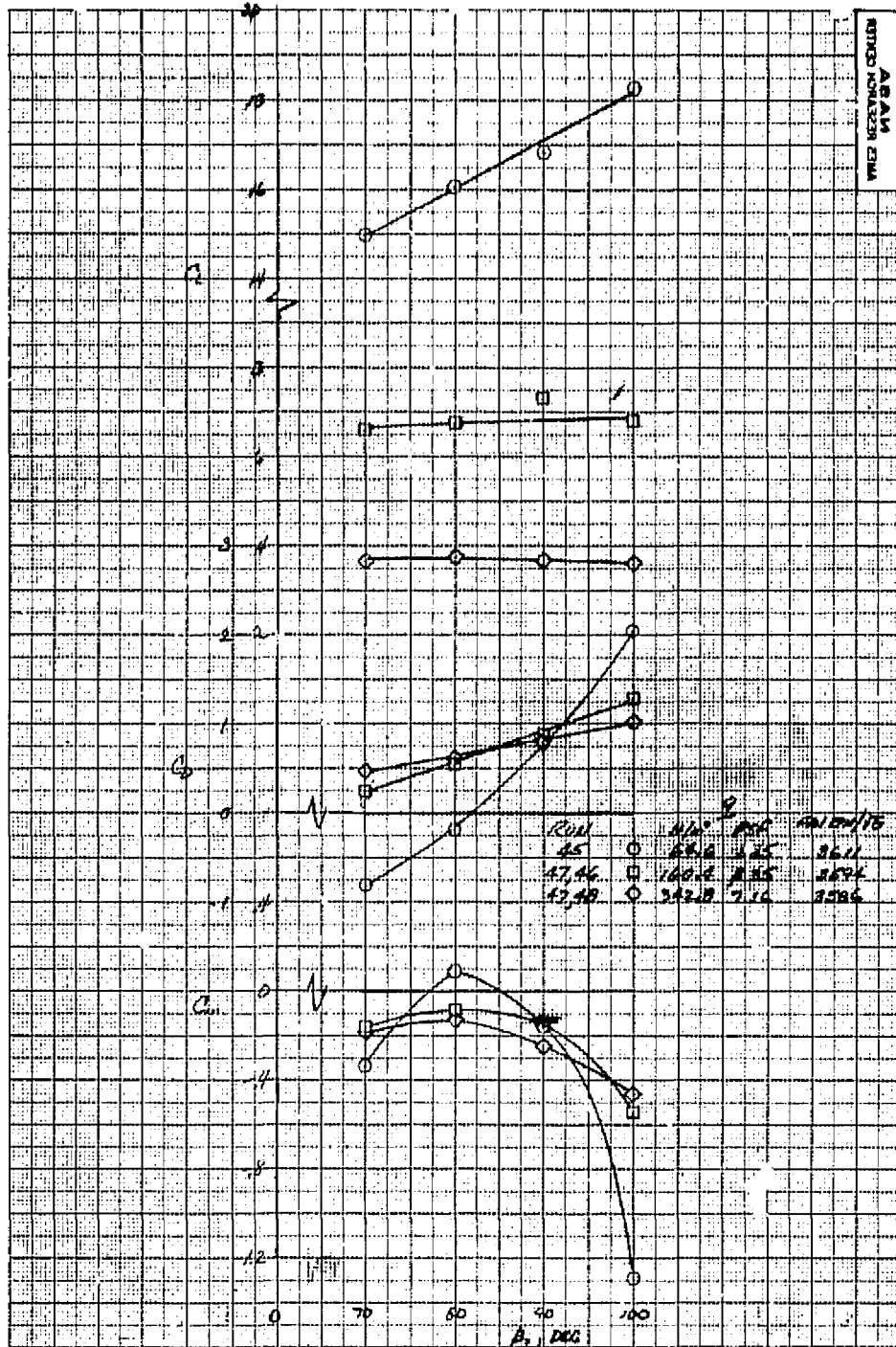
(a) Horizontal tail off.

Figure 22.- Effect of forward lift fan exit louver deflection angle on
the model longitudinal characteristics with three fans operating;
δ_{cn} = 90°, δ_f = 15°, δ_{ail} = 10°, α_u = 0°, β = 0°, δ_R = 0°.
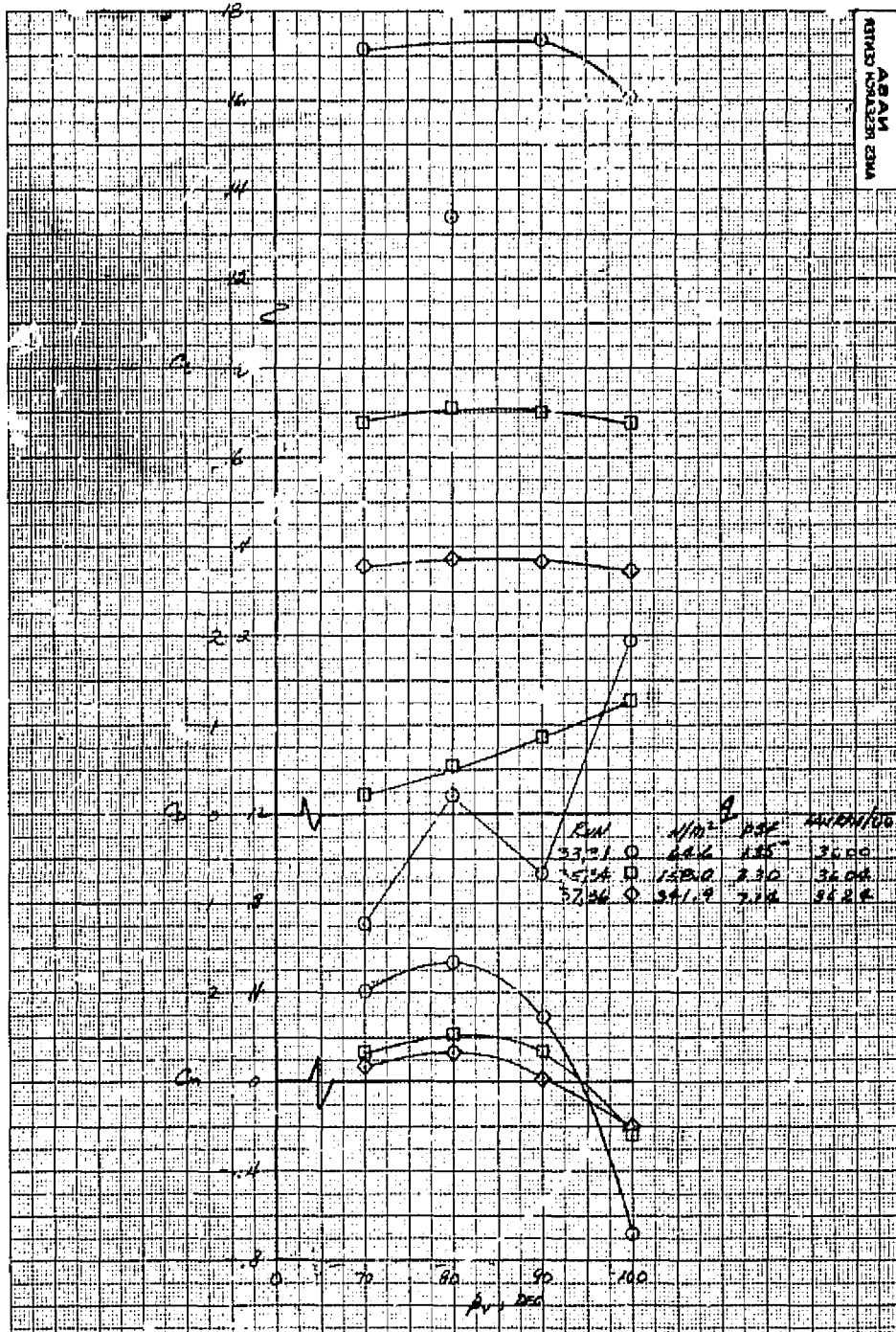
(b) Horizontal tail on, $i_t = 0°$.

Figure 22.- Concluded.
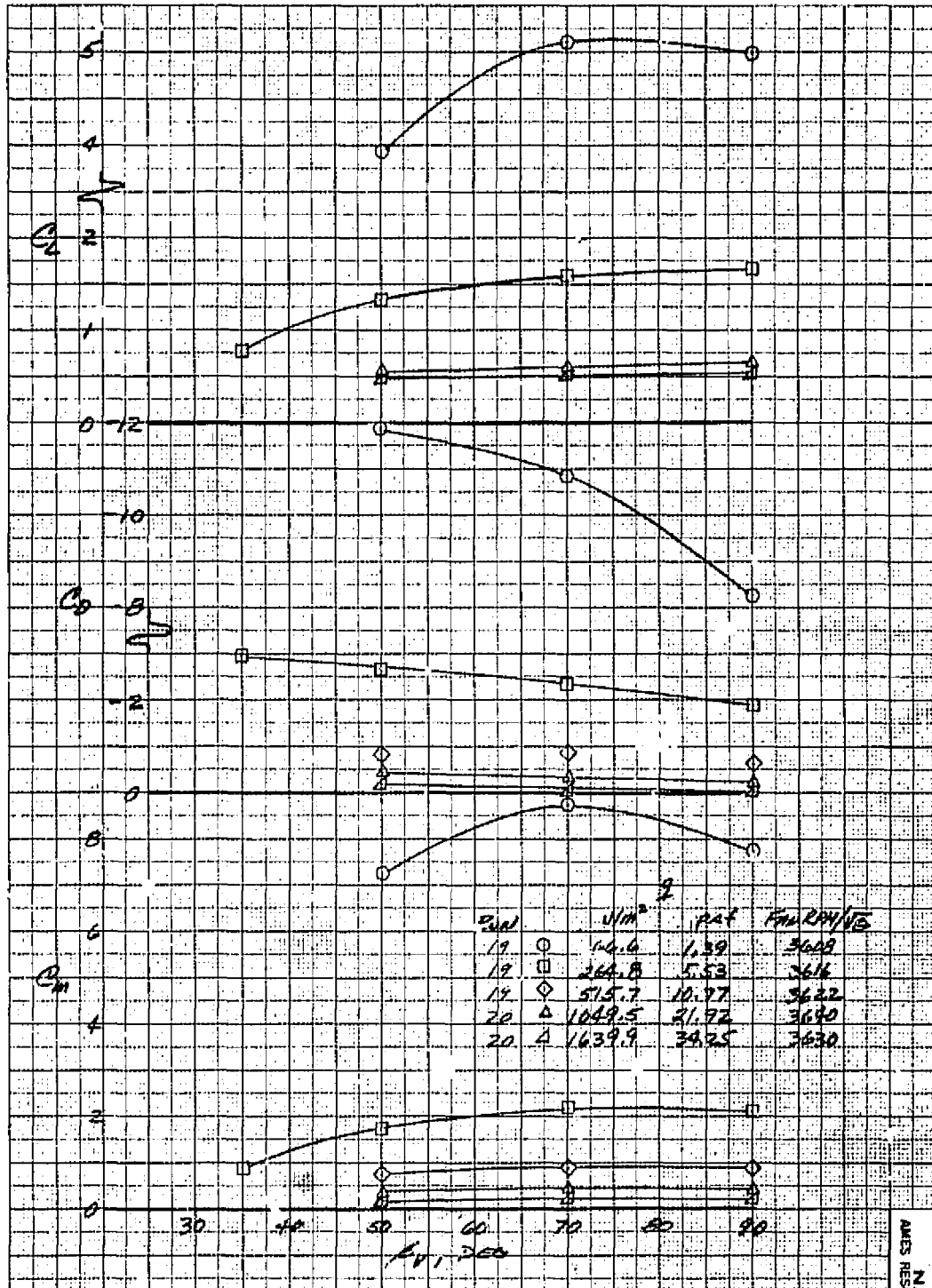
(a) $\alpha_u = 0°$.

Figure 23.- Effect of forward lift fan exit louver deflection angle on model longitudinal characteristics with three fans operating; $\delta_{cn} = 0°$, horizontal tail off, $\delta_f = 15°$, $\delta_{ail} = 10°$, $\beta = 0°$, $\delta_R = 0°$.
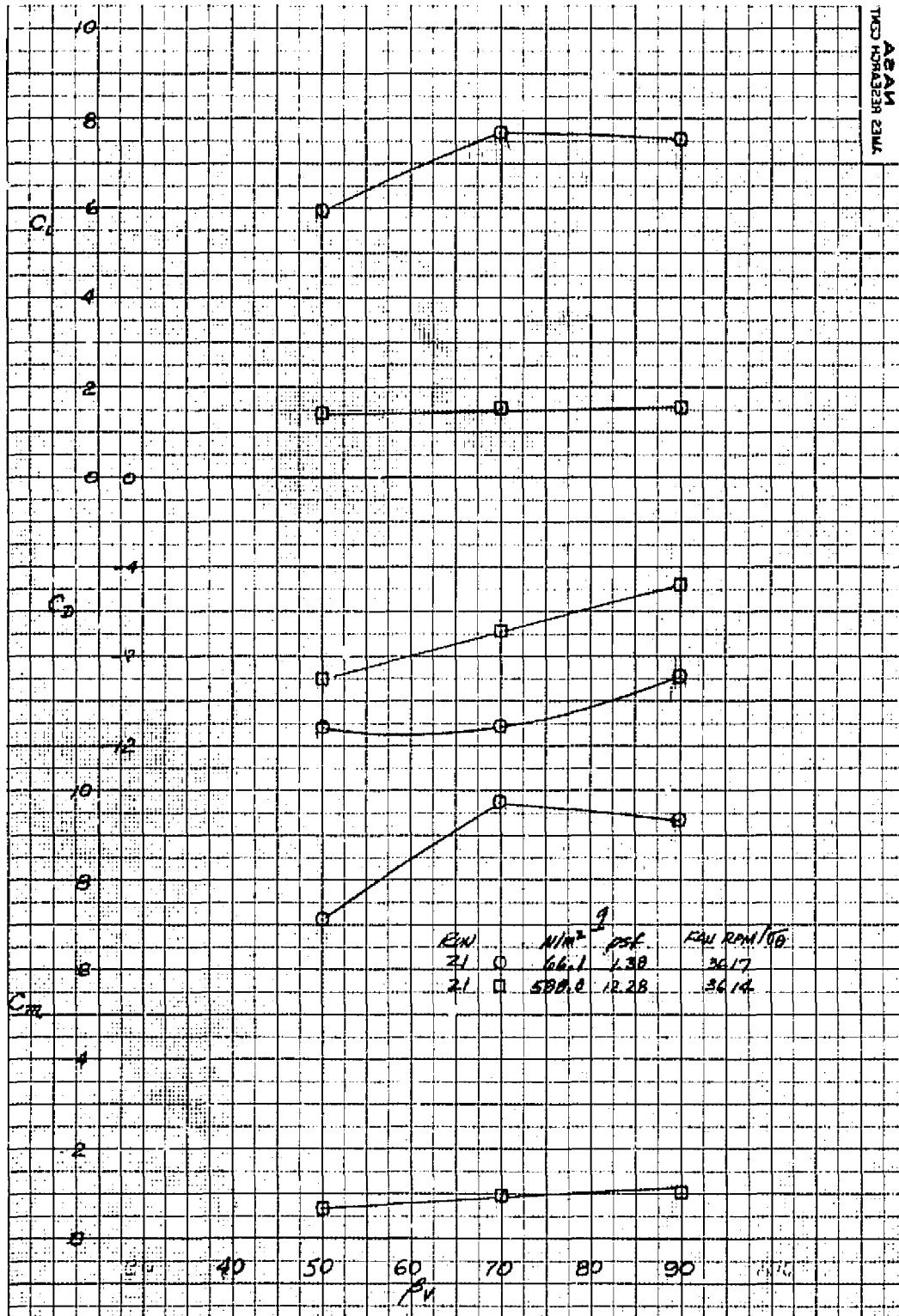
(b) $\alpha_u = 8°$.

Figure 23.- Concluded.
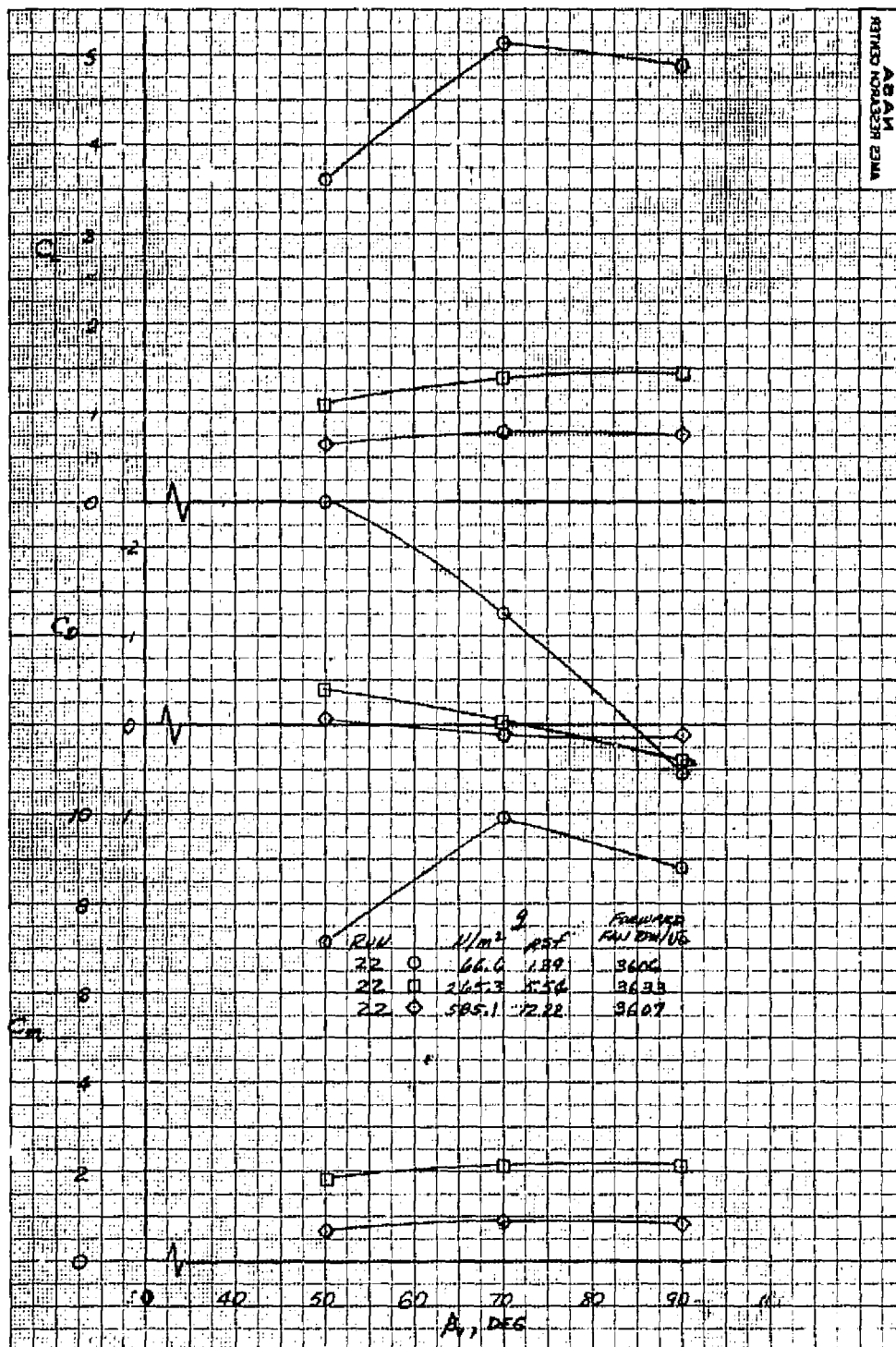
Figure 24.- Effect of forward lift fan exit louver deflection on the model longitudinal characteristics with the cruise fans wind milling; $\delta_{cn} = 0°$, $\delta_f = 15°$, $\delta_{ail} = 10°$, $\alpha_u = 0°$, horizontal tail off, $\beta = 0°$, $\delta_R = 0°$.
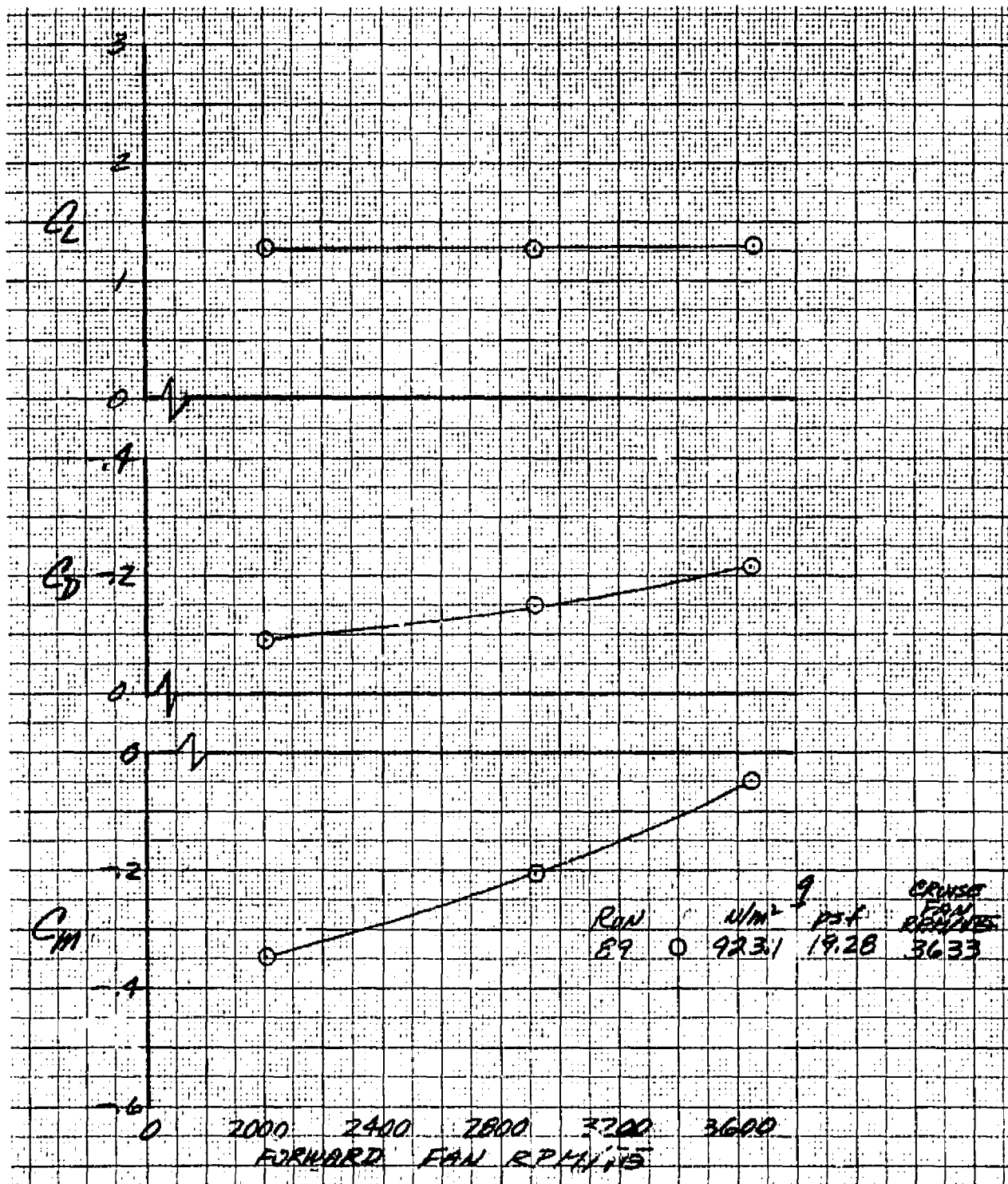
Figure 25.- The effect of forward fan RPM on the longitudinal aerodynamic
characteristics; $\delta_{cn} = 56°$, $\delta_f = 15°$, $\delta_{ail} = 10°$, $i_t = 0°$, $\alpha_u = 0°$,
$\beta_v = 43°$, $\beta = 0°$.
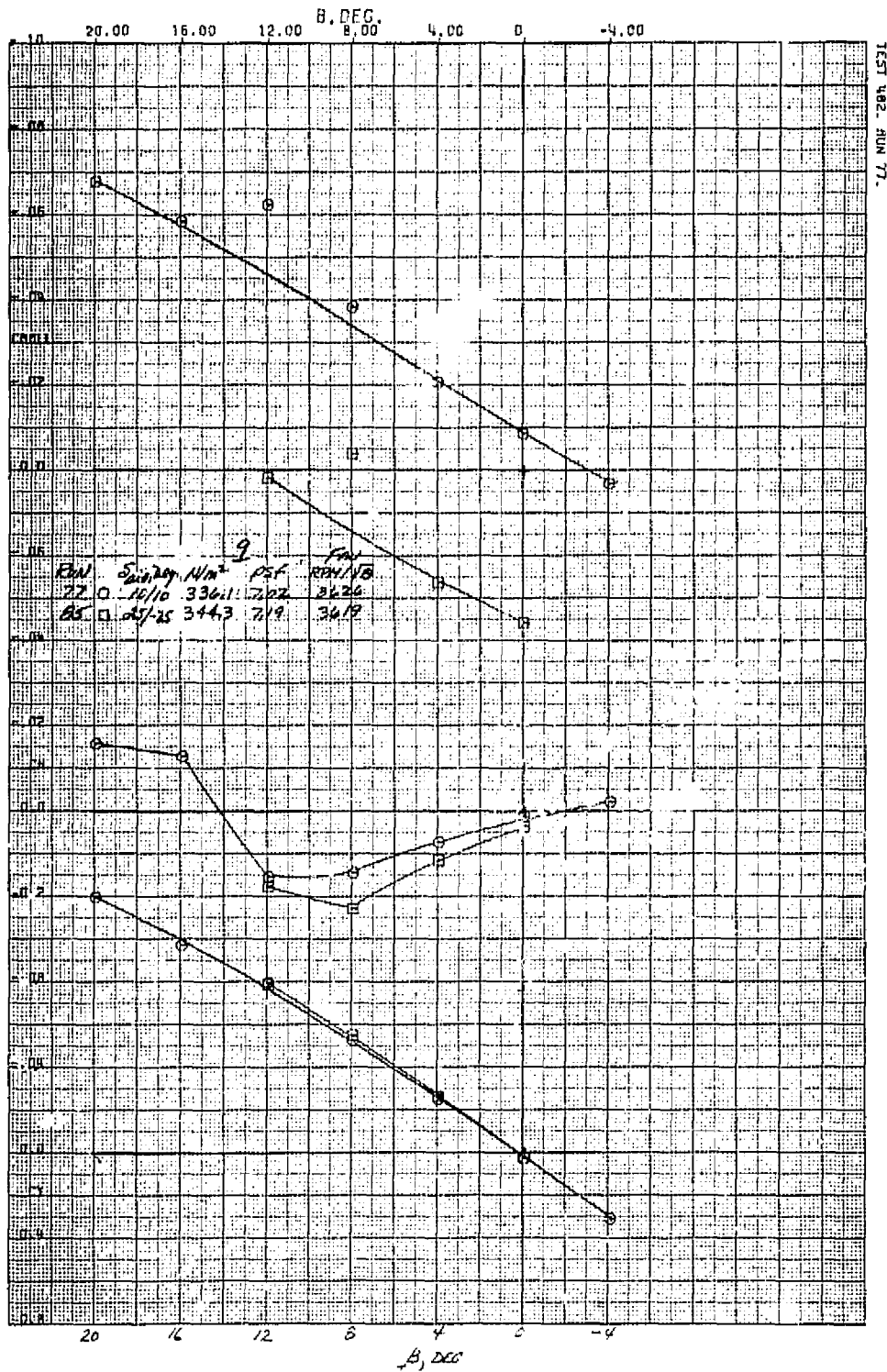
Figure 26.- Variation of side force, yawing-moment, and rolling-moment coefficients with sideslip with three fans operating; $\delta_{cn} = 56°$, $\delta_f = 15°$, $\delta_{ail} = 10°$, $\beta_v = 43°$, $i_t = 0°$, $\alpha_u = 0°$, $\delta_R = 0°$.
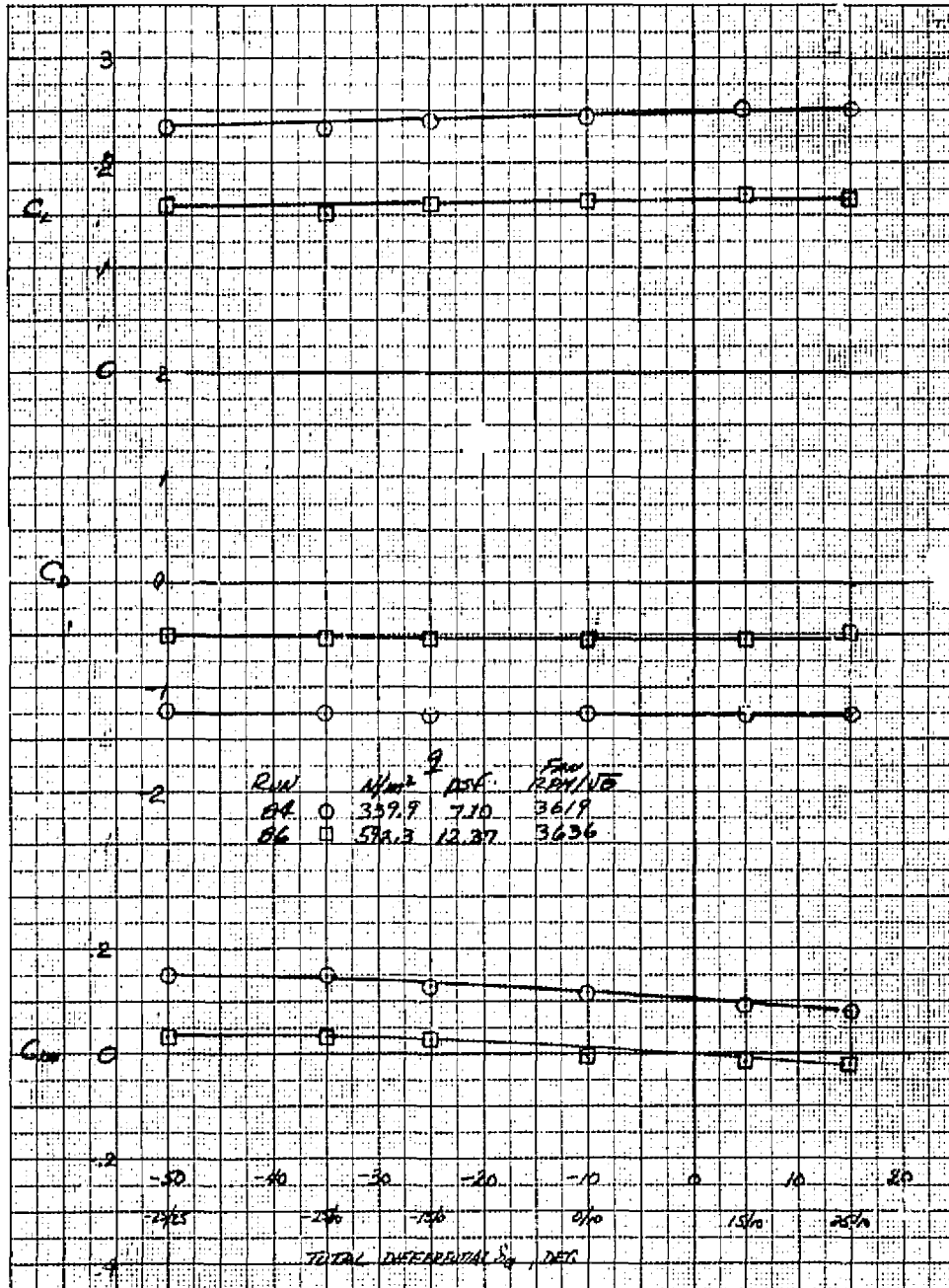
(a) Longitudinal characteristics.

Figure 27.— The effect of the differential aileron deflection on the model aerodynamic characteristics with three fans operating; $\delta_{cn} = 56°$, $\beta_v = 43°$, $\delta_f = 15°$, $i_t = 0°$, $\beta = 0°$, $\delta_R = 0°$, $\alpha_u = 0°$.
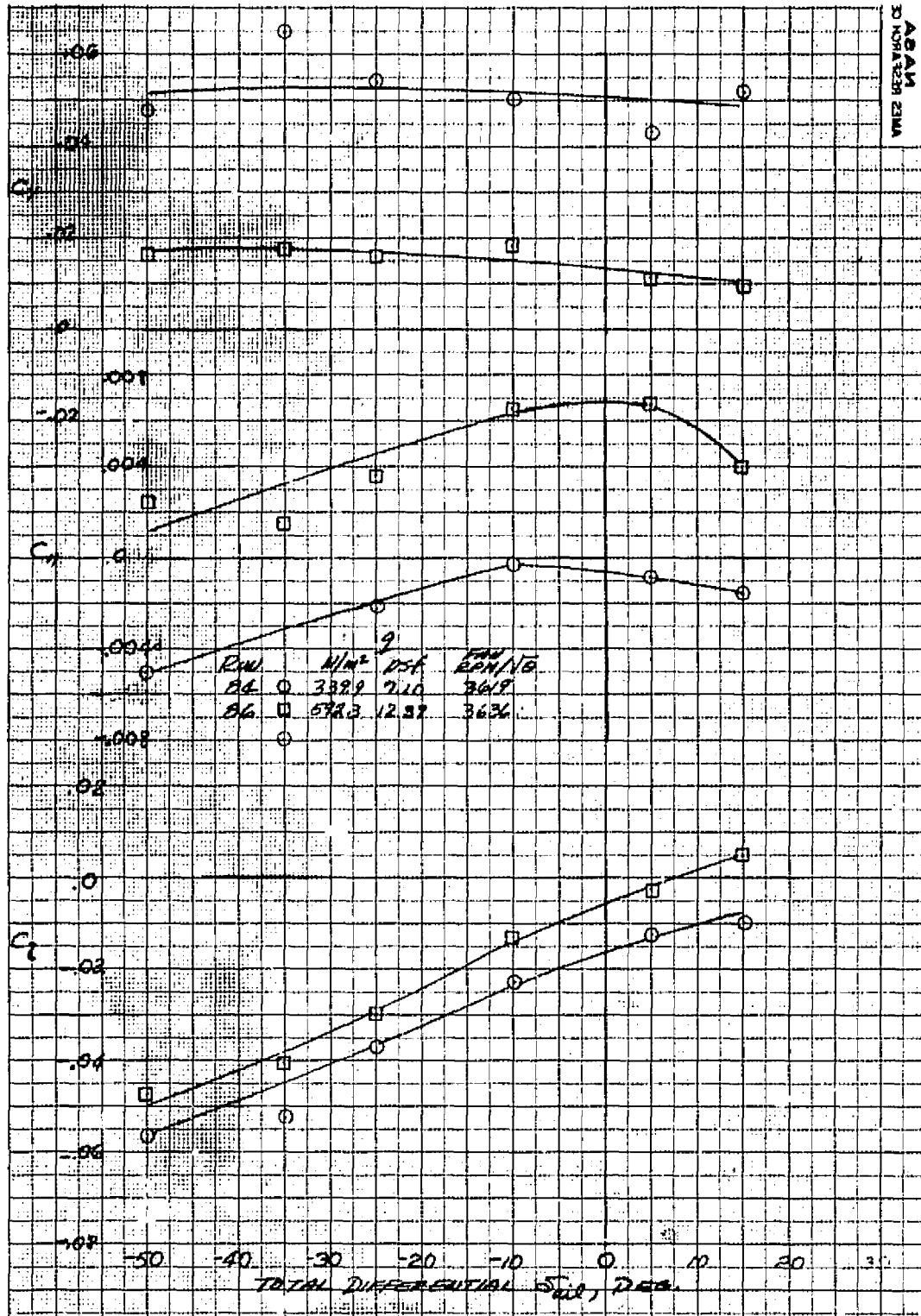
(b) Lateral characteristics.

Figure 27.- Concluded.

89
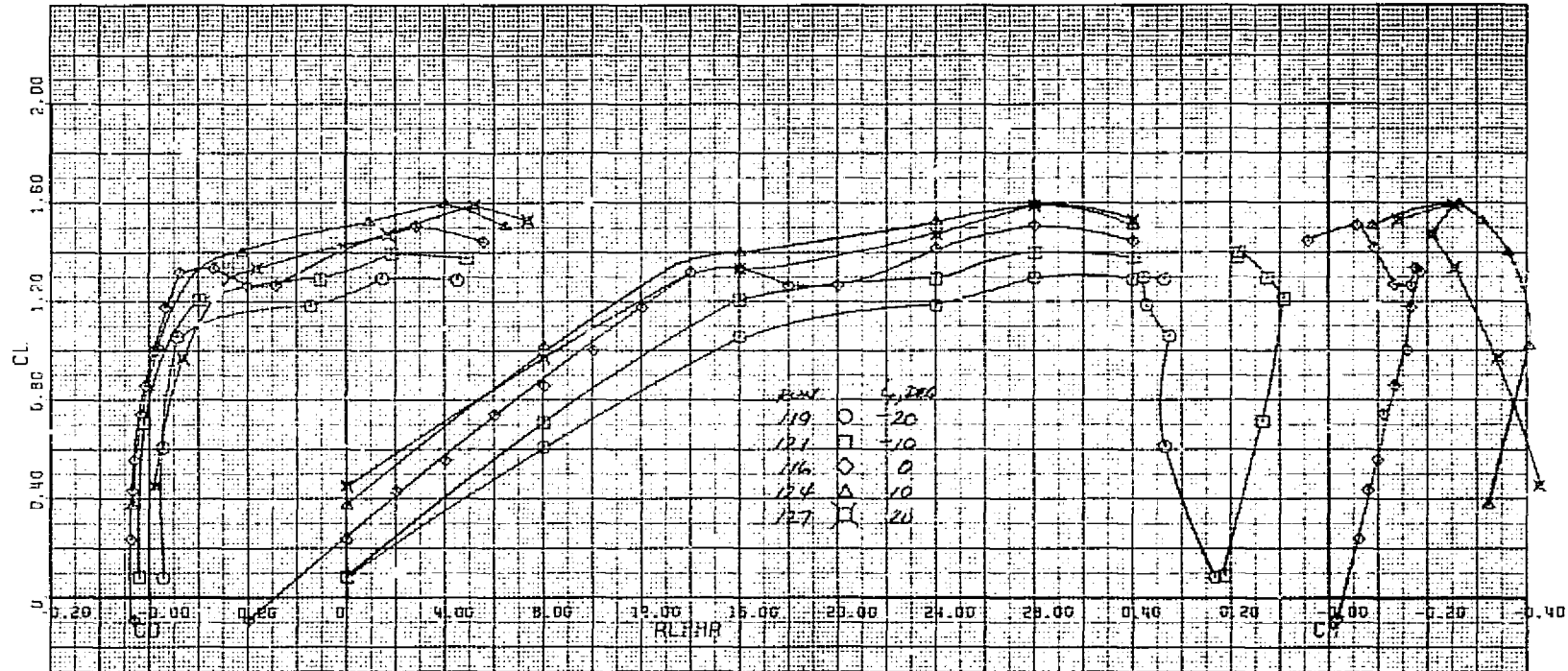
(a) Cruise fan RPM/$\sqrt{\theta}$ = 2727.

Figure 28.— Longitudinal characteristics of the model in the cruise
configuration; forward fan inlet and exit covered, $\delta_{cn} = 0°$,
$\delta_f = 0°$, $\delta_{ail} = 0°$, $\beta = 0°$, $\delta_R = 0°$, q = 1637.0 N/m²(34.19 psf).
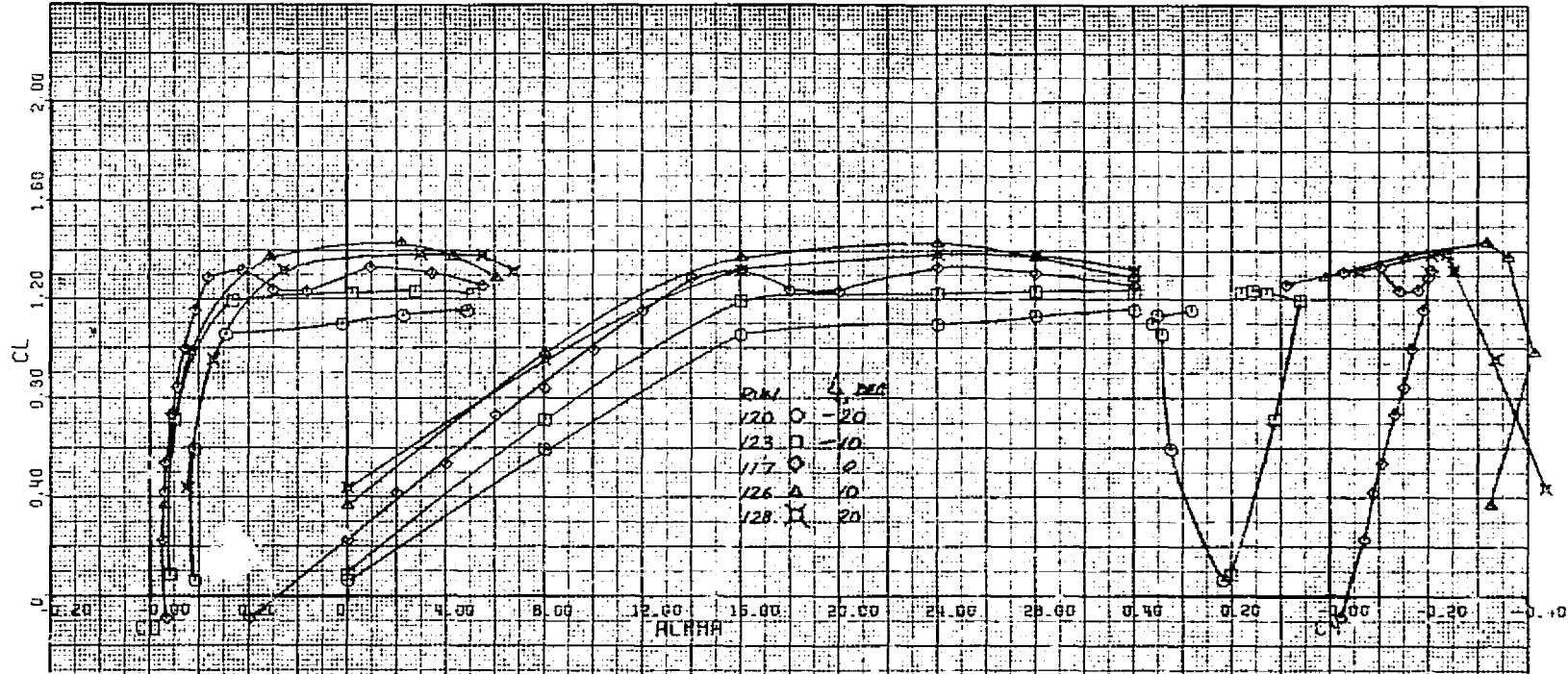
(b) Cruise fan RPM/$\sqrt{\theta}$ = 2170.

Figure 28.- Continued.
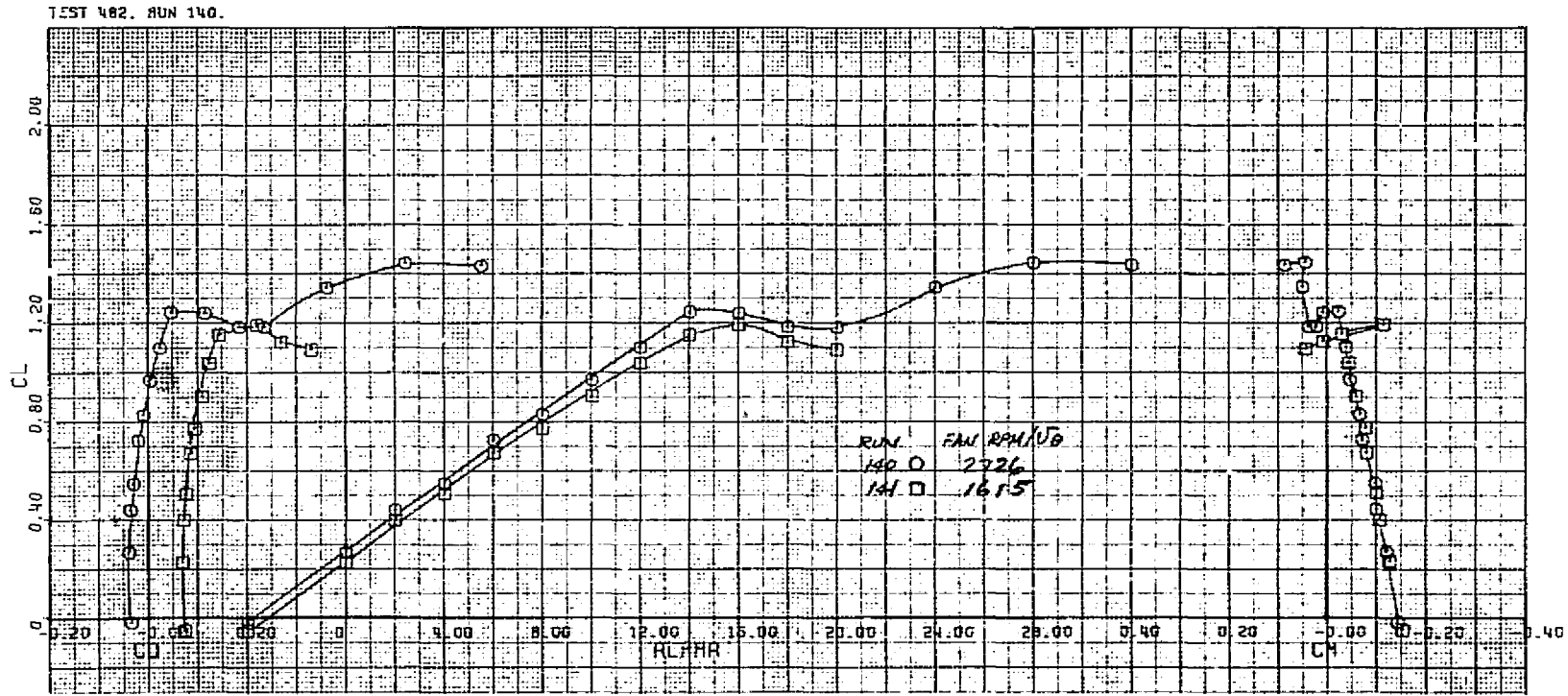
TEST 482. RUN 140.

Figure 29.- Longitudinal characteristics of the model in the cruise
configuration with the horizontal tail off; forward fan inlet
and exit covered, $\delta_{cn} = 0°$, $\delta_f = 0°$, $\delta_{ail} = 0°$, $\beta = 0°$, $\delta_R = 0°$,
$q = 1639.4$ N/m^2(34.24 psf).

(a) Longitudinal characteristics.

Figure 30.- Aerodynamic characteristics of the model in the cruise
configuration with the rudder deflected; forward fan inlet and
exit covered, $\delta_R = 23°$, $\delta_{cn} = 0°$, $\delta_f = 0°$, $\delta_{ail} = 0°$, $i_t = 0°$,
$\beta = 0°$, $q = 1639.4$ N/m^2(34.24 psf).

TEST 482. RUN 134.
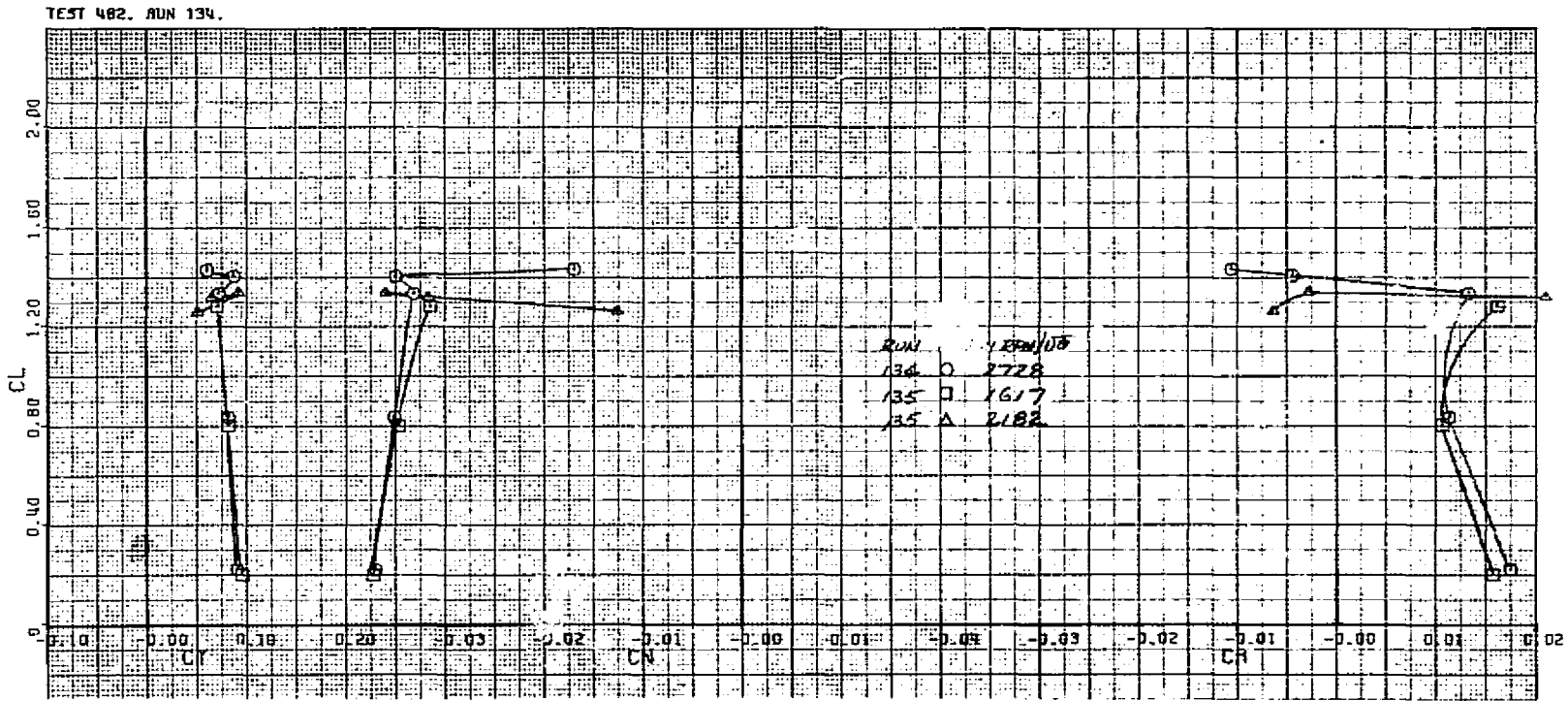
(b) Lateral characteristics.

Figure 30.- Concluded.
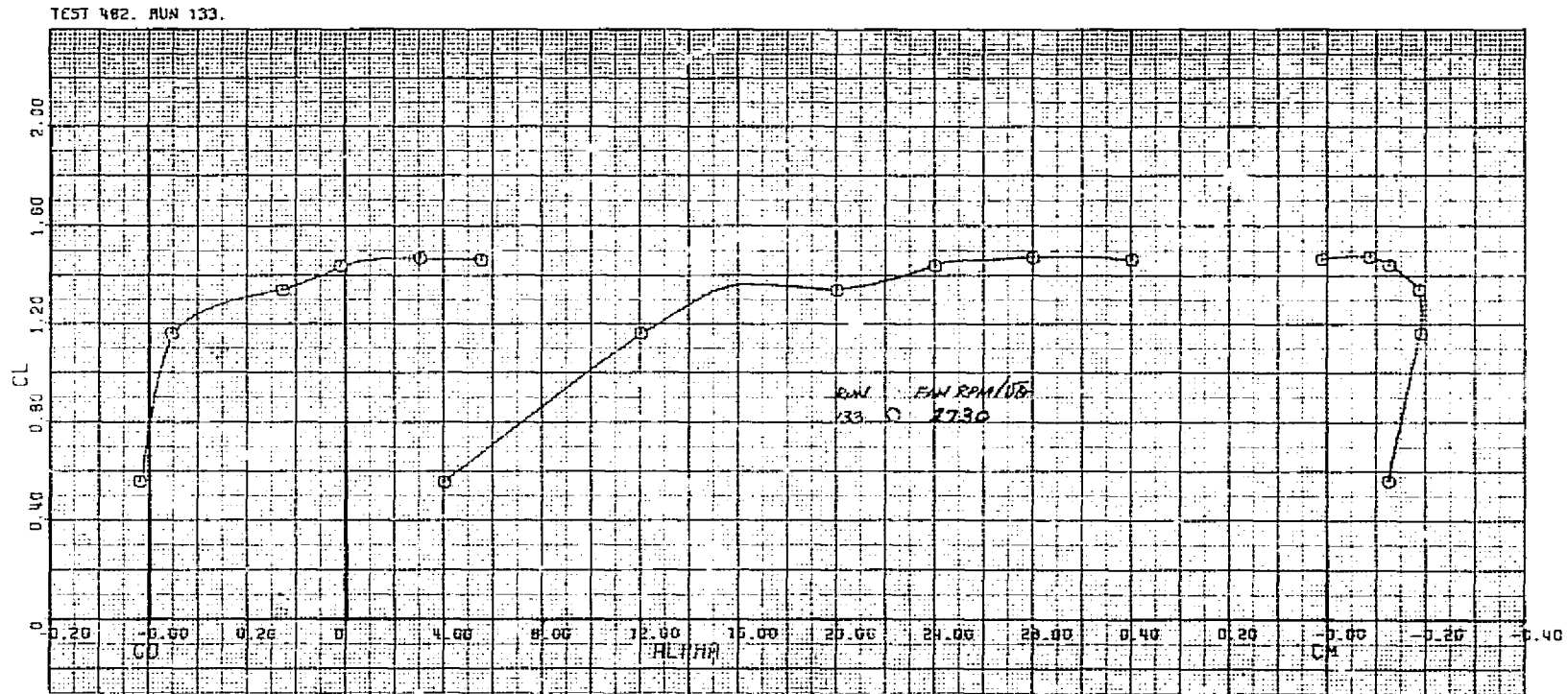
(a) Longitudinal characteristics.

Figure 31.- Aerodynamic characteristics of the model with sideslip of 8°; fow.rd fan covered, $\delta_{cn} = 0°$, $\delta_f = 0°$, $\delta_{ail} = 0°$, $i_t = 0°$, $\delta_R = 0°$, q = 1639.4 N/m^2(34.24 psf).
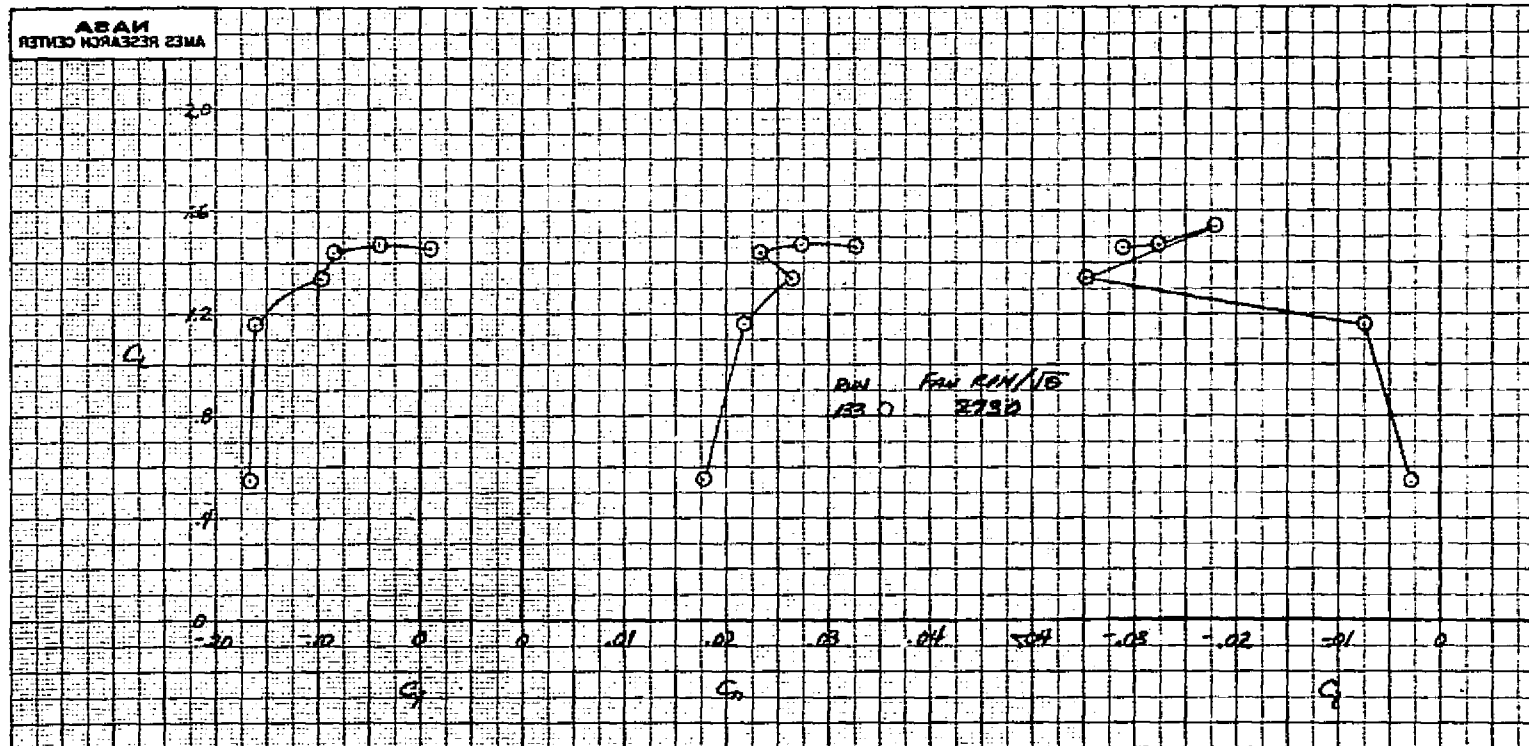
(b) Lateral characteristics.

Figure 31.- Concluded.
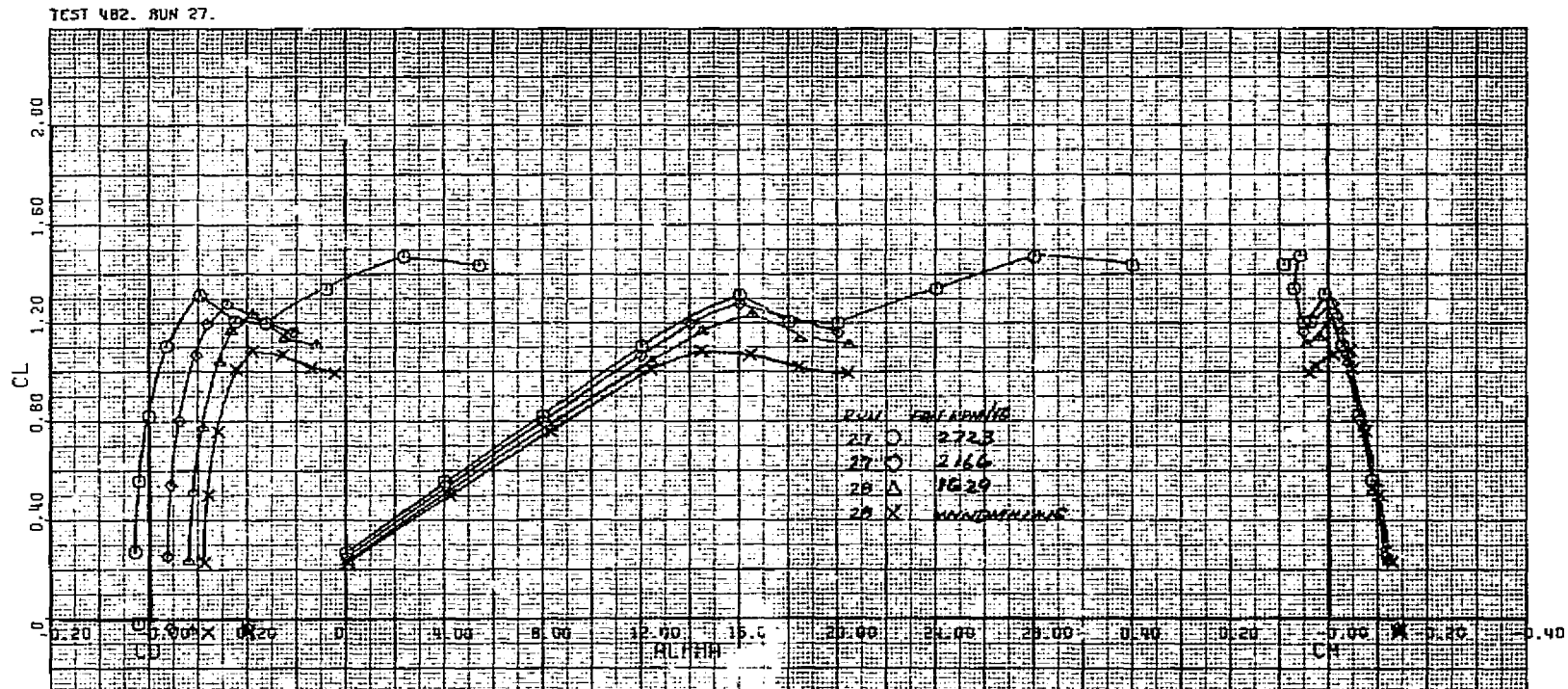
Figure 32.– Longitudinal charac.e. jitcs of the model with the horizontal
tail off; forward fan inlet covered, $\delta_{cn} = 0°$, $\beta_v = 0°$, $\delta_f = 0°$,
$\delta_{ail} = 0°$, $\beta = 0°$, $\delta_R = 0°$, $q = 1637.0$ N/m^2(34.19 psf).
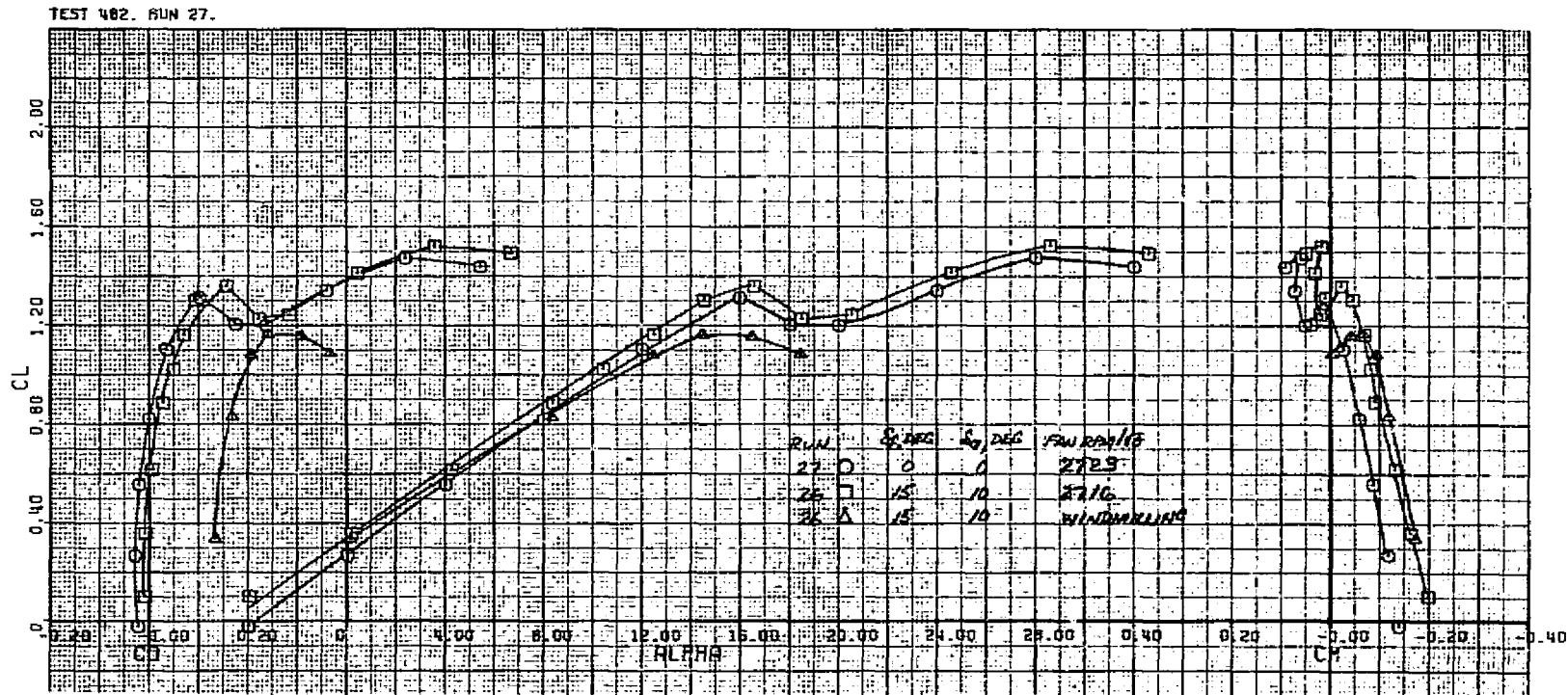
Figure 33.- Longitudinal characteristics of the model with the flaps and ailerons deflected; forward fan inlet covered, $\delta_{cn} = 0°$ $\beta_v = 0°$, horizontal tail off, $\beta = 0°$, $\delta_R = 0°$, $q = 1635.6$ N/m^2(34.16 psf).
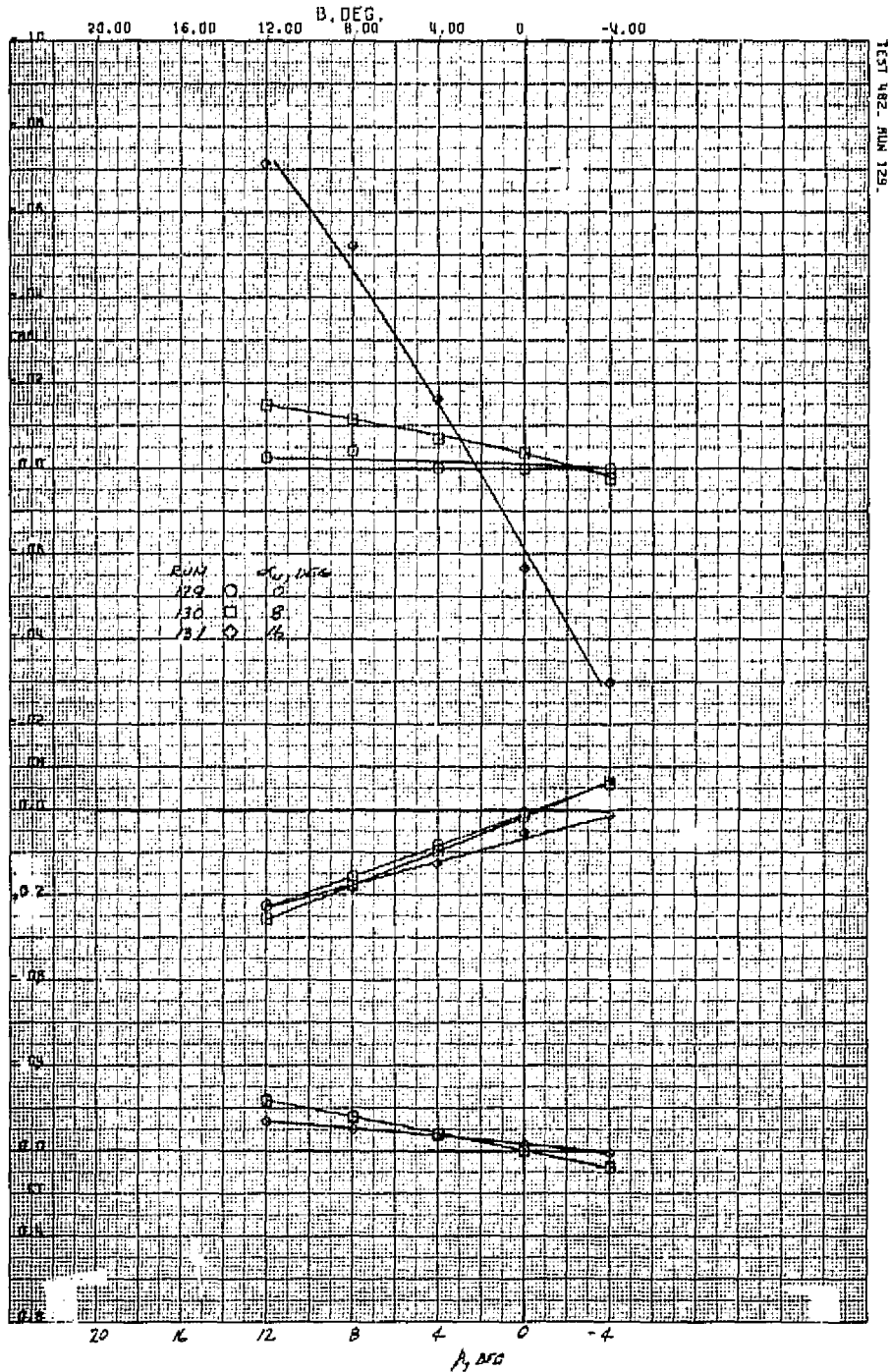
(a) Fan RPM/$\sqrt{\theta}$ = 2723.

Figure 34.- Variation of side force, yawing-moment, and rolling moment coefficients with sideslip; forward fan inlet and exit covered, δ_{cn} = 0°, δ_f = 0°, δ_{ail} = 0°, i_t = 0°, δ_R = 0°, q = 1635.6 N/m^2 (34.17 psf).

100
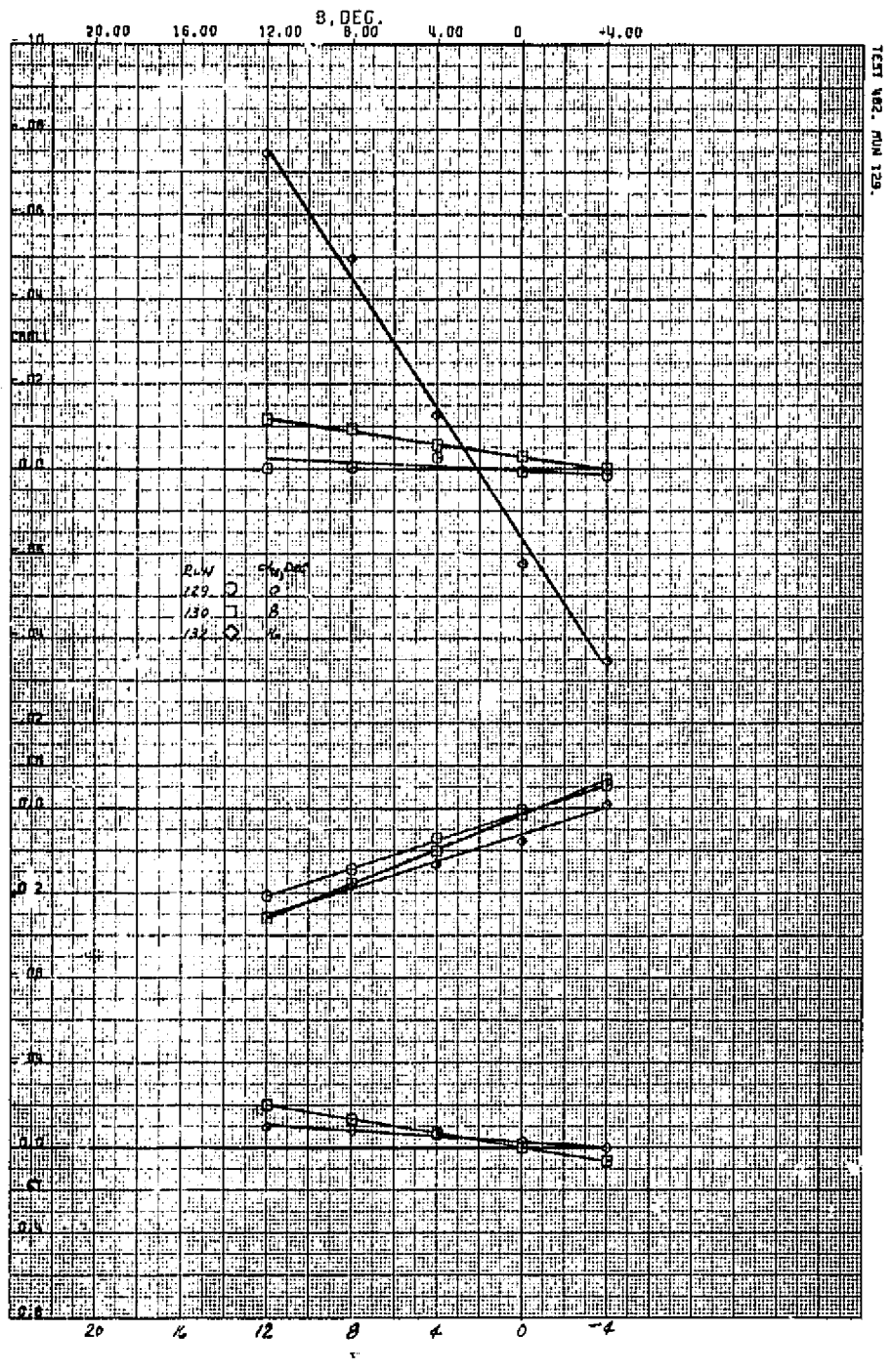
(b) Fan RPM/$\sqrt{\theta}$ = 1614.

Figure 34.- Concluded.
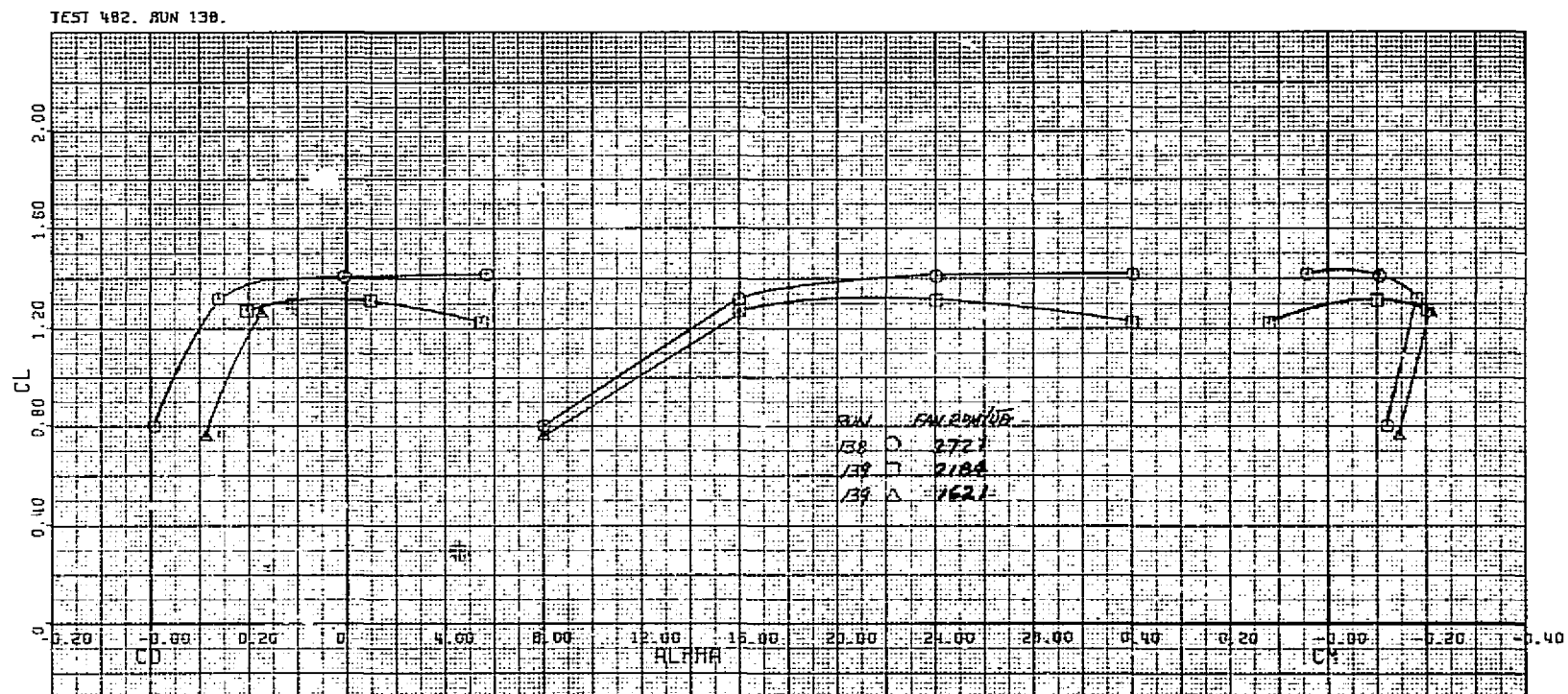
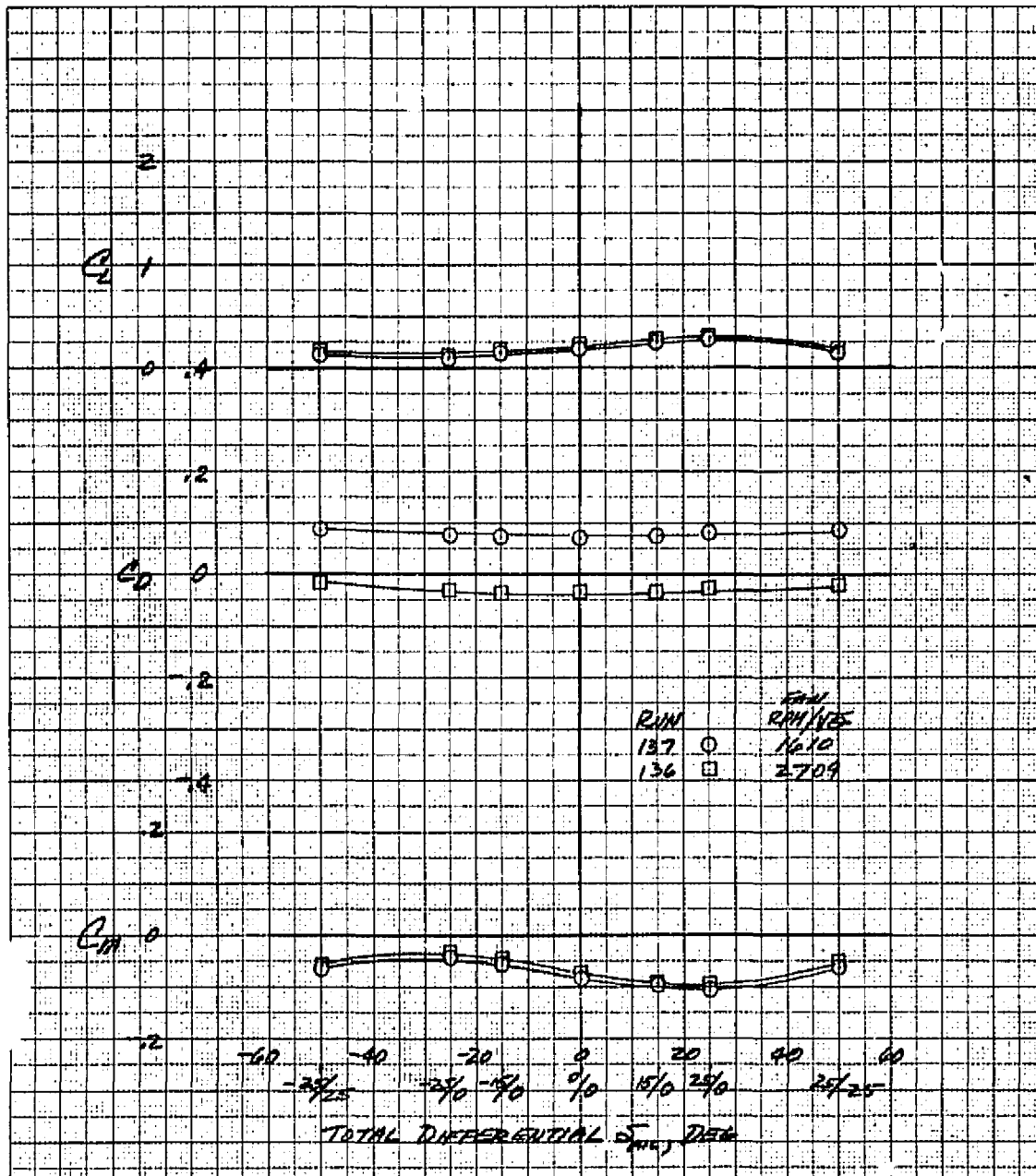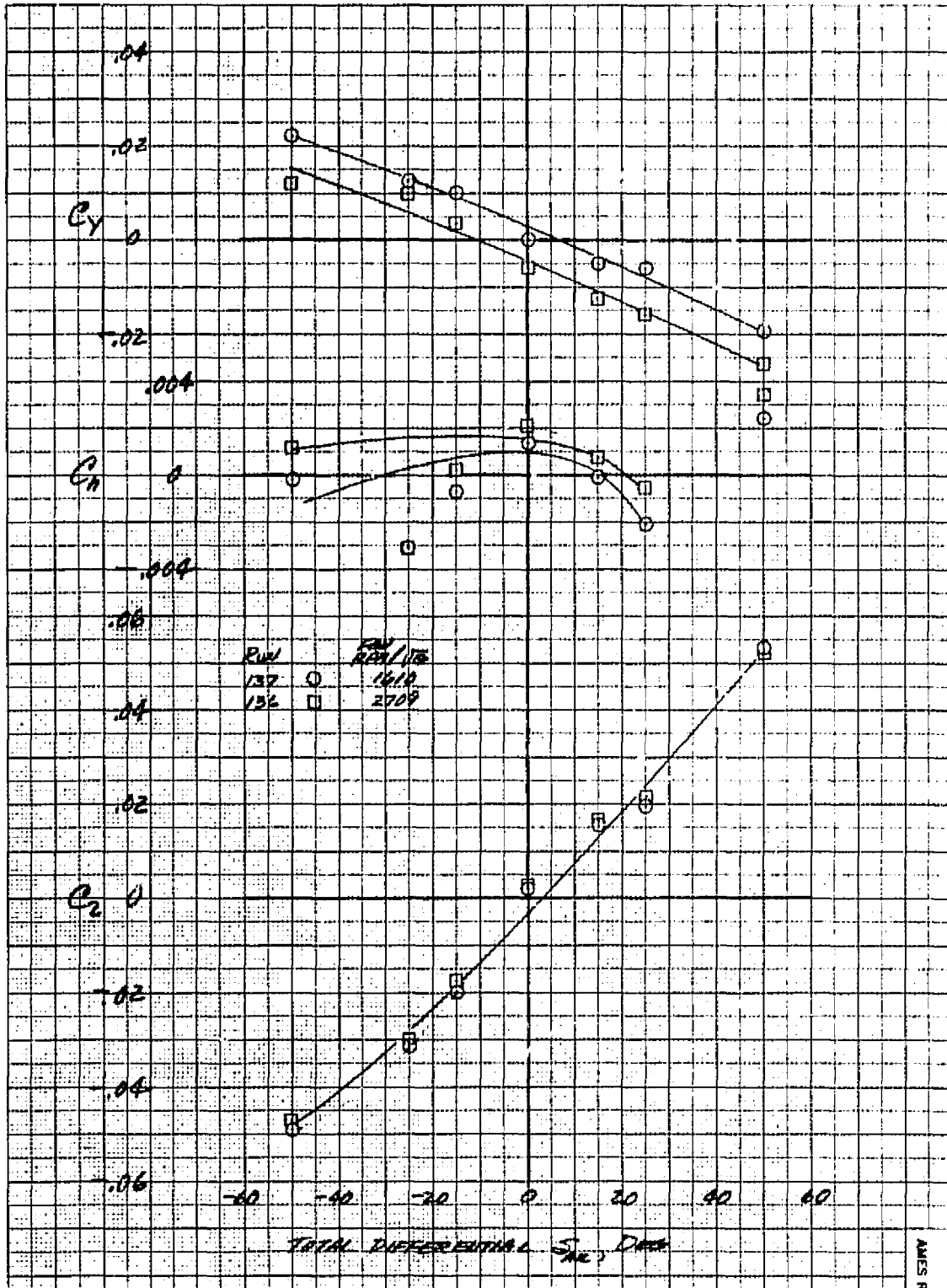(a) Longitudinal characteristics.

Figure 35.- The effect of differential aileron deflection on the model
aerodynamic characteristics; forward fan inlet and exit covered,
$\delta_{ail} = -25°/25°$, $\delta_{cn} = 0°$, $\delta_f = 0°$, $i_t = 0°$, $\beta = 0°$, $\delta_R = 0°$,
$q = 1638.4$ N/m^2 (34.22 psf).
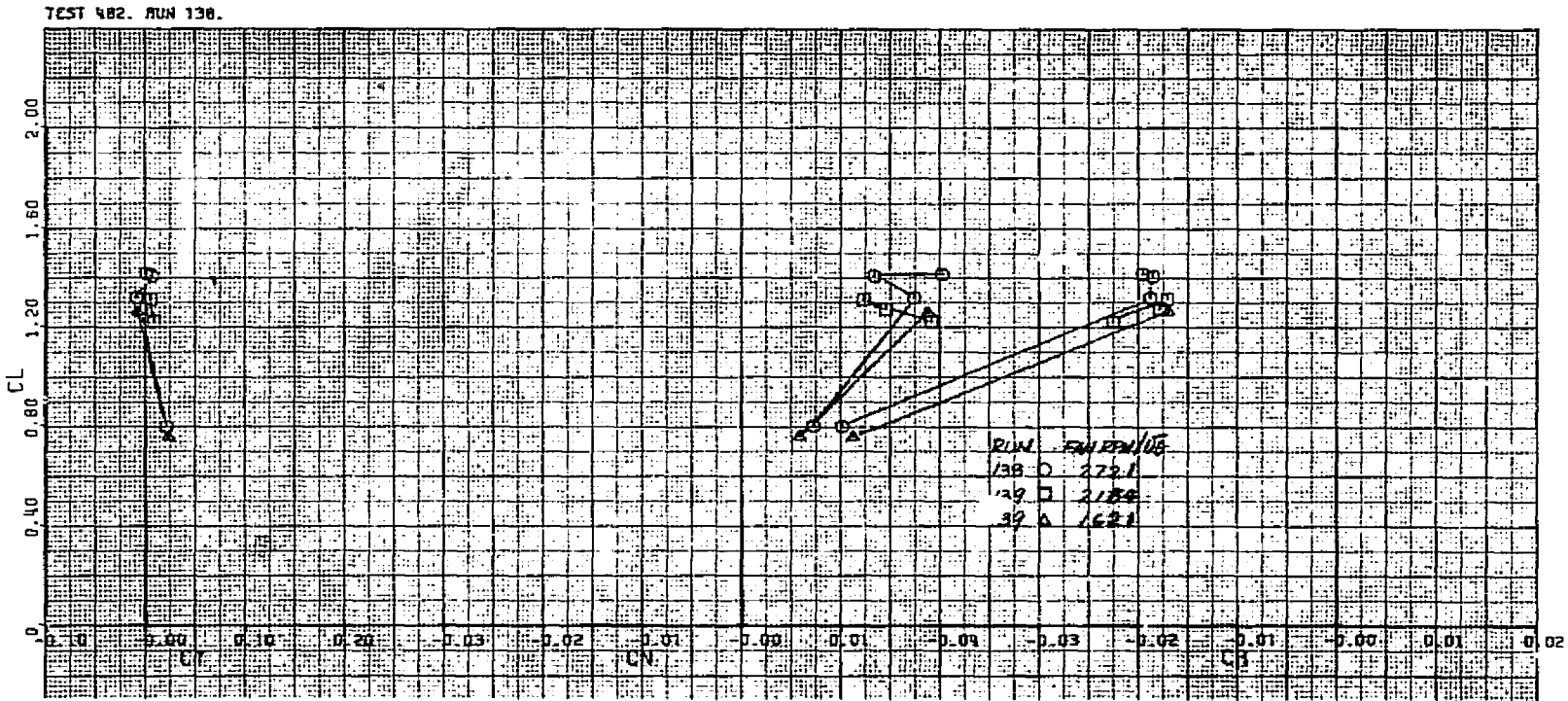
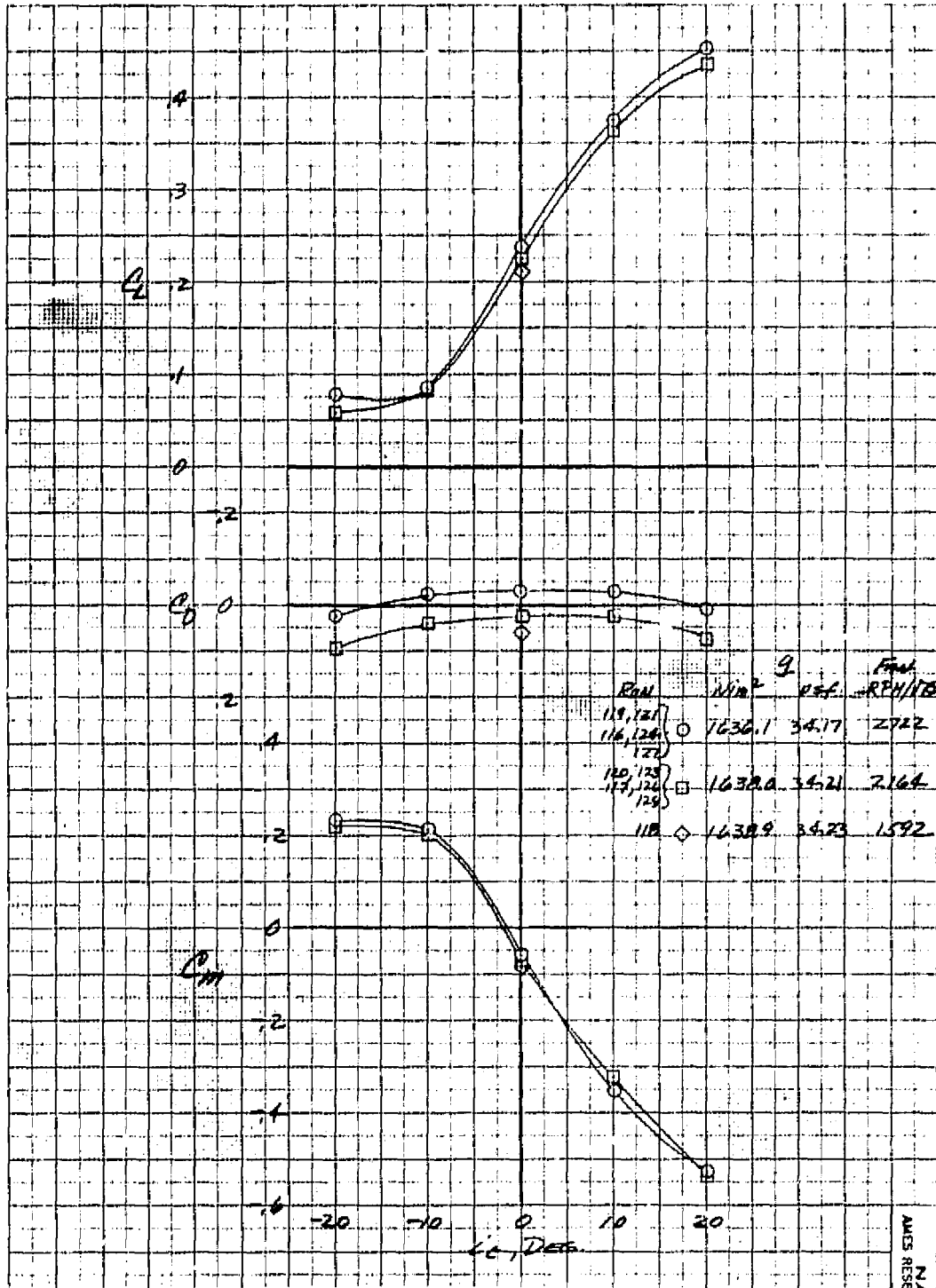(b) Lateral characteristics.

Figure 35.- Concluded.

(a) Longitudinal characteristics.

Figure 36.- The effect of differential aileron deflection on the model
aerodynamic characteristics; forward fan inlet and exit covered,
$\delta_{cn} = 0°$, $\delta_f = 0°$, $i_t = 0°$, $\beta = 0°$, $\alpha_u = 0°$, $q = 1638.0$ N/m^2(34.21 psf),
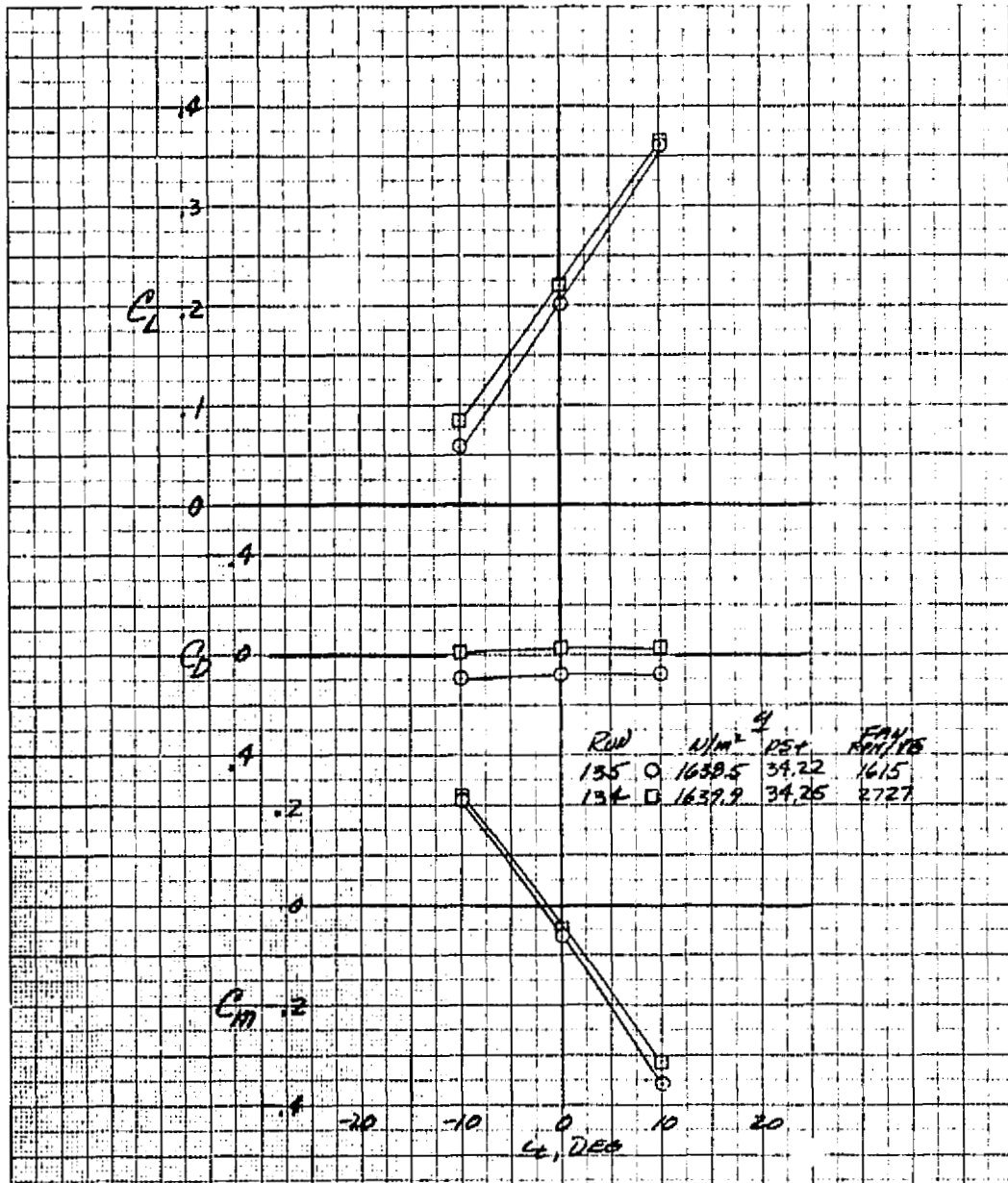$\delta_R = 0°$.

(b) Lateral characteristics.

Figure 36.- Concluded.

(a) $\delta_R = 0$

Figure 37.- The effect of tail incidence on longitudinal aerodynamic
characteristics of the model in the cruise configuration; forward
fan inlet and exit covered, $\delta_{cn} = 0°$, $\delta_f = 0°$, $\delta_{ail} = 0°$, $\alpha_u = 0°$,
$\beta = 0°$.

(b) $\delta_R = 23°$.

Figure 37.- Concluded.